POWER/VOLTAGE INSTABILITY IN AN HVDC LINK CONNECTED TO A WEAK AC SYSTEM

By

Sladjana Elez

A thesis submitted to

Faculty of Graduate Studies

in Partial Fulfilment of the Requirements for

Degree of Master of Science

Department of Electrical Engineering

UNIVERSITY OF MANITOBA

Winnipeg, Manitoba, Canada

May 1996

National Library
of Canada

Acquisitions and
Bibliographic Services Branch

395 Wellington Street
Ottawa, Ontario
K1A 0N4

Bibliothèque nationale
du Canada

Direction des acquisitions et
des services bibliographiques

395, rue Wellington
Ottawa (Ontario)
K1A 0N4

Your file Votre référence

Our file Notre référence

ISBN 0-612-13104-1

Canada

Name _____

Dissertation Abstracts International and *Masters Abstracts International* are arranged by broad, general subject categories. Please select the one subject which most nearly describes the content of your dissertation or thesis. Enter the corresponding four-digit code in the spaces provided.

HVDC systems

SUBJECT TERM

0544

SUBJECT CODE

UMI

Subject Categories

THE HUMANITIES AND SOCIAL SCIENCES

COMMUNICATIONS AND THE ARTS
Architecture 0729
Art History 0377
Cinema 0900
Dance 0378
Fine Arts 0357
Information Science 0723
Journalism 0391
Library Science 0399
Mass Communications 0708
Music 0413
Speech Communication 0459
Theater 0465

EDUCATION
General 0515
Administration 0514
Adult and Continuing 0516
Agricultural 0517
Art 0273
Bilingual and Multicultural 0282
Business 0688
Community College 0275
Curriculum and Instruction 0727
Early Childhood 0518
Elementary 0524
Finance 0277
Guidance and Counseling 0519
Health 0680
Higher 0745
History of 0520
Home Economics 0278
Industrial 0521
Language and Literature 0279
Mathematics 0280
Music 0522
Philosophy of 0998
Physical 0523
Psychology 0525
Reading 0535
Religious 0527
Sciences 0714
Secondary 0533
Social Sciences 0534
Sociology of 0340
Special 0529
Teacher Training 0530
Technology 0710
Tests and Measurements 0288
Vocational 0747

LANGUAGE, LITERATURE AND LINGUISTICS
Language
- General 0679
- Ancient 0289
- Linguistics 0290
- Modern 0291

Literature
- General 0401
- Classical 0294
- Comparative 0295
- Medieval 0297
- Modern 0298
- African 0316
- American 0591
- Asian 0305
- Canadian (English) 0352
- Canadian (French) 0355
- English 0593
- Germanic 0311
- Latin American 0312
- Middle Eastern 0315
- Romance 0313
- Slavic and East European 0314

PHILOSOPHY, RELIGION AND THEOLOGY
Philosophy 0422
Religion
- General 0318
- Biblical Studies 0321
- Clergy 0319
- History of 0320
- Philosophy of 0322

Theology 0469

SOCIAL SCIENCES
American Studies 0323
Anthropology
- Archaeology 0324
- Cultural 0326
- Physical 0327

Business Administration
- General 0310
- Accounting 0272
- Banking 0770
- Management 0454
- Marketing 0338

Canadian Studies 0385
Economics
- General 0501
- Agricultural 0503
- Commerce-Business 0505
- Finance 0508
- History 0509
- Labor 0510
- Theory 0511

Folklore 0358
Geography 0366
Gerontology 0351
History
- General 0578
- Ancient 0579
- Medieval 0581
- Modern 0582
- Black 0328
- African 0331
- Asia, Australia and Oceania 0332
- Canadian 0334
- European 0335
- Latin American 0336
- Middle Eastern 0333
- United States 0337

History of Science 0585
Law 0398
Political Science
- General 0615
- International Law and Relations 0616
- Public Administration 0617

Recreation 0814
Social Work 0452
Sociology
- General 0626
- Criminology and Penology ... 0627
- Demography 0938
- Ethnic and Racial Studies 0631
- Individual and Family Studies 0628
- Industrial and Labor Relations 0629
- Public and Social Welfare 0630
- Social Structure and Development 0700
- Theory and Methods 0344

Transportation 0709
Urban and Regional Planning 0999
Women's Studies 0453

THE SCIENCES AND ENGINEERING

BIOLOGICAL SCIENCES
Agriculture
- General 0473
- Agronomy 0285
- Animal Culture and Nutrition 0475
- Animal Pathology 0476
- Food Science and Technology 0359
- Forestry and Wildlife 0478
- Plant Culture 0479
- Plant Pathology 0480
- Plant Physiology 0817
- Range Management 0777
- Wood Technology 0746

Biology
- General 0306
- Anatomy 0287
- Biostatistics 0308
- Botany 0309
- Cell 0379
- Ecology 0329
- Entomology 0353
- Genetics 0369
- Limnology 0793
- Microbiology 0410
- Molecular 0307
- Neuroscience 0317
- Oceanography 0416
- Physiology 0433
- Radiation 0821
- Veterinary Science 0778
- Zoology 0472

Biophysics
- General 0786
- Medical 0760

EARTH SCIENCES
Biogeochemistry 0425
Geochemistry 0996
Geodesy 0370
Geology 0372
Geophysics 0373
Hydrology 0388
Mineralogy 0411
Paleobotany 0345
Paleoecology 0426
Paleontology 0418
Paleozoology 0985
Palynology 0427
Physical Geography 0368
Physical Oceanography 0415

HEALTH AND ENVIRONMENTAL SCIENCES
Environmental Sciences 0768
Health Sciences
- General 0566
- Audiology 0300
- Chemotherapy 0992
- Dentistry 0567
- Education 0350
- Hospital Management 0769
- Human Development 0758
- Immunology 0982
- Medicine and Surgery 0564
- Mental Health 0347
- Nursing 0569
- Nutrition 0570
- Obstetrics and Gynecology .. 0380
- Occupational Health and Therapy 0354
- Ophthalmology 0381
- Pathology 0571
- Pharmacology 0419
- Pharmacy 0572
- Physical Therapy 0382
- Public Health 0573
- Radiology 0574
- Recreation 0575
- Speech Pathology 0460
- Toxicology 0383

Home Economics 0386

PHYSICAL SCIENCES
Pure Sciences
Chemistry
- General 0485
- Agricultural 0749
- Analytical 0486
- Biochemistry 0487
- Inorganic 0488
- Nuclear 0738
- Organic 0490
- Pharmaceutical 0491
- Physical 0494
- Polymer 0495
- Radiation 0754

Mathematics 0405
Physics
- General 0605
- Acoustics 0986
- Astronomy and Astrophysics 0606
- Atmospheric Science 0608
- Atomic 0748
- Electronics and Electricity 0607
- Elementary Particles and High Energy 0798
- Fluid and Plasma 0759
- Molecular 0609
- Nuclear 0610
- Optics 0752
- Radiation 0756
- Solid State 0611

Statistics 0463

Applied Sciences
Applied Mechanics 0346
Computer Science 0984
Engineering
- General 0537
- Aerospace 0538
- Agricultural 0539
- Automotive 0540
- Biomedical 0541
- Chemical 0542
- Civil 0543
- Electronics and Electrical 0544
- Heat and Thermodynamics ... 0348
- Hydraulic 0545
- Industrial 0546
- Marine 0547
- Materials Science 0794
- Mechanical 0548
- Metallurgy 0743
- Mining 0551
- Nuclear 0552
- Packaging 0549
- Petroleum 0765
- Sanitary and Municipal 0554
- System Science 0790

Geotechnology 0428
Operations Research 0796
Plastics Technology 0795
Textile Technology 0994

PSYCHOLOGY
General 0621
Behavioral 0384
Clinical 0622
Developmental 0620
Experimental 0623
Industrial 0624
Personality 0625
Physiological 0989
Psychobiology 0349
Psychometrics 0632
Social 0451

Nom _____

Dissertation Abstracts International est organisé en catégories de sujets. Veuillez s.v.p. choisir le sujet qui décrit le mieux votre thèse et inscrivez le code numérique approprié dans l'espace réservé ci-dessous.

_____ ☐☐☐ U·M·I

SUJET — CODE DE SUJET

Catégories par sujets

HUMANITÉS ET SCIENCES SOCIALES

COMMUNICATIONS ET LES ARTS
Architecture 0729
Beaux-arts 0357
Bibliothéconomie 0399
Cinéma 0900
Communication verbale 0459
Communications 0708
Danse 0378
Histoire de l'art 0377
Journalisme 0391
Musique 0413
Sciences de l'information 0723
Théâtre 0465

ÉDUCATION
Généralités 515
Administration 0514
Art 0273
Collèges communautaires 0275
Commerce 0688
Économie domestique 0278
Éducation permanente 0516
Éducation préscolaire 0518
Éducation sanitaire 0680
Enseignement agricole 0517
Enseignement bilingue et multiculturel 0282
Enseignement industriel 0521
Enseignement primaire. 0524
Enseignement professionnel 0747
Enseignement religieux 0527
Enseignement secondaire 0533
Enseignement spécial 0529
Enseignement supérieur 0745
Évaluation 0288
Finances 0277
Formation des enseignants 0530
Histoire de l'éducation 0520
Langues et littérature 0279
Lecture 0535
Mathématiques 0280
Musique 0522
Orientation et consultation 0519
Philosophie de l'éducation 0998
Physique 0523
Programmes d'études et enseignement 0727
Psychologie 0525
Sciences 0714
Sciences sociales 0534
Sociologie de l'éducation 0340
Technologie 0710

LANGUE, LITTÉRATURE ET LINGUISTIQUE
Langues
- Généralités 0679
- Anciennes 0289
- Linguistique 0290
- Modernes 0291

Littérature
- Généralités 0401
- Anciennes 0294
- Comparée 0295
- Médiévale 0297
- Moderne 0298
- Africaine 0316
- Américaine 0591
- Anglaise 0593
- Asiatique 0305
- Canadienne (Anglaise) 0352
- Canadienne (Française) 0355
- Germanique 0311
- Latino-américaine 0312
- Moyen-orientale 0315
- Romane 0313
- Slave et est-européenne 0314

PHILOSOPHIE, RELIGION ET THÉOLOGIE
Philosophie 0422
Religion
- Généralités 0318
- Clergé 0319
- Études bibliques 0321
- Histoire des religions 0320
- Philosophie de la religion 0322

Théologie 0469

SCIENCES SOCIALES
Anthropologie
- Archéologie 0324
- Culturelle 0326
- Physique 0327

Droit 0398
Économie
- Généralités 0501
- Commerce-Affaires 0505
- Économie agricole 0503
- Économie du travail 0510
- Finances 0508
- Histoire 0509
- Théorie 0511

Études américaines 0323
Études canadiennes 0385
Études féministes 0453
Folklore 0358
Géographie 0366
Gérontologie 0351
Gestion des affaires
- Généralités 0310
- Administration 0454
- Banques 0770
- Comptabilité 0272
- Marketing 0338

Histoire
- Histoire générale 0578
- Ancienne 0579
- Médiévale 0581
- Moderne 0582
- Histoire des noirs 0328
- Africaine 0331
- Canadienne 0334
- États-Unis 0337
- Européenne 0335
- Moyen-orientale 0333
- Latino-américaine 0336
- Asie, Australie et Océanie 0332

Histoire des sciences 0585
Loisirs 0814
Planification urbaine et régionale 0999
Science politique
- Généralités 0615
- Administration publique 0617
- Droit et relations internationales 0616

Sociologie
- Généralités 0626
- Aide et bien-être social 0630
- Criminologie et établissements pénitentiaires 0627
- Démographie 0938
- Études de l' individu et de la famille 0628
- Études des relations interethniques et des relations raciales 0631
- Structure et développement social 0700
- Théorie et méthodes. 0344
- Travail et relations industrielles 0629

Transports 0709
Travail social 0452

SCIENCES ET INGÉNIERIE

SCIENCES BIOLOGIQUES
Agriculture
- Généralités 0473
- Agronomie. 0285
- Alimentation et technologie alimentaire 0359
- Culture 0479
- Élevage et alimentation 0475
- Exploitation des pâturages 0777
- Pathologie animale 0476
- Pathologie végétale 0480
- Physiologie végétale 0817
- Sylviculture et faune 0478
- Technologie du bois 0746

Biologie
- Généralités 0306
- Anatomie 0287
- Biologie (Statistiques) 0308
- Biologie moléculaire 0307
- Botanique 0309
- Cellule 0379
- Écologie 0329
- Entomologie 0353
- Génétique 0369
- Limnologie 0793
- Microbiologie 0410
- Neurologie 0317
- Océanographie 0416
- Physiologie 0433
- Radiation 0821
- Science vétérinaire 0778
- Zoologie 0472

Biophysique
- Généralités 0786
- Medicale 0760

SCIENCES DE LA TERRE
Biogéochimie 0425
Géochimie 0996
Géodésie 0370
Géographie physique 0368
Géologie 0372
Géophysique 0373
Hydrologie 0388
Minéralogie 0411
Océanographie physique 0415
Paléobotanique 0345
Paléoécologie 0426
Paléontologie 0418
Paléozoologie 0985
Palynologie 0427

SCIENCES DE LA SANTÉ ET DE L'ENVIRONNEMENT
Économie domestique 0386
Sciences de l'environnement 0768
Sciences de la santé
- Généralités 0566
- Administration des hôpitaux 0769
- Alimentation et nutrition 0570
- Audiologie 0300
- Chimiothérapie 0992
- Dentisterie 0567
- Développement humain 0758
- Enseignement 0350
- Immunologie 0982
- Loisirs 0575
- Médecine du travail et thérapie 0354
- Médecine et chirurgie 0564
- Obstétrique et gynécologie 0380
- Ophtalmologie 0381
- Orthophonie 0460
- Pathologie 0571
- Pharmacie 0572
- Pharmacologie 0419
- Physiothérapie 0382
- Radiologie 0574
- Santé mentale 0347
- Santé publique 0573
- Soins infirmiers 0569
- Toxicologie 0383

SCIENCES PHYSIQUES
Sciences Pures
Chimie
- Généralités 0485
- Biochimie 487
- Chimie agricole 0749
- Chimie analytique 0486
- Chimie minérale 0488
- Chimie nucléaire 0738
- Chimie organique 0490
- Chimie pharmaceutique 0491
- Physique 0494
- PolymÈres 0495
- Radiation 0754

Mathématiques 0405
Physique
- Généralités 0605
- Acoustique 0986
- Astronomie et astrophysique 0606
- Électronique et électricité 0607
- Fluides et plasma 0759
- Météorologie 0608
- Optique 0752
- Particules (Physique nucléaire) 0798
- Physique atomique 0748
- Physique de l'état solide 0611
- Physique moléculaire 0609
- Physique nucléaire 0610
- Radiation 0756

Statistiques 0463

Sciences Appliqués Et Technologie
Informatique 0984
Ingénierie
- Généralités 0537
- Agricole 0539
- Automobile 0540
- Biomédicale 0541
- Chaleur et thermodynamique 0348
- Conditionnement (Emballage) 0549
- Génie aérospatial 0538
- Génie chimique 0542
- Génie civil 0543
- Génie électronique et électrique 0544
- Génie industriel 0546
- Génie mécanique 0548
- Génie nucléaire 0552
- Ingénierie des systèmes 0790
- Mécanique navale 0547
- Métallurgie 0743
- Science des matériaux 0794
- Technique du pétrole 0765
- Technique minière 0551
- Techniques sanitaires et municipales 0554
- Technologie hydraulique 0545

Mécanique appliquée 0346
Géotechnologie 0428
Matières plastiques (Technologie) 0795
Recherche opérationnelle 0796
Textiles et tissus (Technologie) 0794

PSYCHOLOGIE
Généralités 0621
Personnalité 0625
Psychobiologie 0349
Psychologie clinique 0622
Psychologie du comportement 0384
Psychologie du développement 0620
Psychologie expérimentale 0623
Psychologie industrielle 0624
Psychologie physiologique 0989
Psychologie sociale 0451
Psychométrie 0632

THE UNIVERSITY OF MANITOBA

FACUTY OF GRADUATE STUDIES

COPYRIGHT PERMISSION

POWER/VOLTAGE INSTABILITY IN AN HVDC LINK CONNECTED TO A WEAK AC SYSTEM

BY

SLADJANA ELEZ

A Thesis/Practicum submitted to the Faculty of Graduate Studies of the University of Manitoba in partial fulfillment of the requirements for the degree of

MASTER OF SCIENCE

ACKNOWLEDGEMENTS

The author expresses her sincere gratitude to her advisor, Dr.Prof. A. Gole who always lent support, and provided his expertise and incisive suggestions towards the completion of this project. I have benefited immensely from association with Dr.Gole and will appreciate such relationship for many years to come.

A very special word of thanks is reserved for Dr. J.Chand of Manitoba Hydro for suggesting this topic, and also for his technical advice and support. The financial support of Manitoba Hydro for this project is gratefully acknowledged.

ABSTRACT

This thesis discusses the effect of different representations of the synchronous machine and its excitation system on the voltage stability in a dc link connected to a weak ac system. Four different synchronous machine models are considered. Indices for steady state stability such as Control Sensitivity Index (CSI) and Maximum Available Power (MAP) are evaluated first for each model and are followed by a subsequent detailed analysis using an electromagnetic transient simulation program PSCAD/EMTDC.

The results show that mere steady state analysis based on the MAP indices is not enough for the calculation of the critical ESCR such that dc system connected to a weak ac system operate reliably. The representation of the synchronous machine as a fixed voltage source behind transient reactance is suitable model for an initial guess for the critical Effective Short Circuit Ratio (ESCR). However, the dynamics of the synchronous machine and exciter play a significant role in determination of the critical ESCR not only in system stability but also in ensuring that the system has acceptable transient performance.

It is found that the system with detailed machine model and exciter which regulates bus voltage has highest critical ESCR. Therefore, the conclusion drawn from the system analysis where machine is modelled as the voltage source behind transient reactance can not be directly used. It is also shown that inability of the synchronous machine to absorb the real power in the steady state makes significant difference during study of the system with detailed machine model and system where machine is modelled as voltage source behind transient reactance.

TABLE OF CONTENTS:

LIST OF FIGURES:

LIST OF THE TABLES:

CHAPTER 1

INTRODUCTION

1.1 The Problem

Ac transmission systems are subject to transient and steady state instability due to the difference in the phase angles at either end of the transmission lines. Dc transmission does not suffer this disadvantage and is widely used to couple ac systems in an asynchronous manner. However, dc transmission systems too can be subject to unstable operation that results from basic characteristics of the conversion process. This is especially true if the dc system is connected to the ac system with weak strength. The strength of the ac system is defined as the ratio of the short circuit MVA at the ac busbar to the dc power taken from the same busbar and is evaluated by numbers called Short Circuit Ratio (SCR) and Effective Short Circuit Ratio (ESCR) [1]. The more complete definition of the SCR and ESCR are given in Chapter 2.

Hvdc convertors (rectifier and inverters) draw lagging reactive current from the ac systems which must be supplied from some other source. Ac harmonic filters provide part of this reactive current. Where the ac system is large compared to the dc link it may have an inherent capability to supply the remainder. However, if the ac system is weak compared

to a dc link the rest of the reactive power has to be supplied with additional devices for reactive power compensation such as synchronous compensators or extra static capacitors or static var compensators (SVC). The main interest of this thesis will be the power/voltage stability of the hvdc system connected to a weak ac system where synchronous compensators is used to compensate for the reactive power.

Even though the SCR and ESCR have been defined a long time ago, it is still not clear how to define SCR and ESCR to take into account the synchronous machine because the synchronous machines reactance doesn't have the fixed value during transients. The voltage stabilizing effect of the synchronous machine if a fast exciter is employed to control bus voltage is also neglected in the evaluation of the SCR and ESCR. The simplest machine model consisting of the fixed voltage behind a transient reactance is considered most appropriate for system stability analysis based on SCR and ESCR analysis. However, in the light of the modern fast acting exciters there are some indications that subtransient reactance would be more appropriate for machine modelling when system operating limits have to be determined. The question which arises here and is of the interest in this research is how different levels of machine model affects the critical ESCR, and which machine model is most appropriate for machine representation when ESCR analysis is performed.

1.2 Objective

An hvdc transmission system supplying a weak ac receiving system is known to present problems of voltage/power stability for which in many cases the best economic solution will be to add a reactive compensator to the receiving bus. One way to compensate reactive power is to add synchronous compensator in shunt with the weak ac system bus. Besides, reactive power compensation employing a fast acting exciter as the dynamic voltage regulator for the synchronous compensator provides voltage stabilising properties. Furthermore, assuming the simplest connection scheme, the synchronous compensator is connected via individual coupling transformers to the high-voltage bus bar. The synchronous transient reactance plus the coupling transformer's reactance is connected in parallel with the ac system impedance, thereby lowering its value and increasing the ac system strength or Short Circuit Ratio (SCR)[1].

The main objective of the thesis is to investigate the power/voltage stability of the dc system connected to a very weak ac system when a synchronous machine is added at the inverter side ac bus to compensate for reactive power and to support voltage. This thesis discusses the results of research showing how different representations of the synchronous machine and dynamic voltage control affect voltage stability at hvdc converter terminals connected to a weak ac system. Four representations of the synchronous machine used to supply reactive power in the hvdc/ac system are considered, and the performance of each representation is simulated using the electromagnetic transient simulation program PSCAD/EMTDC. The aim is to investigate the validity of representations of various detail

for an accurate picture of the systems true behaviour. Model based on the steady state equations where the synchronous machine is represented as a fixed voltage behind a transient Xd' and sub-transient Xd" reactance (Thevenin equivalent) was considered first. Performance of such a system is then compared with performance of the system where a detailed model of the synchronous machine described with Park's equations is used. Two cases are considered. In one case the machine's field voltage is kept constant during simulation while in the other case the machine's field voltage is dynamically adjusted using the exciter to keep bus voltage at 1pu.

Studies using the "Control Sensitivity Index (CSI)" [4] and "Maximum Power Curve (MPC)" [2] analysis methods with different synchronous machine models are conducted. These are then compared with results from time domain simulation. The objective of the steady state CSI analysis is to find the critical ESCR below which the system in the power control mode becomes steady state unstable while the objective of the MPC analysis is to provide information about maximum available power (MAP) for different ESCR. The MPC analysis also provides the theoretical MPCs curves based on the steady state equation which are compared with the MPC obtained by simulation of the system with different synchronous machine representations.

The objective of the time domain analysis using PSCAD/EMTDC is to find the critical ESCR for each model. These results can then be compared with results obtained from analysis of steady state CSI and MPC indices. The first case is the steady state critical ESCR, and the other two are one phase fault recovery critical ESCR and three phase fault

recovery critical ESCR. The steady state critical ESCR refers to the lowest ESCR below which the hvdc/ac system can not be brought up to steady state due to the very weak strength of the ac system. The terms one and three phase fault recovery critical ESCR refer to the lowest ESCR below which the hvdc/ac system can not recover after one and three phase fault clearing respectively.

1.3 Thesis Outline

The hvdc system used for the power/voltage stability study in this thesis is fully described in Chapter 2. The benchmark model developed by CIGRE [8] is used as the base hvdc system model. Some modification of the original benchmark model [3] were necessary in order to design the appropriate study system for the research conducted in the thesis.

The results of the steady state system analysis are presented in Chapter 3. The two steady state analyses are conducted the Control Sensitivity Index (CSI) and Maximum Power Curve (MPC) analysis. Subsequently, results of the steady state analysis are compared with simulation results. At the end, the conclusion drawn from the steady state analysis are outlined.

In Chapter 4 the results of the time domain analysis are presented. The critical ESCR for the steady state results are derived by simulation as are also the critical ESCR values for one and three phase fault recovery. Adding more synchronous machines to deliver the

same amount of the reactive power affects the critical ESCR. The critical ESCR is also affected by exciter gains. Those effects on the critical ESCR are also presented in this chapter.

Finally, in the Chapter 5, the conclusion based on the results obtained in Chapter 3 and 4 are outlined, and recommendations for further research are suggested.

CHAPTER 2

STUDY SYSTEM

In this chapter the definition of the Short Circuit Ratio (SCR) and Effective Short Circuit Ratio (ESCR) and detailed description of the studied system are presented. The study system is developed using the CIGRE benchmark model [8] as the reference system since the benchmark model has been established to provide a common reference system to researchers conducting comparative performance studies. However, some modification of the original CIGRE benchmark model are made in order to establish the appropriate model for the studies conducted herein.

2.1 Definition of SCR and ESCR

The strength of the ac system is measured in terms of the Short Circuit Ratio (SCR) or Effective Short Circuit Ratio (ESCR). The SCR and ESCR indicate the relative strength of the ac system with respect to the rated dc power. There are several definitions of SCR and ESCR; therefore, in order avoid any ambiguity that may arise, this section shows how the SCR and ESCR are calculated in this study.

The SCR is defined as the ratio of the short circuit MVA of the ac system at the ac busbar with the dc blocked, and the ac voltage re-adjusted to its nominal voltage Vt to the rated dc power Pd at that bus [1]. This ratio is equivalent to the system Thevenin admittance expressed in per unit with the rated dc power as the MVA base and rated ac voltage as the voltage base. Figure 2.1.1 shows the equivalent circuit of the inverter ac system used during our study. Referring to figure 2.1.1, the calculation of the SCR, equation (1.1), includes the receiving system impedance Zs, the local load impedance Zll, and the transient synchronous machine reactance Xd' while the filter impedance Zf is not included in the calculation of the SCR. However, if the filter impedance Zf is included in the calculation of the MVA of the ac system, then the ratio is called ESCR, equation (1.2).

.

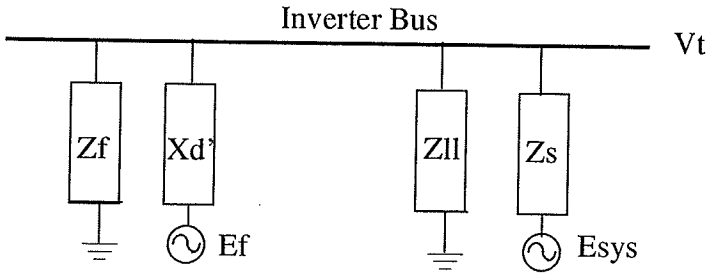

Figure 2.1.1: The SCR and ESCR definition.

$$SCR = \left(\frac{1}{Zsys} + \frac{1}{Zll} + \frac{1}{Xd'}\right)Z_{base} \qquad (1.1)$$

$$ESCR = \left(\frac{1}{Zsys} + \frac{1}{Zll} + \frac{1}{Xd'} + \frac{1}{Zf}\right)Z_{base} \qquad (1.2)$$

where

$$Z_{base} = \frac{Vt^2}{Pdc}$$

2.2. The Study Hvdc/ac System

The system used for the study is shown in Figure 2.2.1. It is the CIGRE benchmark model [3] which has been established to provide a common reference system to researchers conducting comparative performance studies. It is a 1000MW, 500 KV, 12 pulse monopolar hvdc system. The rectifier SCR is $2.5\angle 84^\circ$ and is kept constant during the study while the SCR at the inverter end is changed according to the study requirements. Some modifications of the original CIGRE benchmark model were necessary in order to create a system model appropriate for studies presented in this thesis. From the original CIGRE benchmark model the fixed capacitor banks at the inverter end were replaced by a synchronous condenser. Furthermore, the high and low frequency damping filters at the inverter end were resized to provide 300 Mvar while the synchronous condenser provides around 260 Mvar to fully compensate the inverter reactive power requirement. A local load of 300MVA with power factor 0.95 was added at the inverter bus to represent the damping and regulating effects of the local load.

In the steady state it is considered that the rated value of the dc current is 2kA, the dc power is 1000MW at the middle of the dc line, and the voltage at the inverter ac bus is

230kV. The steady state of the system which gives 1pu value for the dc current, the dc voltage, and the inverter ac bus voltage will be referred to as "1pu steady state" throughout the thesis. All presented results will consider capability of the dc system connected to a very weak ac system to be in the 1pu steady state.

The ESCR of the ac system at the inverter end is changed according to study requirements. The ESCR changes are made in such way that the ac system impedance frequency response profile remains essentially unchanged (see Appendix I). If the ESCR has to be reduced, the magnitude of the system impedance is increased by multiplying the original impedance magnitude by a constant larger than one. If the ESCR has to be increased the magnitude of the system impedance is decreased by multiplying the original impedance magnitude by a constant smaller than one. Changes in the ESCR are done in this way in order to ensure that the phase angle of the system impedance Zs remains the same while its magnitude changes according to the study requirements. The system impedance Zs is shown in figure 2.2.1 in the dashed-line box. The magnitude of the Zs is multiplied with the parameter k. The ESCR is reduced by increasing the parameter k, and conversely the ESCR is increased by decreasing the parameter k. During simulation the ac system strength is changed such that the SCR (or corresponding ESCR) of the system takes a value from the table given in Appendix II.

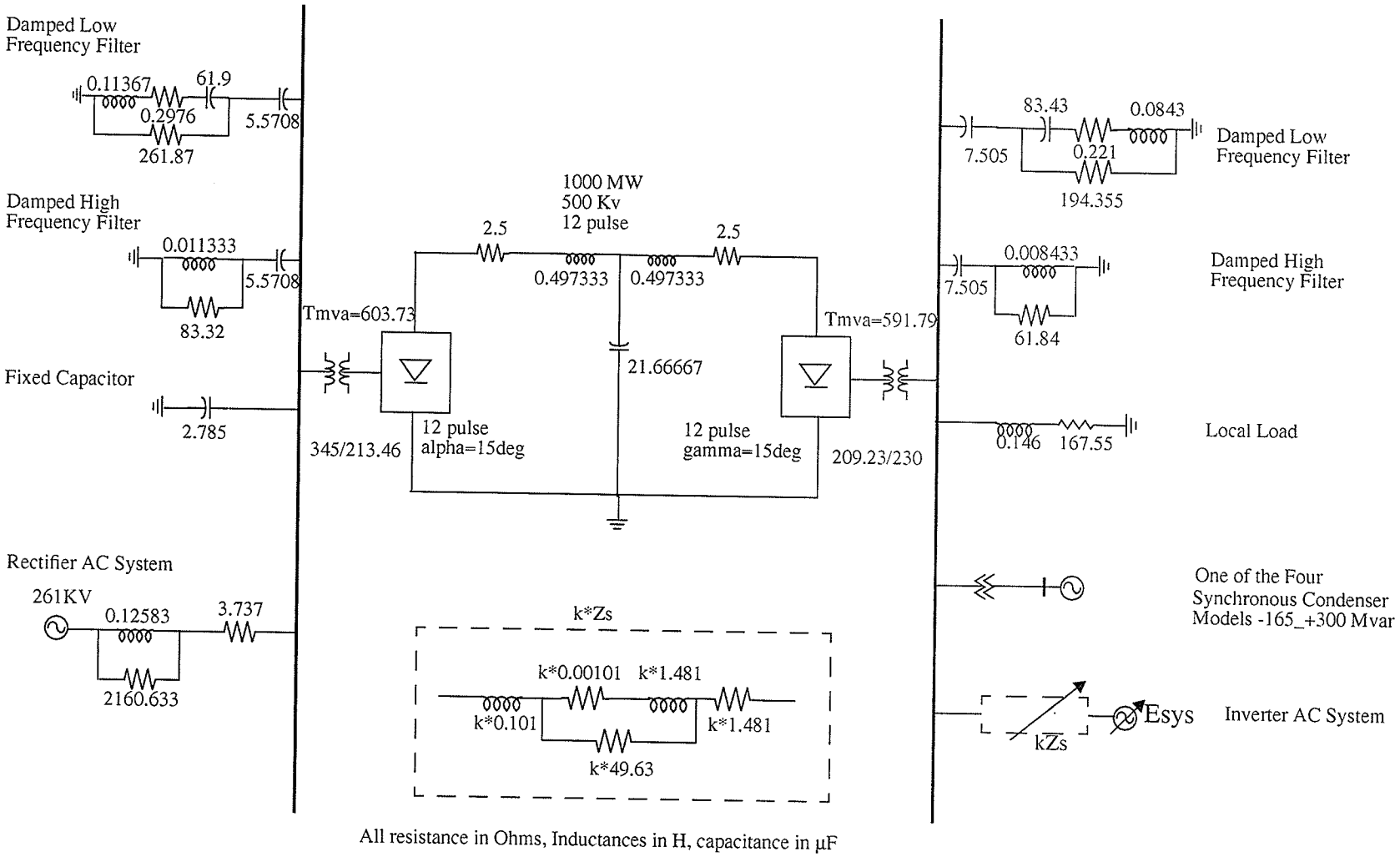

Figure 2.2.1: The Study System (Modified CIGRE benchmark model for 60Hz system)

2.3 Dc Control

The rectifier is in the constant power control mode while the inverter is in the minimum extinction angle (or gamma) control mode with γ=15deg. The power order is passed through a power/voltage divider circuit to generate the appropriate current order, figure 2.3.1a.

2.3.1 Power/Current Control

It is assumed that the rectifier is in the constant power control mode for 1pu steady state. However, for low ESCR's the voltage at the bus bar becomes more sensitive to dc current increases which leads to the power control mode becoming unstable; and the system collapses. In order to avoid system collapse when power control becomes unstable due to low ESCR of the ac system, the following strategy for the power/current control at the rectifier end is applied:

In constant power control mode, the manually set power order is divided by the dc voltage measured at the rectifier side, thus producing the dc current order. This order is passed to the rectifier and inverter current controllers as shown in Figure 2.3.1a. In order to avoid system collapse the power control mode is replaced with current control mode if all three phase voltages at the inverter ac side fall below 0.94pu for more than 30ms. In the current control mode the power order is divided with the fixed dc voltage instead of the measured

dc voltage. The fixed dc voltage has a value equal to rated dc voltage. While the system is in the current control mode, if all phase voltages rise above 0.98pu for more than 100ms, it is again safe to operate the system in power control mode. Therefore, the power order is divided by measured dc voltage at the rectifier side, and the power control takes place instead of the current control, figure 2.3.1b.

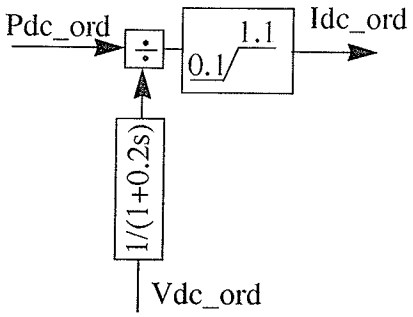

(a)

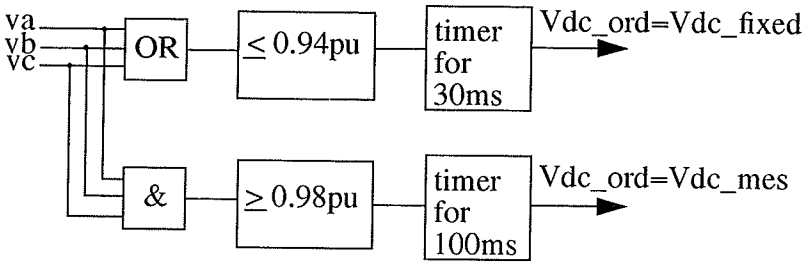

(b)

Figure 2.3.1: The Power/Current Control.

2.4 The Study System Model With Different Synchronous Machine Models

It seems that the modelling of the synchronous machine plays an important role when the critical SCR and ESCR has to be determined in order to ensure that a dc system connected to a very weak ac system operates reliably. Several representation for the synchronous machine are possible. We often model the machine as a fixed voltage behind a transient reactance Xd' or a sub-transient reactance Xd". This Thevenin equivalent machine model is the simplest machine model which is used in SCR and ESCR system analysis. Here we compare this simple model with the detailed machine model where the machine is modelled using Park's equations while the machine's field voltage is kept constant. The detailed machine model contains internal electro-mechanical machine dynamics but excludes exciter dynamics. One question which arises here is which reactance (Xd' or Xd") is more appropriate for representing the machine for steady state voltage stability analysis.

The most accurate model is the detailed machine model including exciter dynamics with its time constants and field forcing limits. The model where machine and exciter as a dynamic voltage regulator are fully modelled gives the most complete and accurate picture about hvdc system behaviour. Let us compare the performance of the complete system model with the system performance where the machine is modelled as a voltage source behind the transient reactance Xd'. The voltage source is automatically adjusted to keep bus voltage at 1pu. This comparison should provide the answer to the suitability of a

voltage source behind a transient reactance type of machine representation.

One of the objectives of the thesis is to determine how the synchronous machine modelling affects critical ESCR. In order to do that, the following four models of the synchronous machine connected to an hvdc system are investigated.

2.4.1 Model 1

The synchronous machine is modelled as a fixed voltage source behind a (sub-) transient reactance.

In this test model, figure 2.4.1, the synchronous machine is replaced with a fixed field voltage behind its sub-transient reactance Xd" and transient reactance Xd'. In other words, in this simplest machine model the Thevenin equivalent of the synchronous machine is used, and other machine dynamics are neglected.

In the time domain analysis this system model contains dynamics of the dc system and its control while internal electro-mechanical dynamics of the synchronous machine and dynamics of the exciter are neglected.

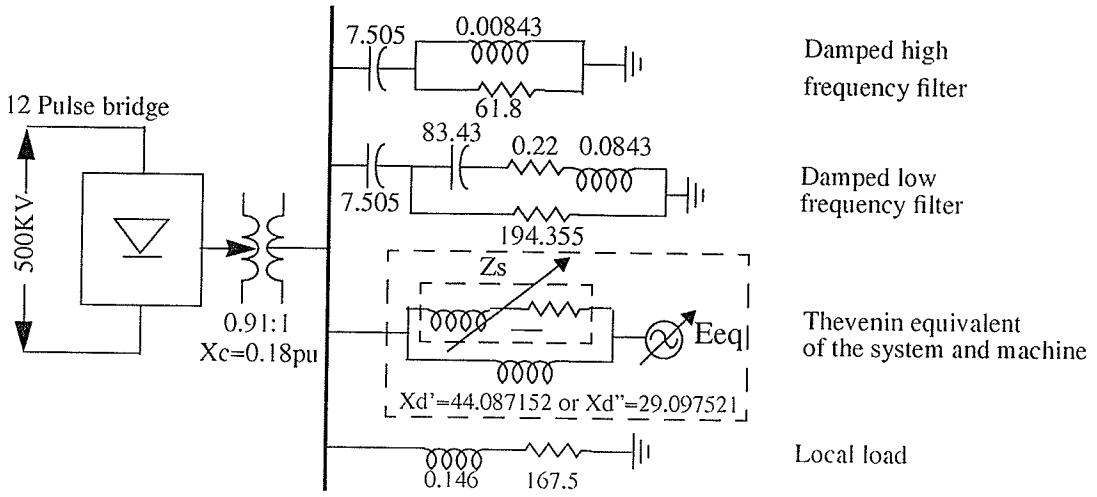

Figure 2.4.1: The study system model 1.

2.4.2 Model 2

Detailed Machine Model With Fixed Field Voltage (Without Exciter)

In order to investigate how critical ESCR is affected by simplifying the synchronous machine model to a fixed voltage behind a transient reactance, the machine is modelled in detail, and field voltage is kept constant. In this model, the synchronous machine is represented with Park's equations while the machine field voltage is kept constant during simulation as in figure 2.4.2. The fixed field voltage is manually adjusted to provide 1pu bus bar voltage at the inverter ac side. In the time domain analysis this system model contains dynamics of the dc control and internal electro-mechanical dynamics of the synchronous

machine while the dynamics of the exciter are neglected.

A synchronous machine of rating -165-+300Mvar is used for the time domain simulation. The machine parameters are given in Appendix III. At steady state, the filters supply 300Mvar, and the machine's field voltage is adjusted so that the synchronous compensator supplies the remaining 260Mvar to fully compensate for reactive power.

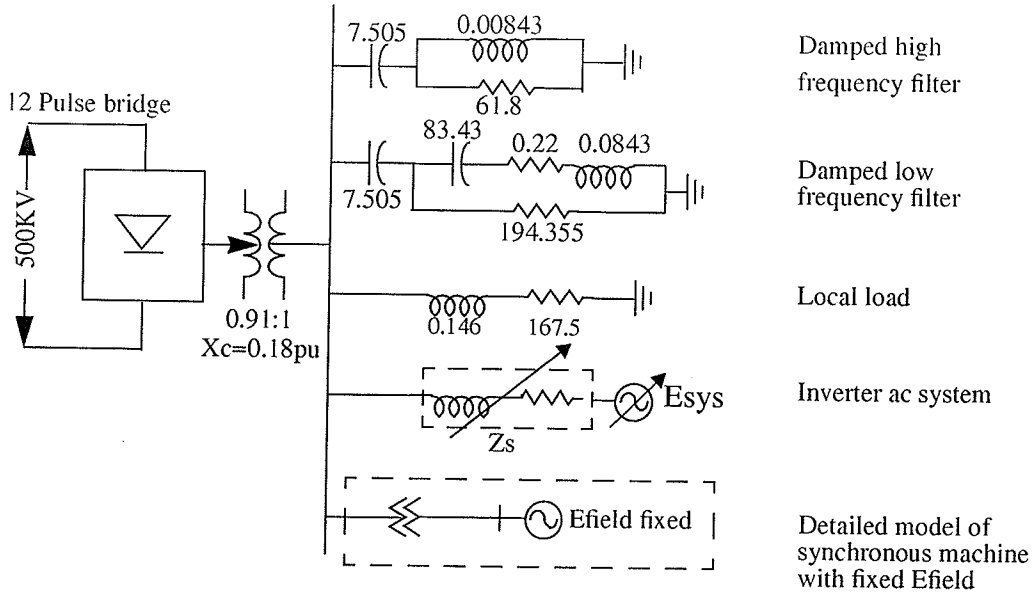

Figure 2.4.2: The study system model 2.

2.4.3 Model 3

Detailed Machine Model With Exciter

In this model the synchronous machine is represented with Park's equations where the machine field voltage is dynamically adjusted by a fast acting exciter to keep bus voltage at the inverter ac bus at 1pu as in Figure 2.4.3. In the time domain analysis this system model contains full system dynamics including dynamics of the dc control, internal electro-mechanical dynamics of the synchronous machine, and dynamics of the exciter as automatic voltage regulator.

Two different exciter models are used during the study. The gain Ka is changed in parametric studies in order to investigate the effect of the gain on the critical ESCR.

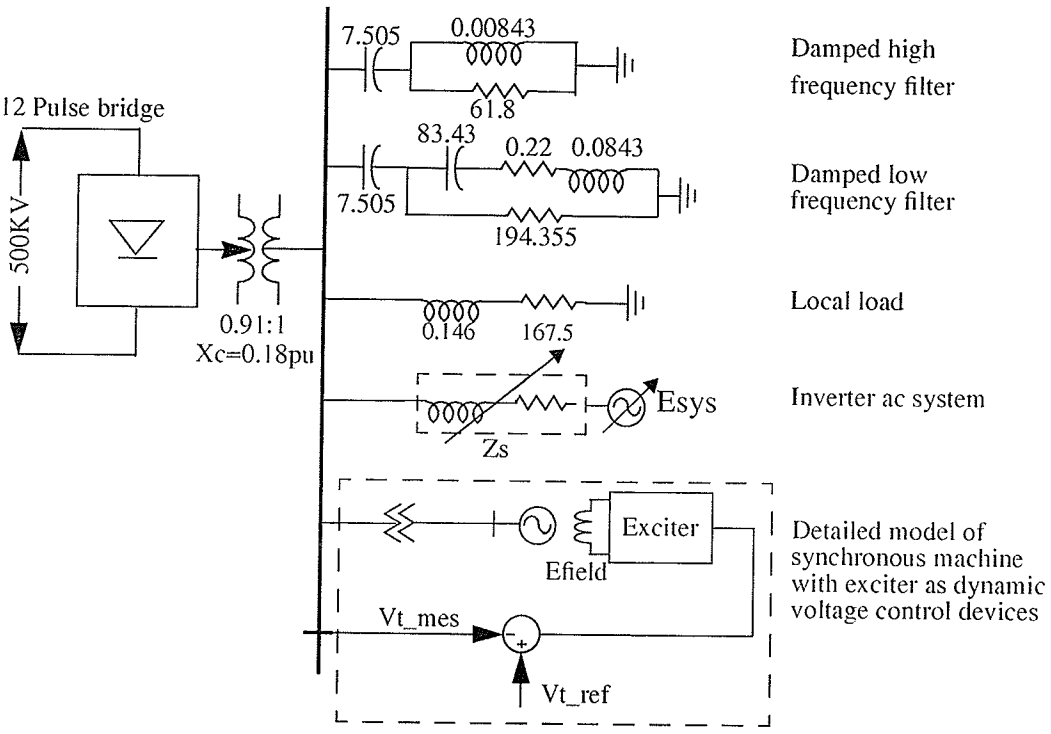

Figure 2.4.3: The study system model 3.

Figure 2.4.4 shows exciter model 1 which corresponds to an exciter with characteristics similar to a modern fast acting exciter such as the MIL manufactured exciter in the Manitoba Hydro System. Figure 2.4.5 shows the exciter model 2 which corresponds to the exciter with typical time constants and field forcing limits which corresponds to those available on modern day exciters. A 3% current droop based on full range of the compensator is used.

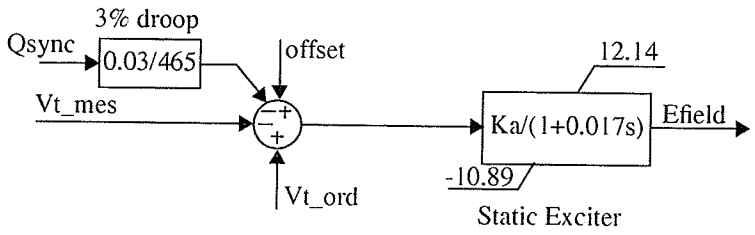

Figure 2.4.4: Exciter model 1.

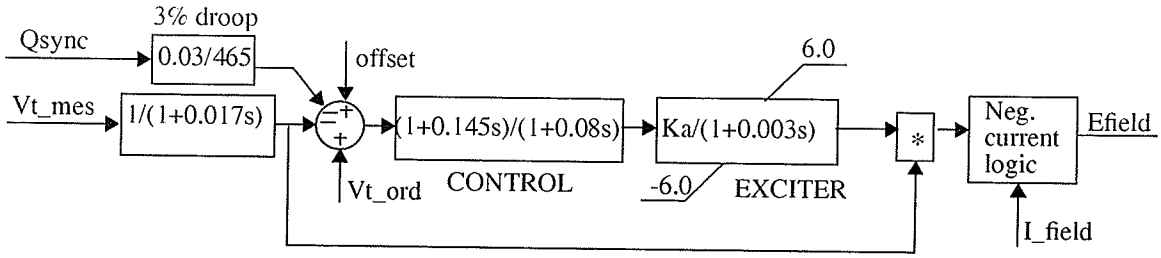

Figure 2.4.5: Exciter model 2.

2.4.4 Model 4

Idealised Synchronous Condenser (Exciter Model)

Model 4 is very similar to model 1. However, in this model the synchronous machine is modelled as a voltage dependant ac voltage source behind a transient reactance. The emf of the ac source Esys is automatically adjusted to keep bus voltage Vt at 1pu, figure 2.4.6. The PI regulator with the gain equal to 500 and integral time constant equal to 0.001s is

used to adjust Esys to keep bus voltage at 1pu. This model like model 1 does not contain machine and exciter dynamics. On the other hand, this model includes the feature of a fast automatic bus voltage regulator.

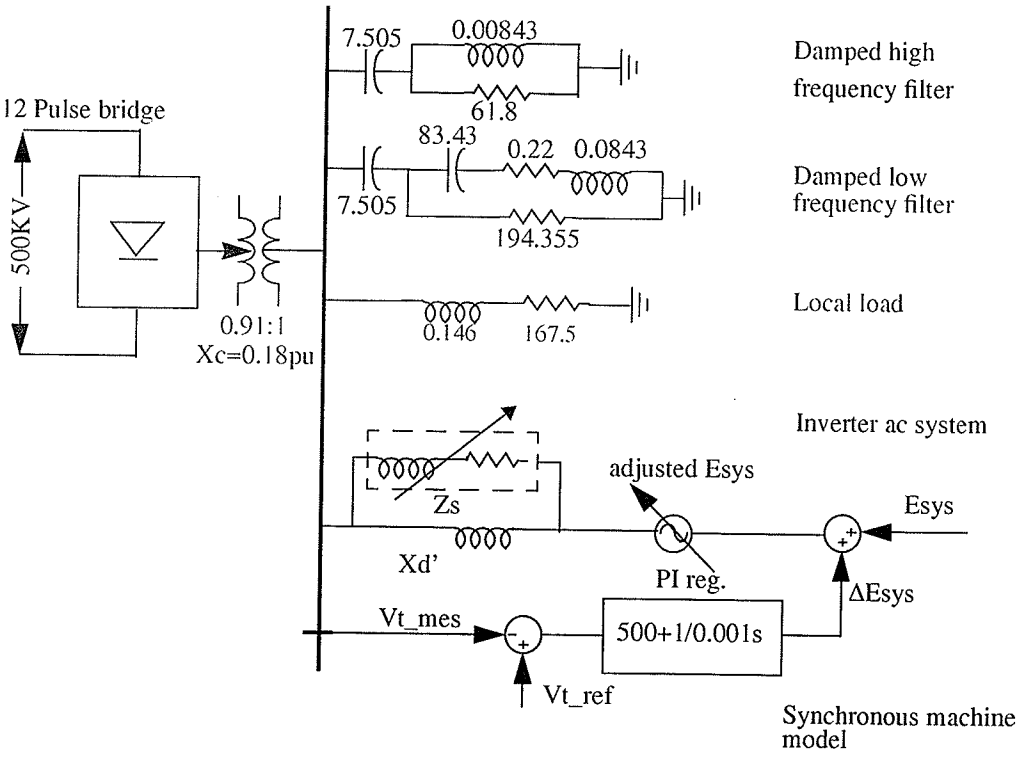

Figure 2.4.6: The study system model 4.

CHAPTER 3

STEADY STATE ANALYSIS

In this chapter the steady state analysis of the system under study is conducted. The methods of Control Sensitivity Index (CSI) and the Maximum Power Curve (MPC) analysis are applied in order to determine the critical effective short circuit ratio (ESCR) below which the system in power control mode becomes unstable. Theoretical MPC's based on the steady state equations, are calculated where the machine is replaced with a fixed voltage behind a sub-transient or a transient reactance. These curves are then compared with MPC's obtained by simulation to see how the theoretical MPC matches with the simulated MPC. After that, the simulated MPC of the system with detailed machine models described by Park's equations is compared with the theoretical MPC where the machine is replaced by its transient Xd' and sub-transient Xd" reactances, respectively.

3.1 Theoretical background

There is a maximum limit to the power that can be injected into the ac network at the point of connection of a dc system inverter. The relation between the "Maximum Available Power" (MAP) transmitted by the dc system and the ac system impedance, as seen from

the converter ac bus, has been expressed in terms of dc power versus dc current characteristics called "Maximum Power Curves (MPC)". The concept of "Maximum Power Curves" (MPC) for the hvdc system with rectifier in constant power control, and the inverter in constant extinction angle γ control is introduced by Ainsworth [2]. The peak of the MPC is the Maximum Available Power (MAP) or Peak Available Power (PAP) for the system with given system impedance Zs or ESCR.

The stability of the hvdc system in power control mode is determined by the MPC. The MPC tells how much dc current can be increased in order to increase the delivered dc power. However, the dc current increase causes the converter ac bus voltage to decrease due to increased reactive power demand of the converter. After some point, any further increase in the dc current results in a decrease in the bus voltage such that the dc power reduces. This causes the system in the constant power control mode to become unstable. In other words, any further dc current increase will reduce delivered dc power and render a feedback control system in power control to become unstable.

Recently, Nayak et al [4] developed the concept of "Control Sensitivity Index (CSI)" for the control stability analysis of hvdc convertors connected to a weak ac system. The "Control Sensitivity Index" is based on relating the sensitivity of the power system response to the output of the controller under consideration. It is defined for a particular control mode as the rate of change of the controlled (controller input) quantity with respect to the controlling quantity (controller output). This definition is illustrated in the figure 3.1.1. The CSI focuses directly on the controller input/output characteristics and indicates how the

controller affects the stability of the system. The indication of the instability onset for particular control mode is when the CSI for that control mode changes sign. The CSI concept for power control mode like the MPC concept gives the critical short circuit which indicates onset of instability of the system in power control mode.

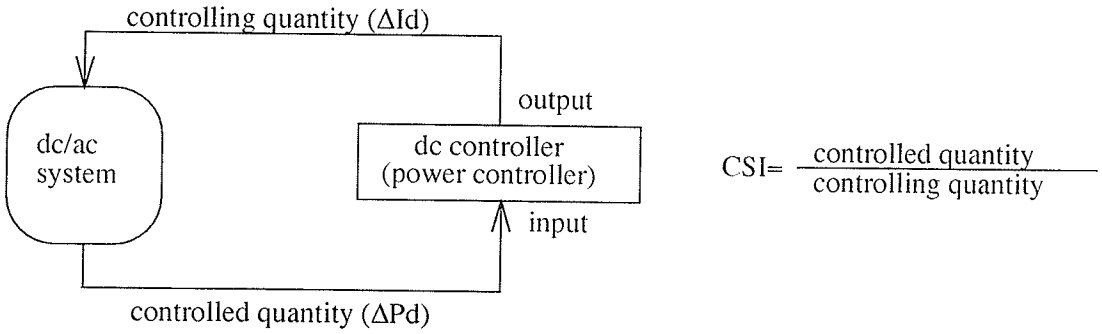

Figure 3.1.1: The definition of CSI.

3.2 Control Sensitivity Index (CSI) ΔPd/ΔId Analysis

The "Control Sensitivity Index (CSI)" indicates how the employed control modes affect the stability of the hvdc system. The CSI is based on analysing the sensitivity of the power system response to a change in an output quantity of the controller under consideration. If the hvdc system is in the constant power control mode the controller normally adjusts the current order so that the ordered power is maintained. The power controller is designed to increase current Id in order to increase ordered power Pd. However, if the hvdc system is connected to a sufficiently weak ac system the increase in dc current beyond a certain crit-

ical value can actually lead to decrease in dc power. In this case the power control will act in a direction to increase dc current to attempt to maintain the ordered power. However on the contrary, the power will reduce, and that will ultimately lead to system collapse. The CSI for the power control mode is defined as $\Delta Pd/\Delta Id$, and it is positive for normal system operation. If by reducing ESCR of the ac system the CSI i.e $\Delta Pd/\Delta Id$ becomes negative; it indicates that system has become unstable as then an attempt by the controller to increase power actually results in reduced power output. This causes a system collapse unless a control strategy other than power control (such as current control) is applied.

3.2.1 Control Sensitivity Index $\Delta Pd/\Delta Id$ Calculation

The CSI for the power control mode $\Delta Pd/\Delta Id$ calculation is based on the steady state equations. A straightforward implementation of the SCR concept results in a simple Thevenin equivalent that can absorb or supply real as well as reactive power. The SCR concept is based on the equivalent ac system impedance without any restriction for reactive and real power supply. This SCR concept is used in model 1 and model 4 (section 2.4) where the synchronous machine is modelled as a voltage source behind transient reactance. The steady state of such a modelled system is described by five steady state equations in complex form as in equations 3.1.

A synchronous machine on the other hand can only supply and absorb a reactive power in the steady state while it can not absorb or supply real power. This constraint on the real

power supply is demonstrated in model 2 and model 3 (section 2.4) where the detailed machine model is used. This is the most accurate model to use. If the synchronous machine is modelled so as to supply required reactive power in to the system while its real power is maintained at zero, the system is then described by six steady state equations in complex form as in equations 3.2.

Steady state equations for model 1:

$$Vt = \frac{\sqrt{2} \cdot Xc \cdot Id}{T \cdot (\cos(\gamma) + \cos(\alpha))}$$

$$\cos(\Phi) = \frac{(\cos(\alpha) - \cos(\gamma))}{2}$$

$$Vd = \frac{3 \cdot \sqrt{2}}{\pi} \cdot T \cdot Vt \cdot \cos(\gamma) - \frac{3}{\pi} \cdot Xc \cdot Id \qquad (3.1)$$

$$Pd = Id \cdot Vd$$

$$\overline{Esys} = Vt - \frac{\overline{Zs} \cdot jXd'}{\overline{Zs} + jXd'} \cdot \left(\frac{Pd}{Vt \cdot \cos(\Phi)} \cdot e^{j\Phi} - \frac{Vt}{\overline{Zf}} - \frac{Vt}{\overline{Zll}} \right)$$

Steady state equations for model 2:

$$Vt = \frac{\sqrt{2} \cdot Xc \cdot Id}{T \cdot (\cos(\gamma) + \cos(\alpha))}$$

$$\cos(\Phi) = \frac{(\cos(\alpha) - \cos(\gamma))}{2}$$

$$Vd = \frac{3 \cdot \sqrt{2}}{\pi} \cdot T \cdot Vt \cdot \cos(\gamma) - \frac{3}{\pi} \cdot Xc \cdot Id \qquad (3.2)$$

$$Pd = Id \cdot Vd$$

$$\overline{Esys} = Vt - \overline{Zs} \cdot \left(\frac{Pd}{Vt \cdot \cos(\Phi)} \cdot e^{j\Phi} - \frac{Vt}{\overline{Zf}} - \frac{Vt}{\overline{Zll}} + \frac{\overline{Qsyn}}{Vt} \right)$$

$$\overline{Qsyn} = \sqrt{3} \cdot Vt \cdot \frac{(Efield \cdot \cos(\delta) - Vt)}{jXd'}$$

where the variables are defined as:

Vt: Line to line voltage on the ac busbar

Xc: Commutation impedance

Id: Dc current

T: Transformer turn ratio

α: Firing angle of inverter

γ: Extinction angle

Φ: Power factor angle of convertor ac current

Vd: Dc voltage

Pd: Dc power

Zf: Impedance of ac filters

Zll: Impedance of local load

Esys: Source voltage of system equivalent

Zs: System impedance equivalent

Xd': Synchronous machine transient reactance

δ: Synchronous machine angle

Qsync: Reactive power supplied by synchronous machine

Efield: Synchronous machine field voltage

The control sensitivity index $\Delta Pd/\Delta Id$ has been computed by linearizing the equations 3.1 and 3.2 and using the numerical Newton-Raphson method [19] to find 1pu steady state solution for different Zs (ESCR). Figure 3.3.1 shows the algorithm for $\Delta Pd/\Delta Id$ calculation. If the synchronous machine is replaced only by a fixed voltage behind its transient Xd' or sub-transient reactance Xd" without any restriction for machine absorbed/supplied real power in steady state, the equations 3.1 are used for the $\Delta Pd/\Delta Id$ calculation. In that case during the steady state calculation it is assumed that:

- The inverter is in the constant extinction angle γ control mode.
- The rectifier is in the constant current Id control mode.
- The inverter is connected to the infinite ac bus with voltage Vt.

However, in the real synchronous machine the real power absorbed/supplied is zero in the steady state. If this assumption is made then the equation 3.2 are used for $\Delta Pd/\Delta Id$ calculation. Therefore, besides the above assumptions the additional assumptions have to be made:

- The machine supplies constant amount of required reactive power Qsync for 1pu steady

state.

- The real power of the synchronous machine is equal zero. Therefore, the angle δ of the synchronous machine is set to zero in the solution.

In other words, the variables γ, Id, and Vt are kept constant during steady state calculation for equations 3.1 while variables γ, Id, Vt, Qsync, and δ are kept constant for equations 3.2.

When the steady state for particular Zs has been reached, a sensitivity analysis is conducted where the equations are solved for a small change in the dc power ΔPd in response to a small change in the dc current ΔId. The solution gives the ratio ΔPd/ΔId for different Zs (ESCR). During ΔPd/ΔId calculation, the quantities |Esys| and γ do not change due to small dc current change, therefore Δ|Esys| and $\Delta\gamma$ are held at zero for the equations 3.1 while for the equations 3.2 the quantities Δ|Esys|, $\Delta\gamma$, $\Delta\delta$, and Δ|Efield| are held at zero.

The programs listing for power control mode CSI calculation are provided in Appendix-IV.

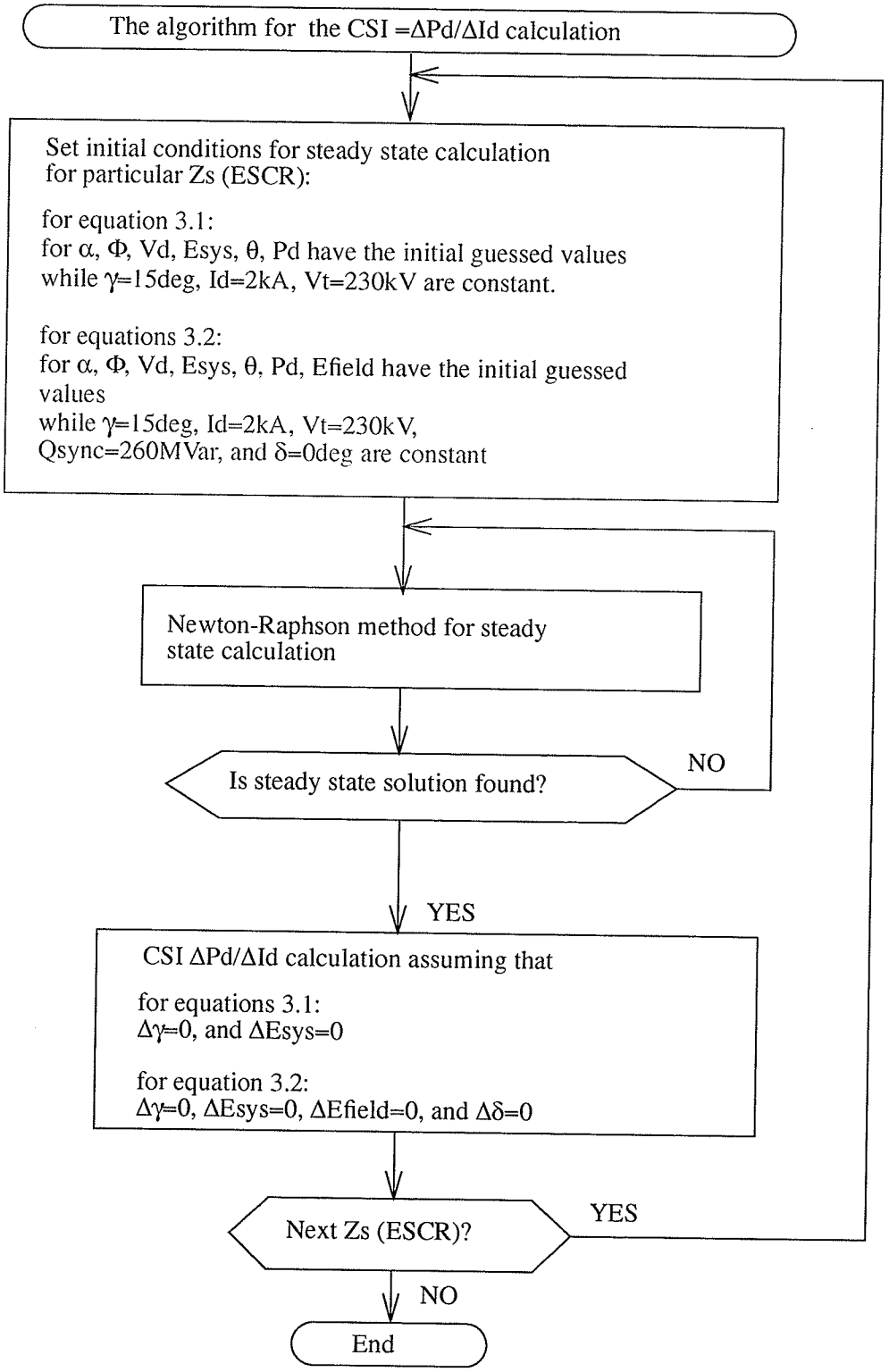

Figure 3.2.1: The algorithm for the CSI=ΔPd/ΔId calculation.

3.2.2 CSI Analysis Results

The results of the CSI analysis are shown in the figures 3.2.2 and 3.2.3. Figure 3.2.2 shows results for both sets of steady state equations. Depending of the steady state equations by which the system is described, the CSI analysis for the power control mode gives different critical ESCR. If the synchronous condenser is represented by a fixed voltage behind its transient reactance Xd', the critical ESCR is equal to 1.554. This is how the calculation is conventionally carried out. However, if the synchronous condenser is modelled by its transient reactance Xd', but its real power is kept at zero then critical ESCR is equal to 1.597.

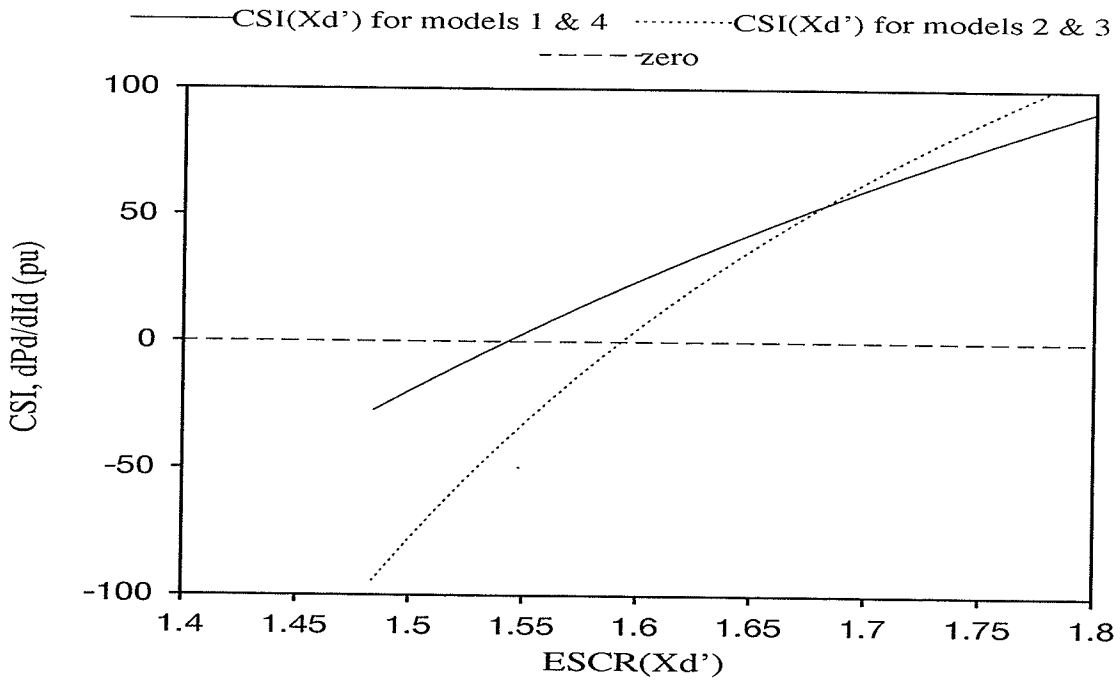

Figure 3.2.2: The CSI for power control mode if machine is modelled as transient reactance Xd'.

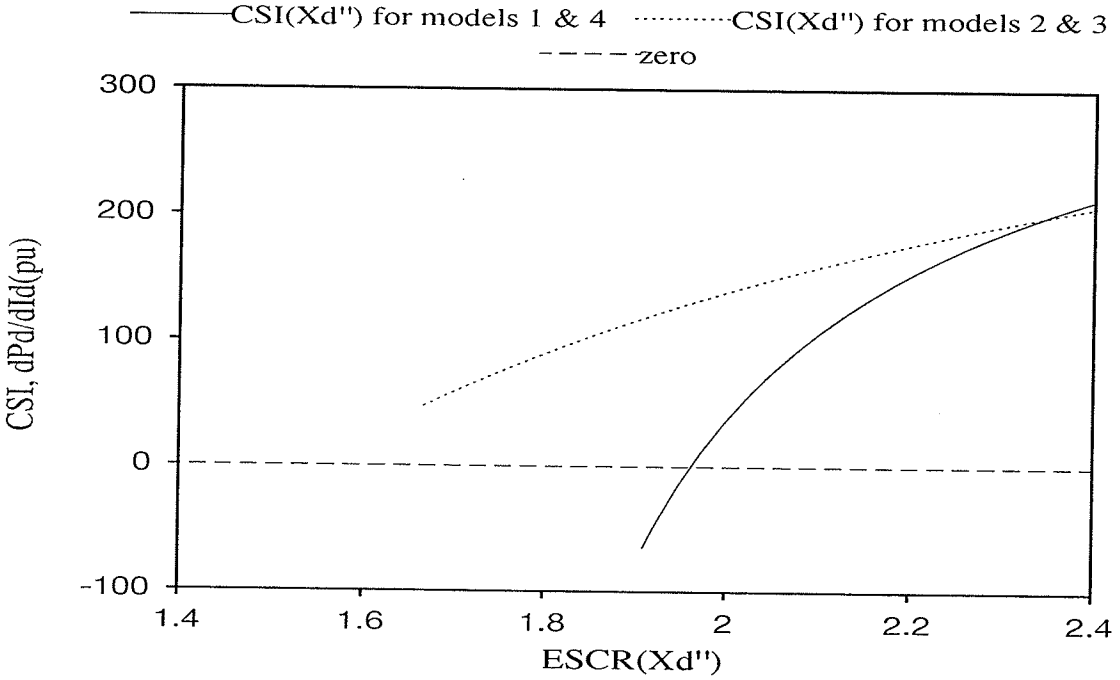

Figure 3.2.3: The CSI for power control mode if machine is modelled as the sub- transient reactance Xd".

Figure 3.2.3 shows CSI results if the synchronous machine is replaced by its sub-transient reactance Xd". With machine represented by Xd" an ESCR of 1.636 results even if the remote ac system is totally disconnected. Consequently, 1.636 is thus the lowest practically achievable ESCR (or 1.033 if Xd' is used instead Xd"). According to figure 3.2.3 it seems that critical ESCR is less than the smallest possible ESCR for model 1. That means that the synchronous machine represented by sub-transient reactance Xd" increases the strength of the ac system such that the system is always steady state stable in the power control mode. On the other hand, the CSI analysis for the model 2 (with additional constraint that machine's real power is equal to zero) gives the critical ESCR(Xd") equal to 1.965 or the corresponding ESCR(Xd') is equal to 1.355.

These results show that representing the machine as a mere fixed voltage behind reactance without any restriction for the machine's real power gives lower critical ESCRs'. This leads to the conclusion that representing the machine as a mere fixed voltage behind reactance gives too optimistic a value for the critical ESCR. This will later be proved in the time domain analysis, as well. Which machine model, whether one with transient Xd' or with sub-transient Xd" reactance is more appropriate for steady state system analysis will be resolved by the MAP and time domain analysis to follow.

3.3. Maximum Power Curve (MPC) Analysis

The "Maximum Power Curve (MPC)" shows the maximum power which can be injected into the ac system at the point of connection of a dc system inverter. For a given ac system strength (i.e. impedance Zs) and other parameters of the hvdc/ac system there will be a unique Pd versus Id characteristics or unique MPC.

Using steady state equations the MPC for the hvdc/ac system with different system impedance Zs (ESCR) are calculated. Those curves are referred further in the this thesis as the theoretical MPC. For an ac system with a given strength two MPC's are calculated. One MPC is calculated such that the synchronous machine is replaced by the transient reactance Xd' while in another MPC calculation the synchronous machine is replaced by the sub-transient reactance Xd".

The MPC's are also calculated by simulation using the EMTDC program. In order to do that, it is assumed that the rectifier is in current control mode and inverter in the γ control mode. Then, during simulation the dc current order is gradually increased from 0 to 1.2pu in the time range of 30 seconds to move the operating point in a quasi-steady manner. Finally, the dc power and the rms voltage at the inverter ac bus are measured and later plotted versus dc current.

In this section comparisons are made to address the following questions:

(i) How does an MPC characteristics calculated from theory agree with one from transient simulation with the impedance of a machine represented as a Thevenin equivalent?

(ii) How does the MPC calculated from theory agree with the simulation MPC that is calculated using a more detailed machine model described by Park's equations?

(iii) How does a theoretical MPC calculated assuming ideal bus voltage control agree with one from simulation where bus voltage is controlled by a fast acting exciter?

3.3.1 The Maximum Power Curve MPC Calculation

This section describes the MPC theoretical calculation using steady state equations. The steady state equations 3.1 are used for MPC calculation assuming some pre-defined starting condition. The dc current order is gradually increased, and dc power is measured. The algorithm for MPC calculation is shown in the figure 3.3.1. For any Zs (ESCR) for which the MPC is to be calculated the system Thevenin voltage Esys is set to provide the 1pu

steady state operating condition. This establishes the steady state condition. After that, the following assumption are made for MPC calculation:

- The inverter is in the constant extinction angle γ control mode.
- The rectifier is in the constant current Id control mode.

In other words, the variable γ, Esys, and Id equal to ordered current are kept constant in equations 3.1 during steady state MPC calculation.

In addition, we realized that in a real synchronous condenser the real power absorbed/supplied is zero in steady state. When we make this assumption a different set of steady state equations must be used as in equations 3.2, and additional assumptions have to be made as follows:

- The machine field voltage Efield doesn't change with change in current order.
- The real power of the synchronous machine is equal zero. Therefore, the angle δ of the synchronous machine is set to be equal to zero.

In other words, the variables γ, Esys, Efield, δ, and Id are kept constant for equations 3.2 during steady state MPC calculation.

The algorithm for MPC calculation is shown in figure 3.3.1, and the programs listing for the MAP calculation are provided in Appendix-V.

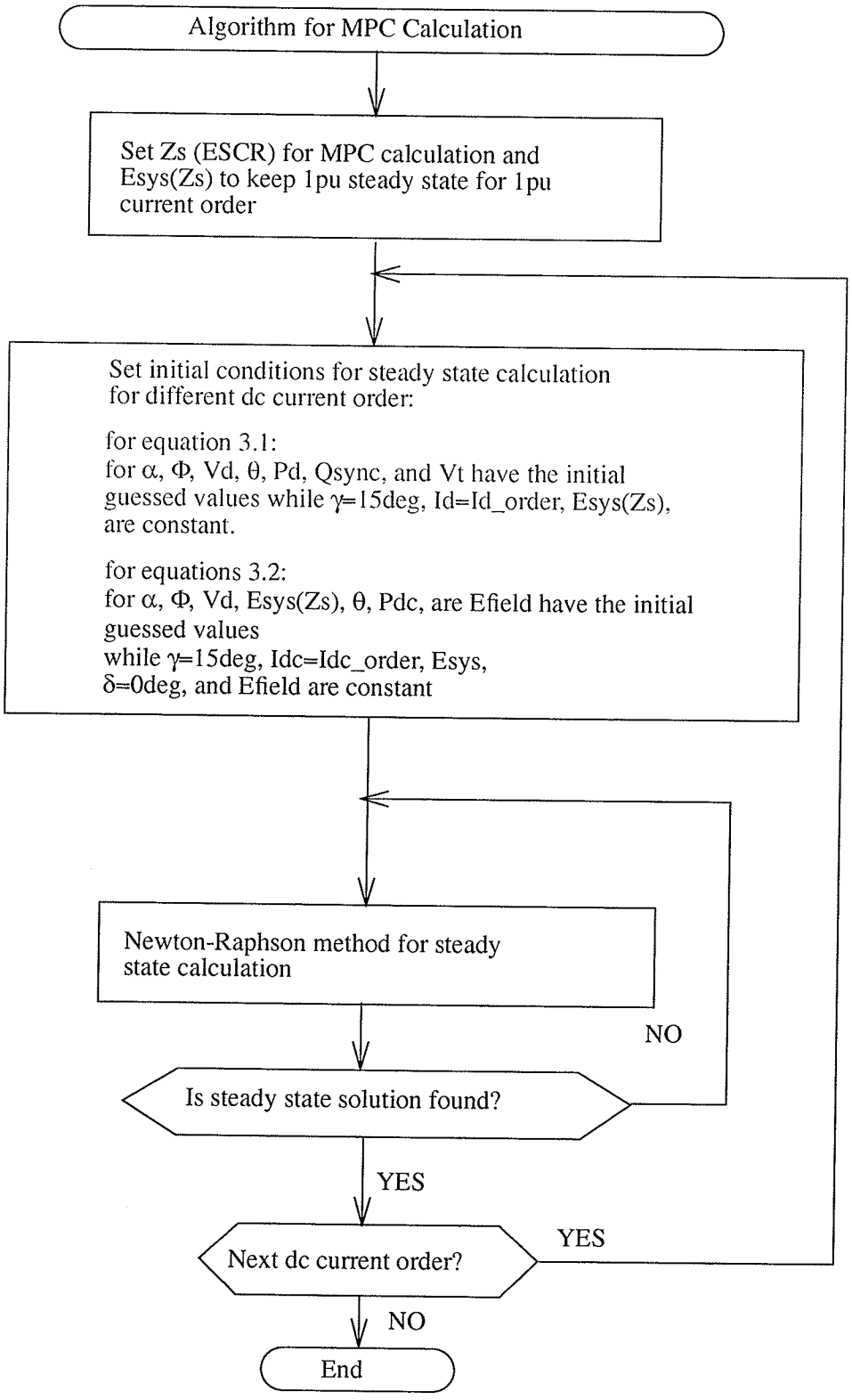

Figure 3.3.1: The algorithm for the MPC calculation.

3.3.2 The MPC Analysis Results

The results of the MPC analysis are now shown. Figure 3.3.2 shows the theoretical MPC's and MPC's obtained by simulation using model 1 where machine is modelled as a fixed voltage behind the transient reactance. For the ESCR(Xd') higher than or equal to 1.554, the system MPC(Xd') calculated with transient reactance Xd' passes through the 1pu steady state system operating point. However, for reduced ESCR equal to 1.534 the system maximum available power MAP is less than 1pu which results in the system being unable to deliver 1pu dc power into the ac system. Because stability of the power control mode is the subject of investigation, the incapability of the system to reach 1pu steady state is designated as unstable for the power control mode. From the figure 3.3.1, it is shown very good agreement between theoretical MPC's and simulation MPC's calculated using EMTDC.

Figure 3.3.3 shows theoretical MPC and simulation MPC obtained using model 2 where internal machine dynamics are fully modelled. The theoretical calculations have been carried out using steady state equations 3.2. It can be noticed that the simulation MPC for lower dc current order matches quite well with the theoretical MPC where the machine is replaced by the sub-transient reactance Xd". However, for the higher dc current order simulation MPC matches better with theoretical MPC where the machine is replaced by the transient reactance Xd'. It is noticed that for dc current order approximately equal to 1.0pu MPC starts to oscillate with increasing oscillations. Those oscillation can be attributed to the dynamics of the synchronous machine. Indeed, figure 3.3.4 shows the same curve

drawn if a machine's inertia is (artificially) increased from 2.15pu to 10pu. The oscillations are then not evident. For ESCR less than or equal to 1.574 the MAP is less then 1pu which means that ordered power can not be delivered in to the system resulting in the instability of the power control mode.

Similarly, Figure 3.3.5 shows the effects of including or not including the Psync=0 (machine's real power equal to zero) constraint. Surprisingly, the curves (with transient reactance Xd') with and without the constraint seem to be quite close to the simulated curve. However, as reported in section 3.2.2, the critical ESCR (i.e. ESCR at which $\Delta Pd/\Delta Id$ changes sign) is more accurately given with the constraint included.

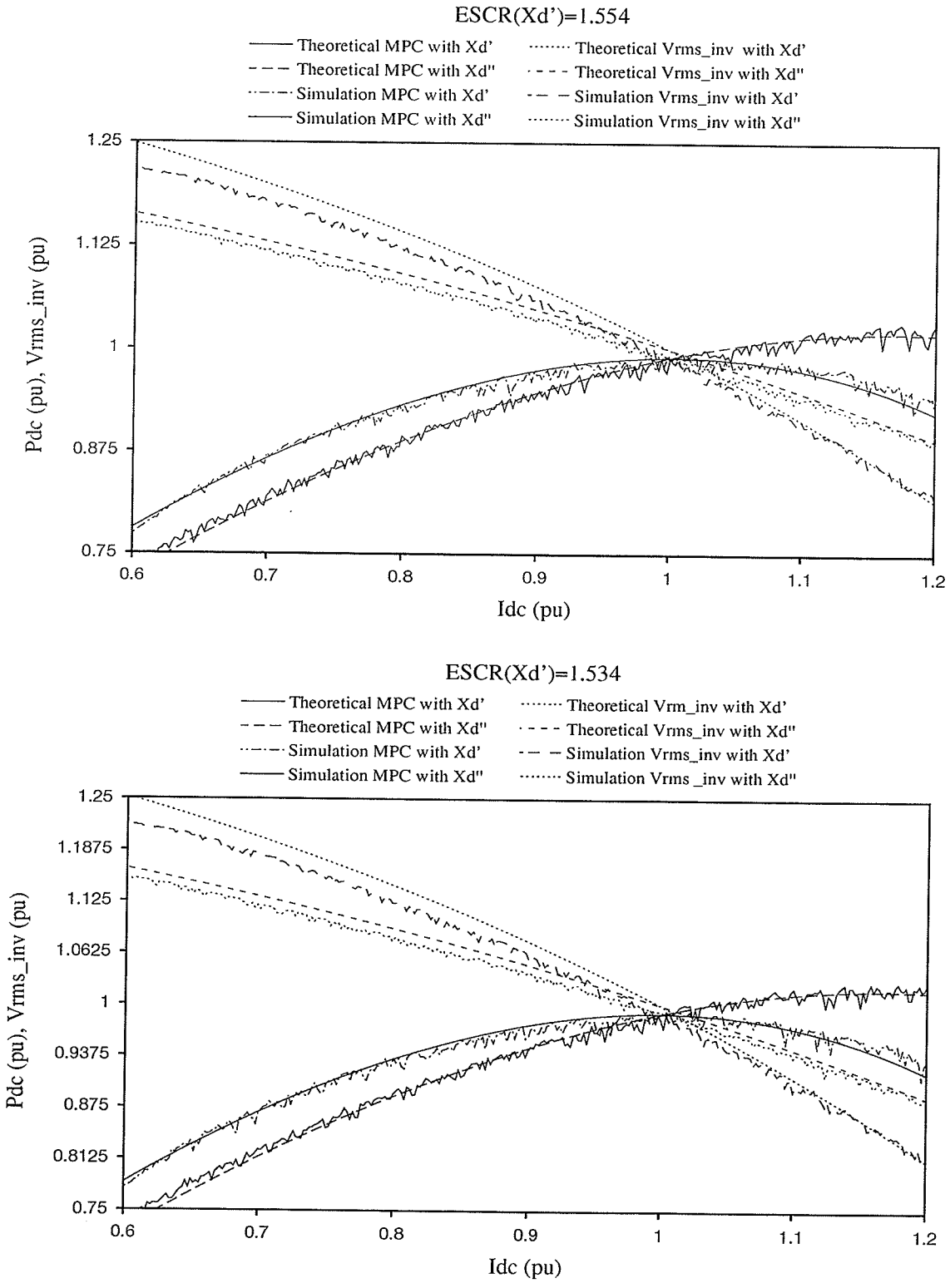

Fig. 3.3.2: The theoretical and simulation MPC for the system model 1.

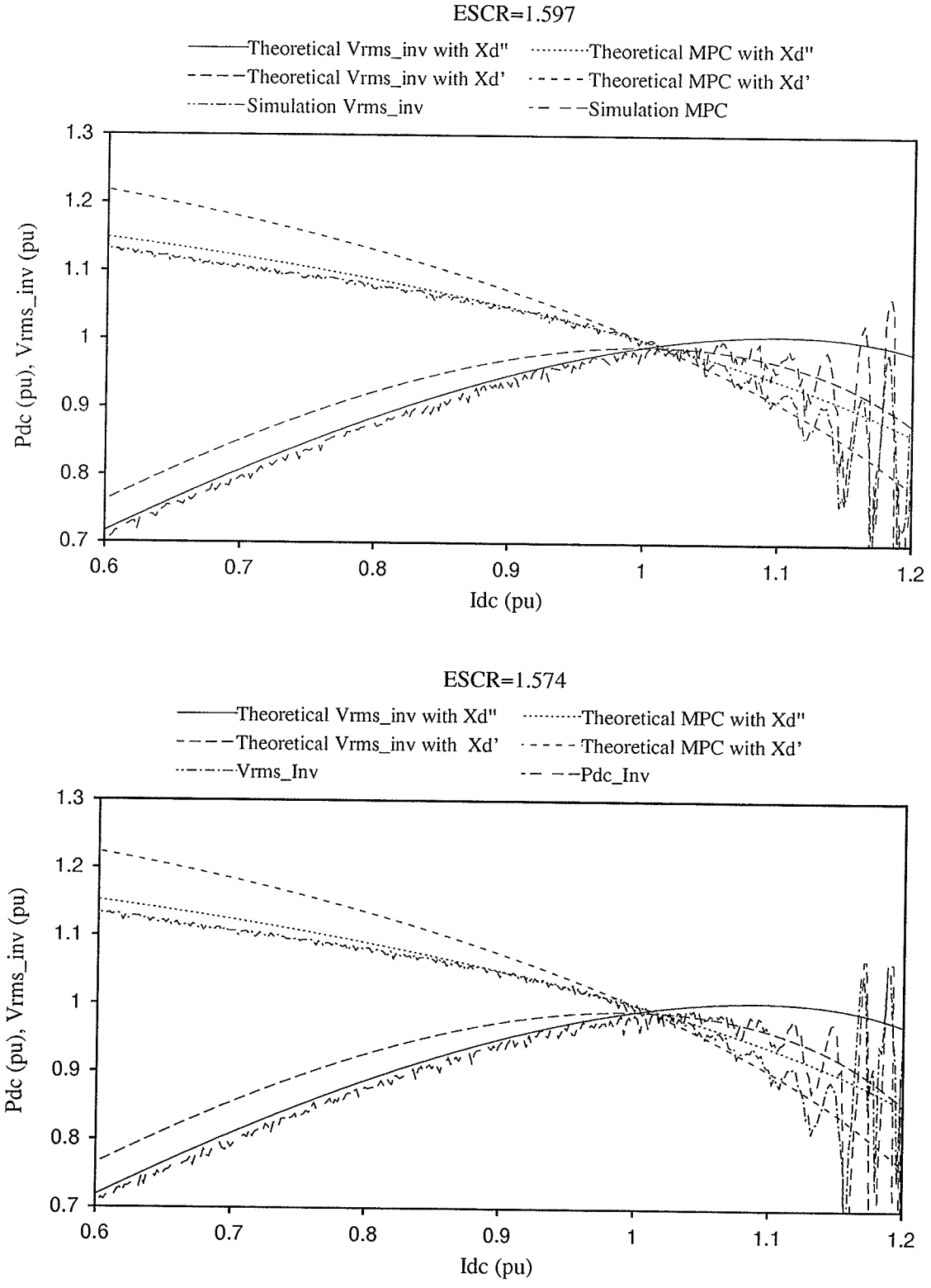

Fig. 3.3.3: The theoretical and simulation MPC for the system model 2.

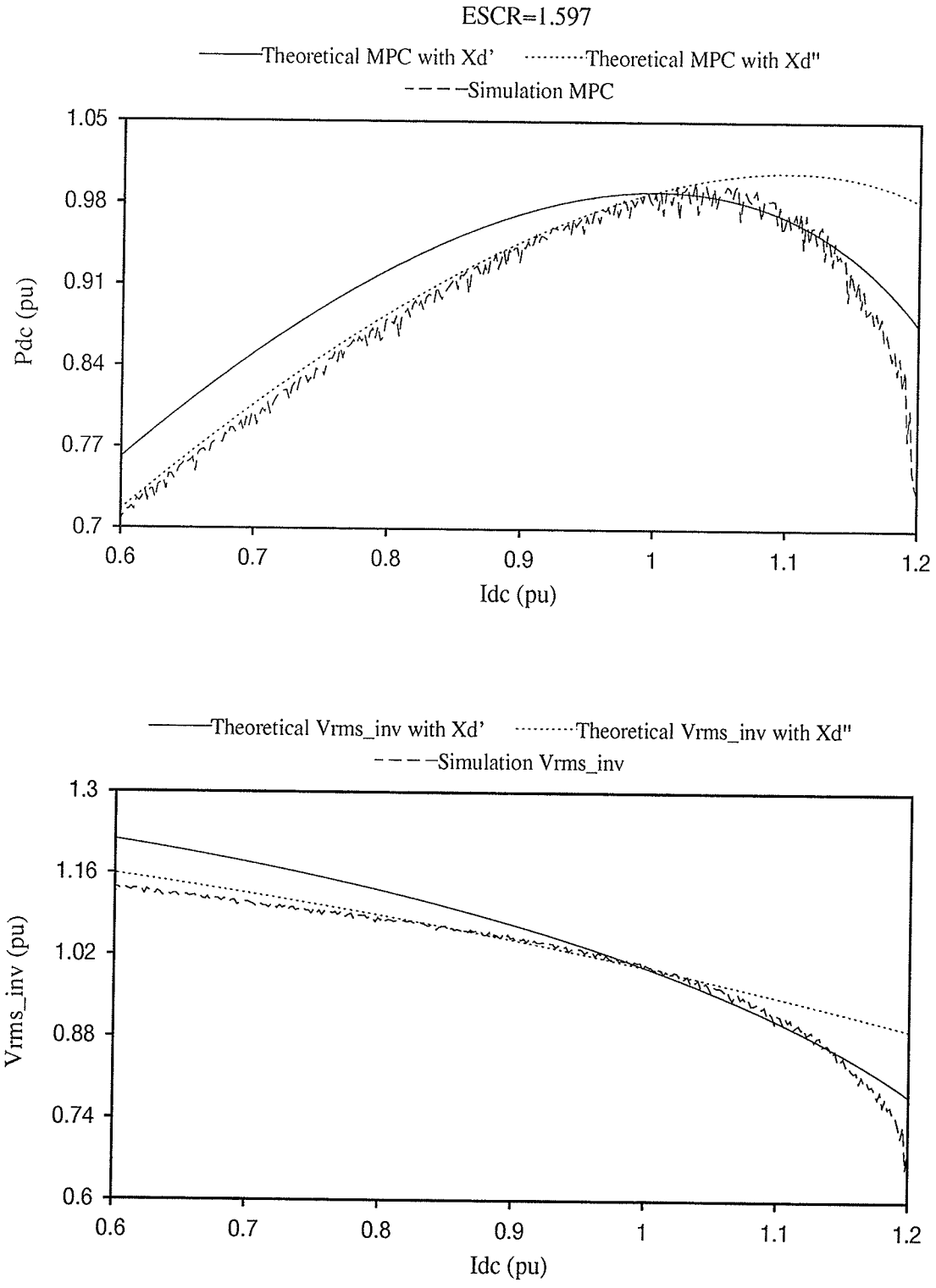

Fig. 3.3.4: The theoretical and simulation MPC for the system model 2. with a larger machine's inertia (H=10pu).

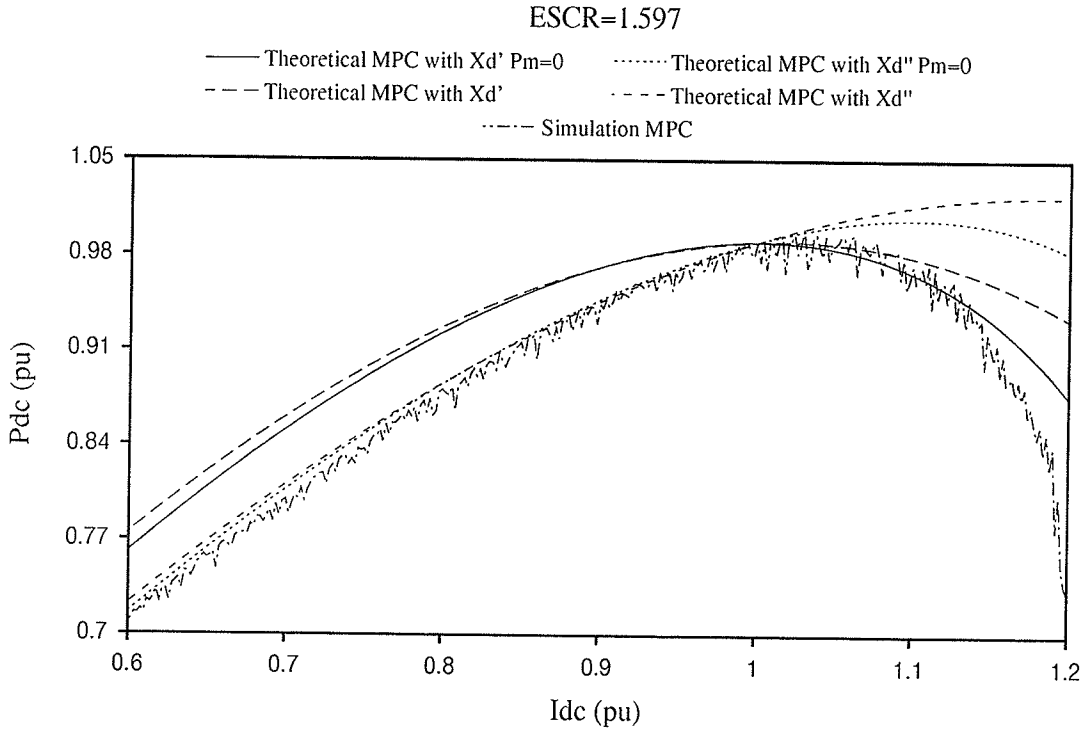

Figure 3.3.5: The theoretical MPC's comparison with the simulation MPC for the system model 2

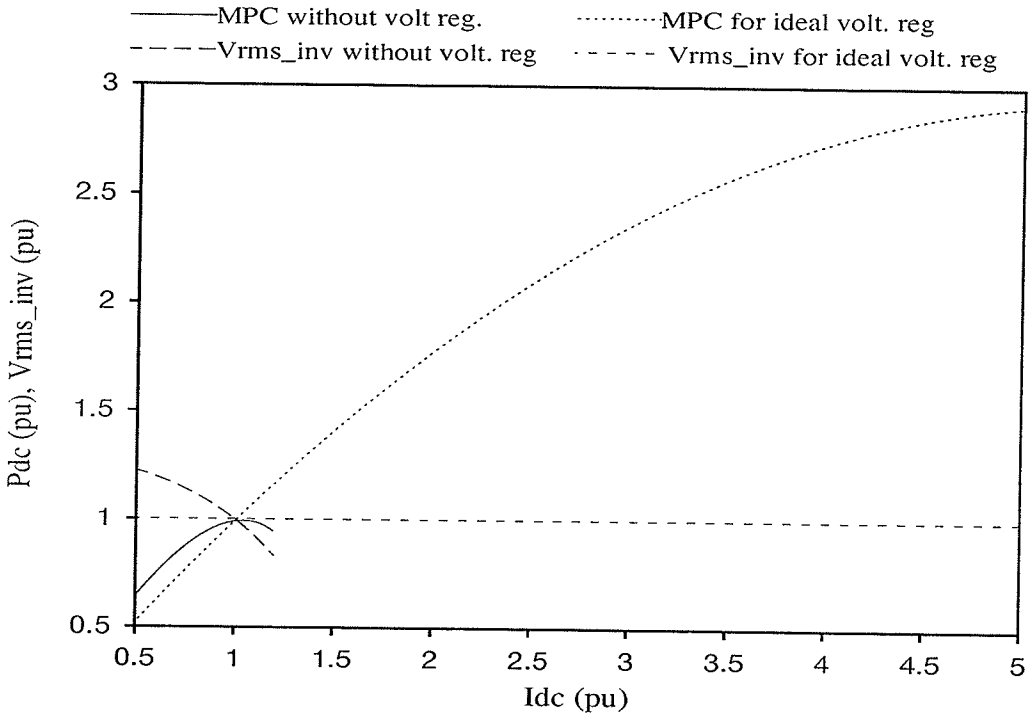

Figure 3.3.6: Theoretical MPC for the ideal voltage control.

The power/voltage instability limit could be greatly improved if it is possible to ideally control the bus voltage. However, in real systems the synchronous machine and the exciter which controls bus voltage contain inherent dynamics, limits, and delays which may not allow this stability improvement to be achieved.

The MPC shown in figure 3.3.6 is calculated using equation 3.2 and assuming that the inverter side ac voltage is ideally controlled. The MPC indicates that the weak ac system does not show signs of the power instability. In fact, according to the MPC from the figure 3.3.6 in the dc current range of our interest from 0.6 to 1.2pu, it can be approximated that dc power increases proportionally to the dc current. During the MPC calculation for this

case, the bus voltage Vt, the extinction angle γ, synchronous machine angle δ equal to zero, and system voltage magnitude |Esys| are kept constant. This MPC is dependant neither on the system impedance Zs nor on the synchronous machine presentation i.e whether it is represented by transient Xd' or sub-transient Xd" reactance. This is to be expected with a device that maintains the bus voltage ideally at 1pu. The parabolic shape of the curve is thus only due to the converter transformer reactance Xc.

Figure 3.3.7 shows simulation MPC's for model 3, where synchronous machine and exciter are fully modelled for the ESCRs equal to 1.711 and 1.746 respectively. It can be seen that inverter side ac voltage can not be "ideally" kept constant as the current order increases. For the ESCR equal to 1.711 the MPC starts to deviate increasingly from its theoretical value, for the dc current order close to 0.9pu, while for the ESCR equal to 1.746 those deviations can be noticed after 1.0pu dc current order. Due to these deviations, for the ESCR equal to 1.711, it can be expected that the system modelled as model 3 will be steady state unstable (verified latter in chapter 4). Even though the theory tells us that the voltage control makes that weak ac system behave as a strong one it is obvious than that in the real system the machine and exciters speed and dynamics significantly affects critical ESCR.

The simulation MPC of the model 4 where the machine is modelled as a dynamically adjusted voltage source to keep bus voltage at 1pu behind a transient reactance is shown in figure 3.3.8. It is then compared with simulation and theoretical MPC for model 3 where machine and exciter are fully modelled to show difference between ideal voltage control

and exciter voltage control which gives a more realistic picture. It can be seen that MPC for model 4 follows the theoretical MPC quite accurately up to 1.12pu current order when the lower limit at the rectifier controller is reached. On the other hand, the simulation MPC for model 3 shows significant oscillations for current order higher then 0.9pu. This ultimately leads to voltage collapse for current order close to 1.11pu. Those oscillations are due to electro-mechanical dynamics of the synchronous machine. Indeed, if the machine inertia is (artificially) increased from 2.15pu to 10pu, the oscillations are not evident as shown in Figure 3.3.9. However, even though the system response is not oscillatory the bus voltage will collapse for same current order close to 1.11pu.

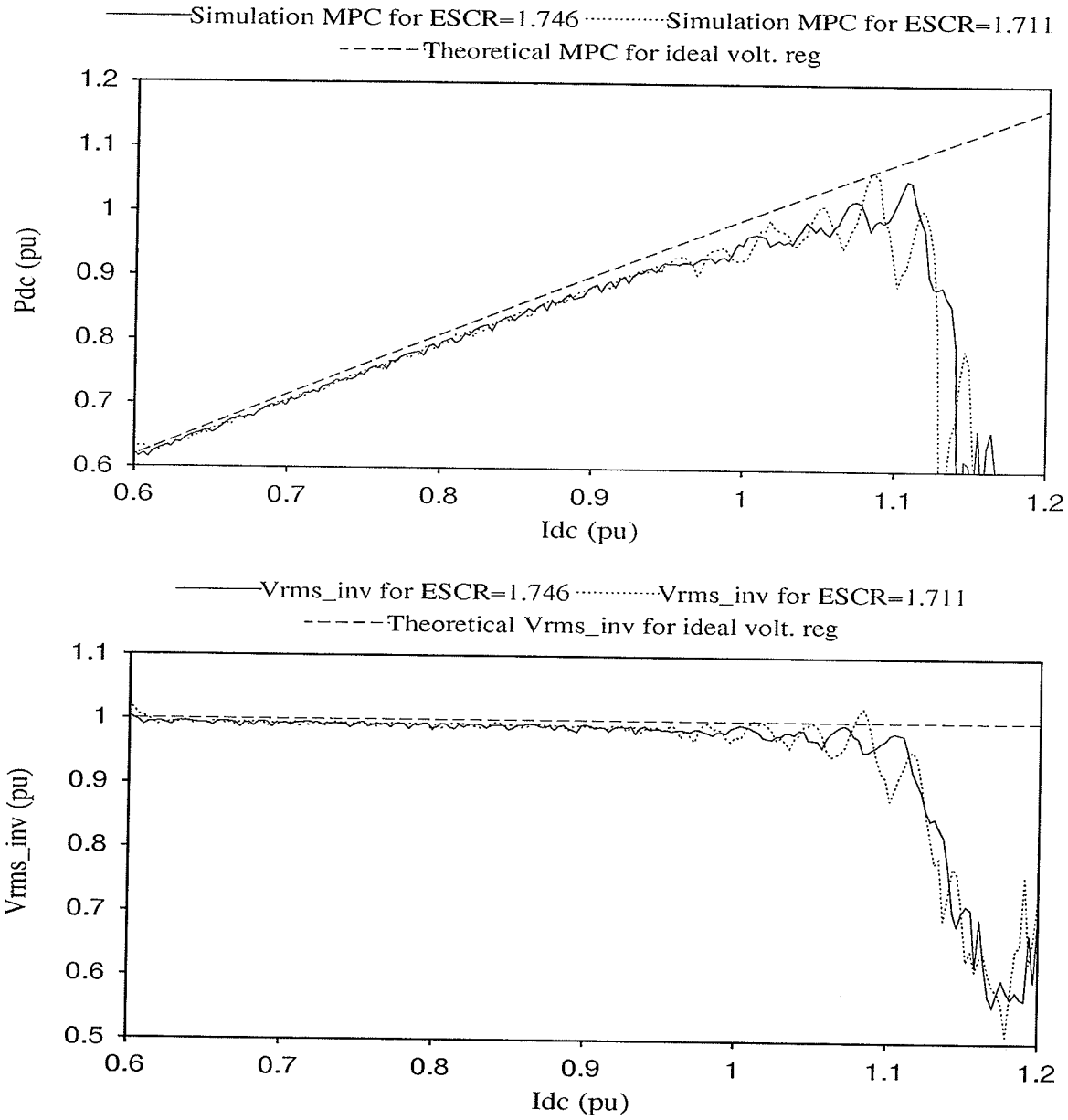

Figure 3.3.7: Theoretical and simulation MPC for system model 3.

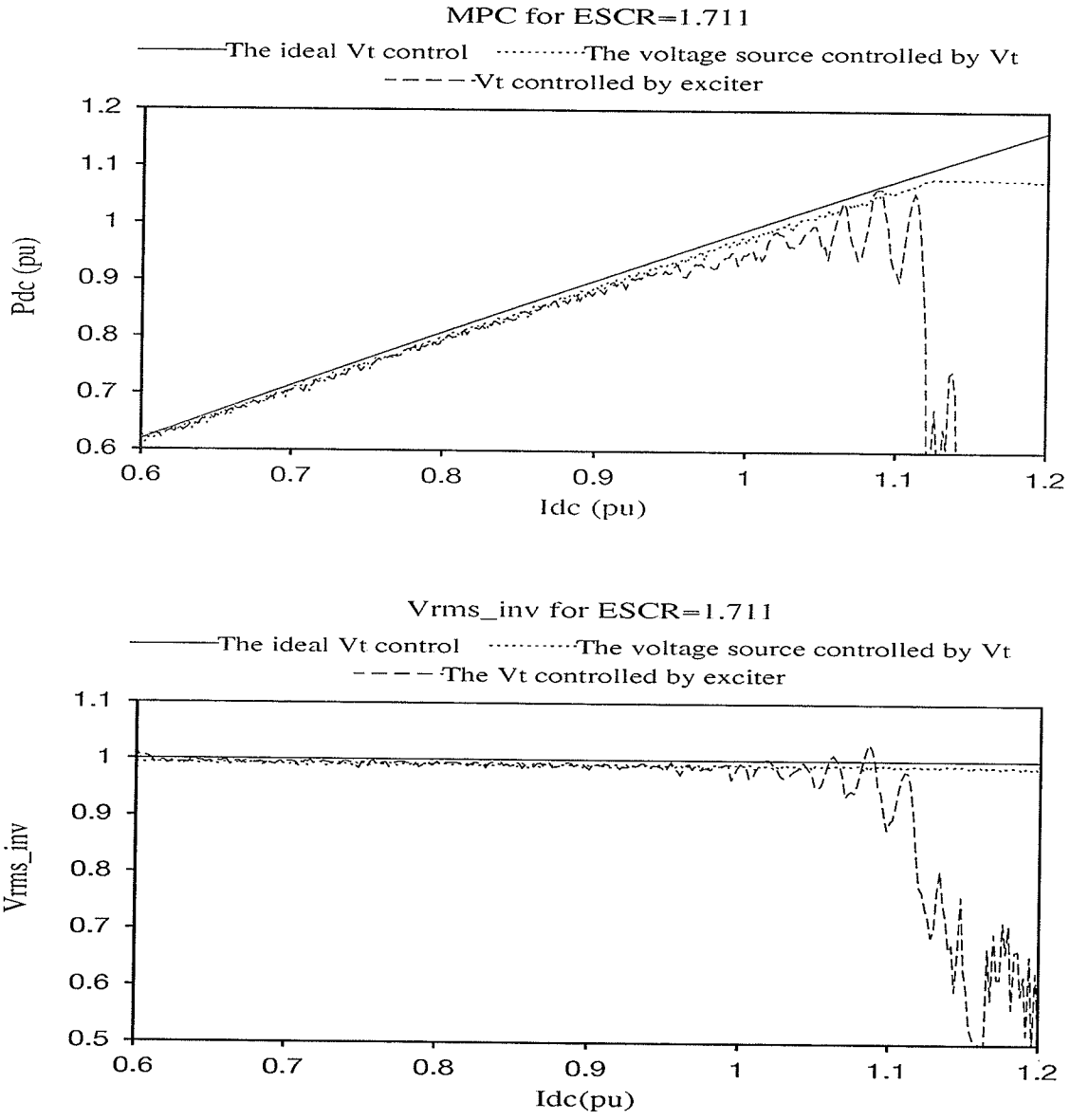

Figure 3.3.8: Theoretical and simulation MPC for the system model 3 and the system model 4.

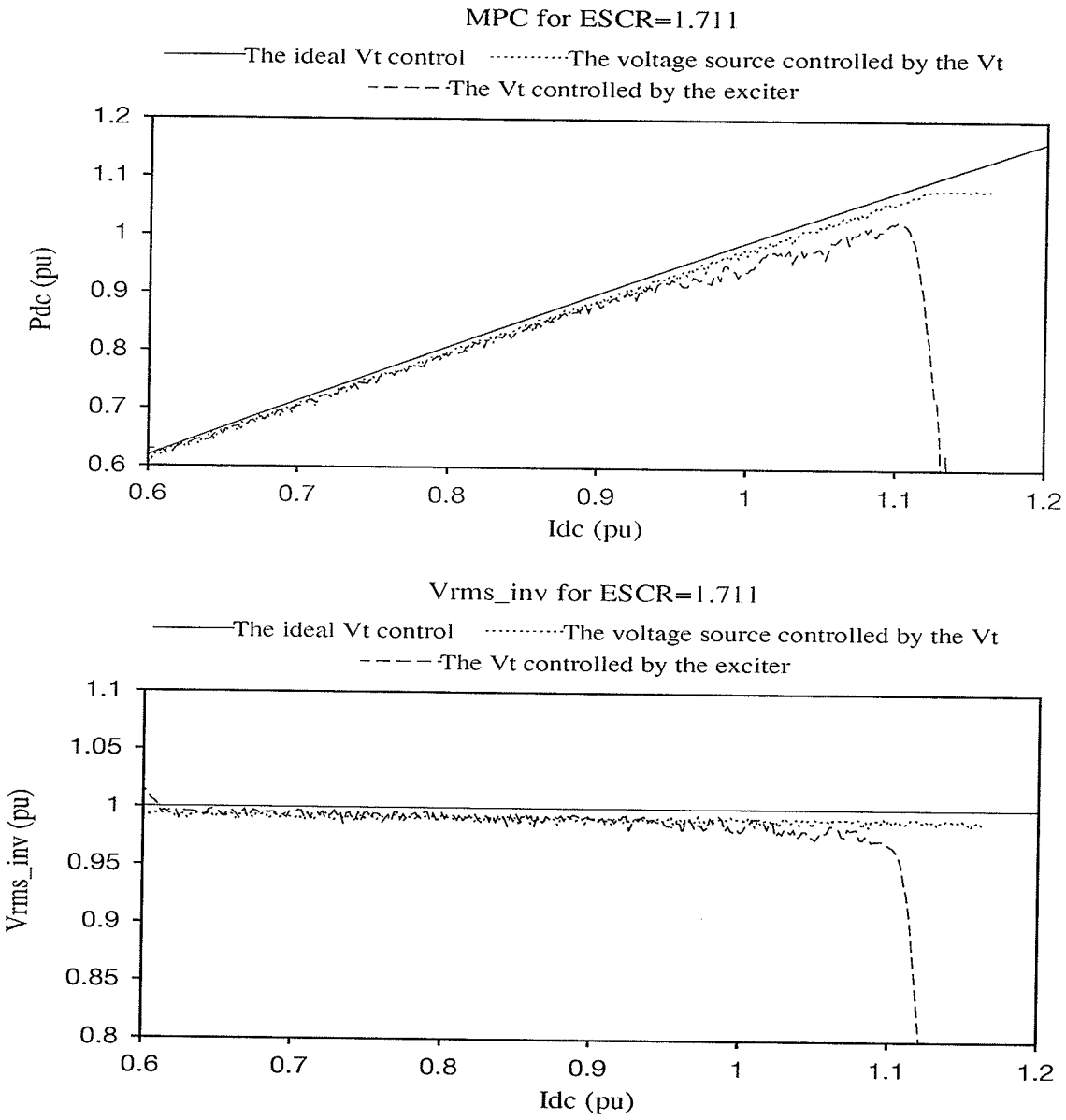

Figure 3.3.9: Theoretical and simulation MPC for the system model 4 and the system model 3 with larger machine's inertia (H=10pu).

3.4 Summary

Table 1 summarises the results of the CSI and MAP analysis. It is shown that the theoretical critical ESCR based on the CSI and the MPC calculation depends on the type of model used. If the synchronous machine is modelled as a fixed voltage behind the transient reactance Xd' (equations 3.1) the calculated steady state critical ESCR(Xd') is equal to 1.554. If it is supposed more realistically, that the machine supplies reactive power in to the system while its real power is equal to zero (equations 3.2) then the calculated critical ESCR(Xd') is higher and equal to 1.597.

Table 1: The critical ESCRs' as result of the CSI and MAP analysis

critical ESCR(Xd')	CSI analysis Theoretical	MAP analysis Theoretical	MAP analysis Simulation
with Xd'	1.554	1.554	1.554
Model 1 (Psync≠0)	stable for all ESCR	stable for all ESCR	stable for all ESCR
with Xd"			
with Xd'	1.597	1.597	1.597
Model 2 (Psync=0)	1.355 or ESCR(Xd")=1.965	1.355	
with Xd"			
Model 3	stable for all ESCR (voltage control dynamic is not included in theoretical calculation)	stable for all ESCR	1.746
Model 4	stable for all ESCR (voltage control dynamic is not included in theoretical calculation)	stable for all ESCR	stable for all ESCR

If the synchronous machine is replaced by a fixed voltage source behind the sub-transient Xd" reactance in equations 3.1, the system is steady state stable for every ESCR. This means that even if the ac system equivalent is completely disconnected, the system is stable at rated voltage and current. In other words, the machine represented by a fixed voltage behind the sub-transient reactance increases ac system strength to such an extent that the system does not ever experience power instability. However in the more realistic case, assuming that machine real power is zero in the steady state as in equations 3.2, and the machine is replaced by sub-transient reactance Xd", the steady state critical ESCR(Xd") is equal to 1.965 if the sub-transient reactance Xd" is used for the ESCR(Xd") calculation. If instead of the sub-transient reactance the transient reactance is used for ESCR(Xd') calculation then the corresponding critical ESCR(Xd') is equal to 1.355.

Comparing theoretical MPC and simulation MPC for model 2 it is obvious that for lower current order the simulated MPC follows theoretical MPC(Xd") where the machine is replaced by its sub-transient reactance Xd". However, for higher current order than 1pu the simulation MPC follows theoretical MPC(Xd') where the machine is replaced by its transient reactance Xd'. This means that instability will occur for higher ESCR than theoretical critical ESCR calculated by using machine model with the sub-transient reactance Xd". This leads to the conclusion that transient reactance Xd' is more appropriate for the ESCR analysis if a steady state critical ESCR has to be determined for the weak ac system.

Very good agreement results between theoretical MPC for ideal terminal voltage control

and simulation MPC for the corresponding model 4, but in model 4 machine and exciter dynamics are neglected while exciter voltage regulating capability is maintained. However, if machine and exciter dynamics are included like in model 3, the simulation MPC shows oscillatory erratic deviations from the theoretical MPC for higher current order. This is due to the internal machine's dynamics. If a machine's inertia is increased the system oscillatory response can be avoided.

CHAPTER 4

TIME DOMAIN ANALYSIS

In this chapter the results of time domain transient analysis of the study system are presented. The analysis is conducted by using the simulation transient package PSCAD/ EMTDC. The aim is to find out how meaningful the critical ESCR calculation is for an operating dc system. For example, the system may be stable at a given operating point considering only the steady state operating condition. However, if a fault is applied and removed, when in this condition, the system may never recover. Thus we wish to determine how applicable the steady state analysis is for determining critical ESCR values for an actual system.

4.1. Objective

The objective of the time domain simulation is to find critical ESCR's for the 1pu steady state and also for one phase, and three phase fault recovery. If initially the system can not be brought up to the 1pu steady state by gradually increasing the power order, steady state instability is present. The lowest ESCR for which the system is still stable is called the steady state critical ESCR. When 1pu steady state is reached an one phase fault is applied,

and after 100ms the fault is cleared. If the system can not attain 1pu steady state again, then we say that "one phase fault instability" has occurred. Similarly, if the system can not recover after the three phase fault is cleared, we say that "three phase fault instability" has occurred. The lowest ESCR for which the system can still recover from one and three phase fault is called one and three phase fault critical ESCR, respectively. An important question is how does this one or three phase critical ESCR compare with earlier 'steady state' critical ESCR. During a fault recovery simulations, the dc system inherent ability to recover from the faults is investigate. In other words, none of the fault clearing strategies are applied. The critical ESCR's presented in this chapter for the fault recovery reflects the system ability to recover from fault without any additional mechanism for the faults clearing.

4.2. Model 1 Time Domain Simulation Results

The purpose of model 1 is to verify the theoretical results obtained in the CSI and the MPC analysis (chapter 3). In this model the synchronous machine is represented by a fixed voltage source behind the transient Xd' and sub-transient reactance Xd" (section 2.4.1). The system with such a simplified machine model is then simulated.

The simulations are conducted in the following way. The ESCR is reduced at the inverter end by increasing Zs while the synchronous machine's reactance is kept constant. For each ESCR the Thevenin equivalent ac voltage is calculated using steady state equation

3.1 to keep the terminal voltage at 1pu. Two cases are investigated. In the first case the synchronous machine is replaced with a fixed voltage behind the transient Xd' reactance, and in the second case machine is replaced by the sub-transient Xd" reactance.

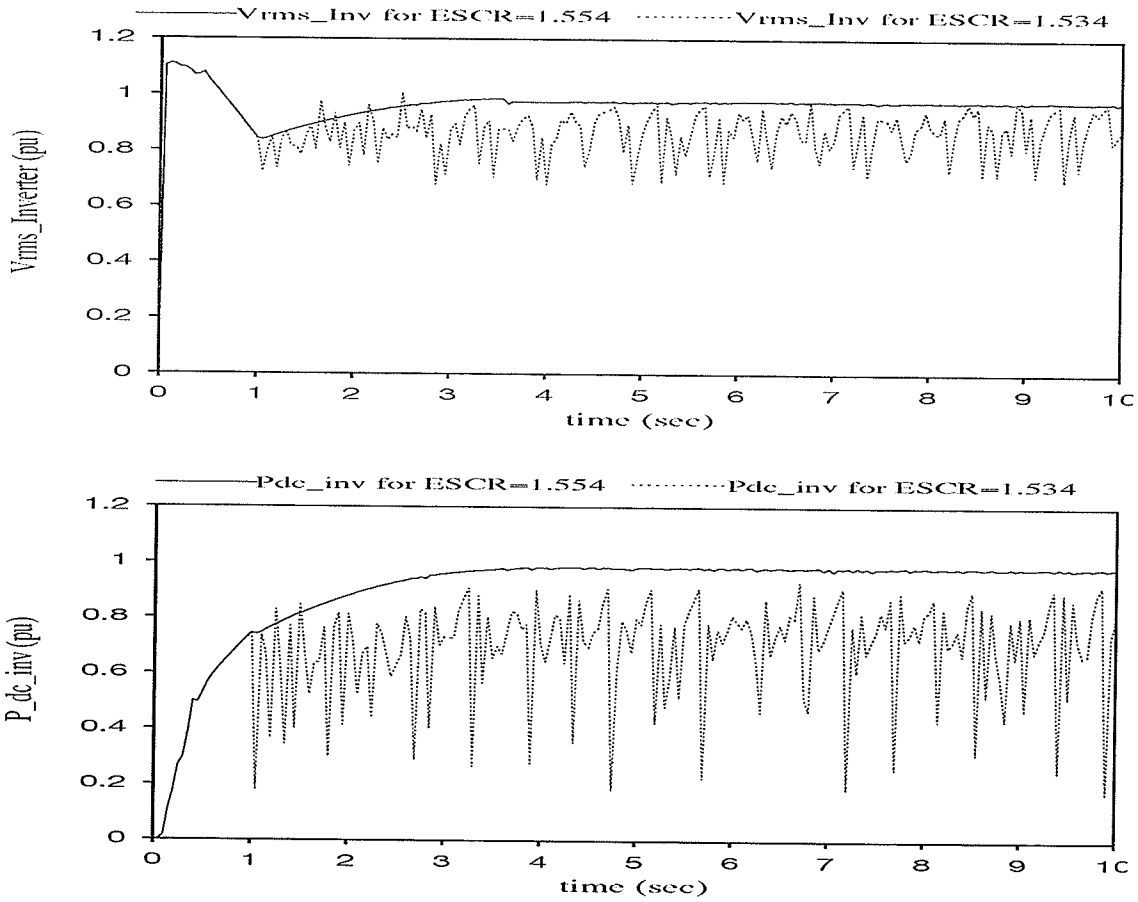

Figure 4.2.1: The steady state stability and instability for model 1 with Xd'.

Simulations show that the system, if machine replaced by the transient reactance Xd', is steady state stable and remains in power control mode for an ESCR higher then or equal to 1.554. If the ESCR is reduced further, the system becomes unstable due to power control mode instability. The power control increases dc current in order to increase power to 1pu but that causes power to decrease. The simulated steady state critical ESCR equal to 1.554

is the same as the critical ESCR found in the CSI analysis.

Figure 4.2.1 shows steady state system power and voltage response for the ESCR equal to 1.554 (stable state) and for the ESCR equal to1.534 (unstable state). The ripples noticed for the unstable case are due to repeated interchanges between constant power and constant current control mode. Figure 4.2.2 show the power and the bus voltage at the inverter side for the three and the one phase fault. The critical ESCR for the one and the three phase fault recovery is the same as the critical ESCR for the steady state stability.

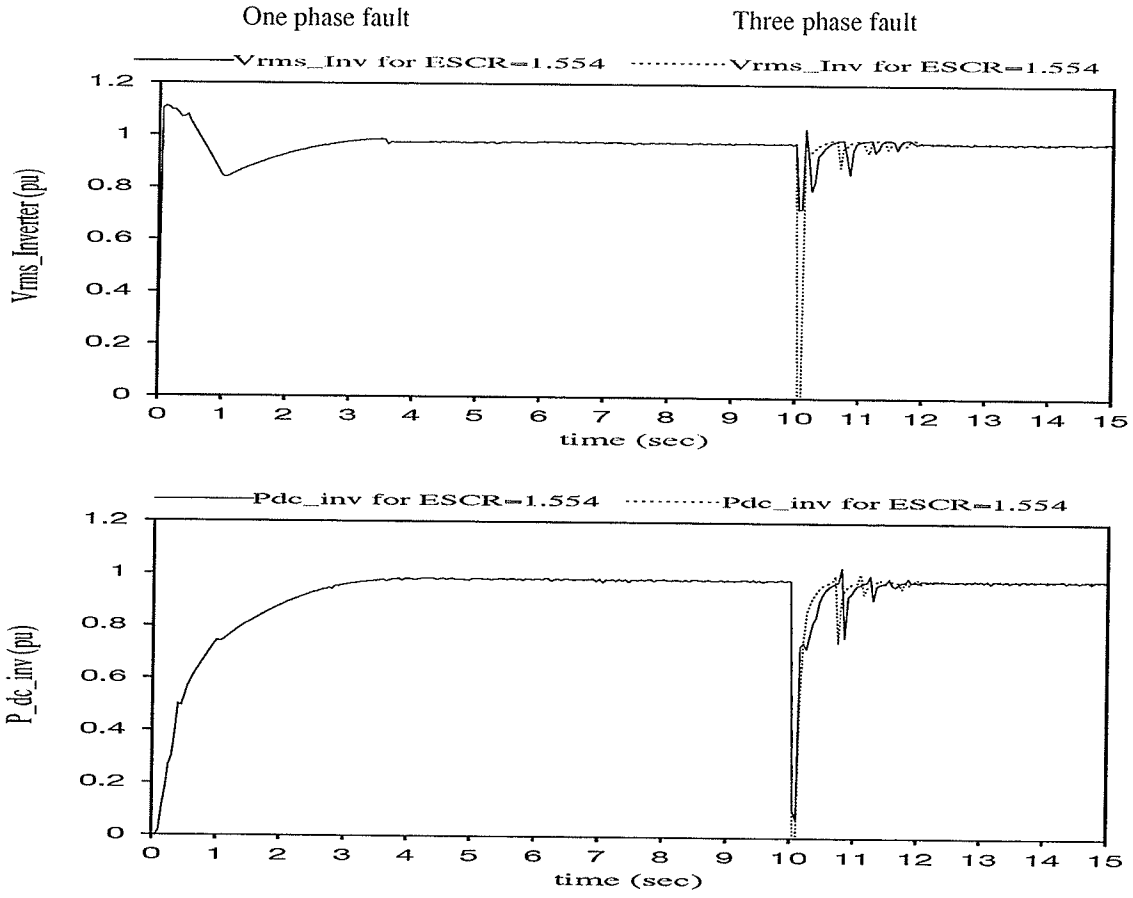

Figure 4.2.2: One phase fault and three phase fault recovery for model 1 with Xd'.

Figure 4.2.3 shows the power and the bus voltage if machine is replaced by sub-transient

reactance Xd" for ESCR(Xd") equal to 1.636 (the lowest ESCR calculated such as the Zs tends to infinity). It is obvious that the system doesn't show the power/voltage instability in the case of the steady state, the one phase fault recovery, and three phase fault recovery. This agrees with results from CSI and MAP analysis.

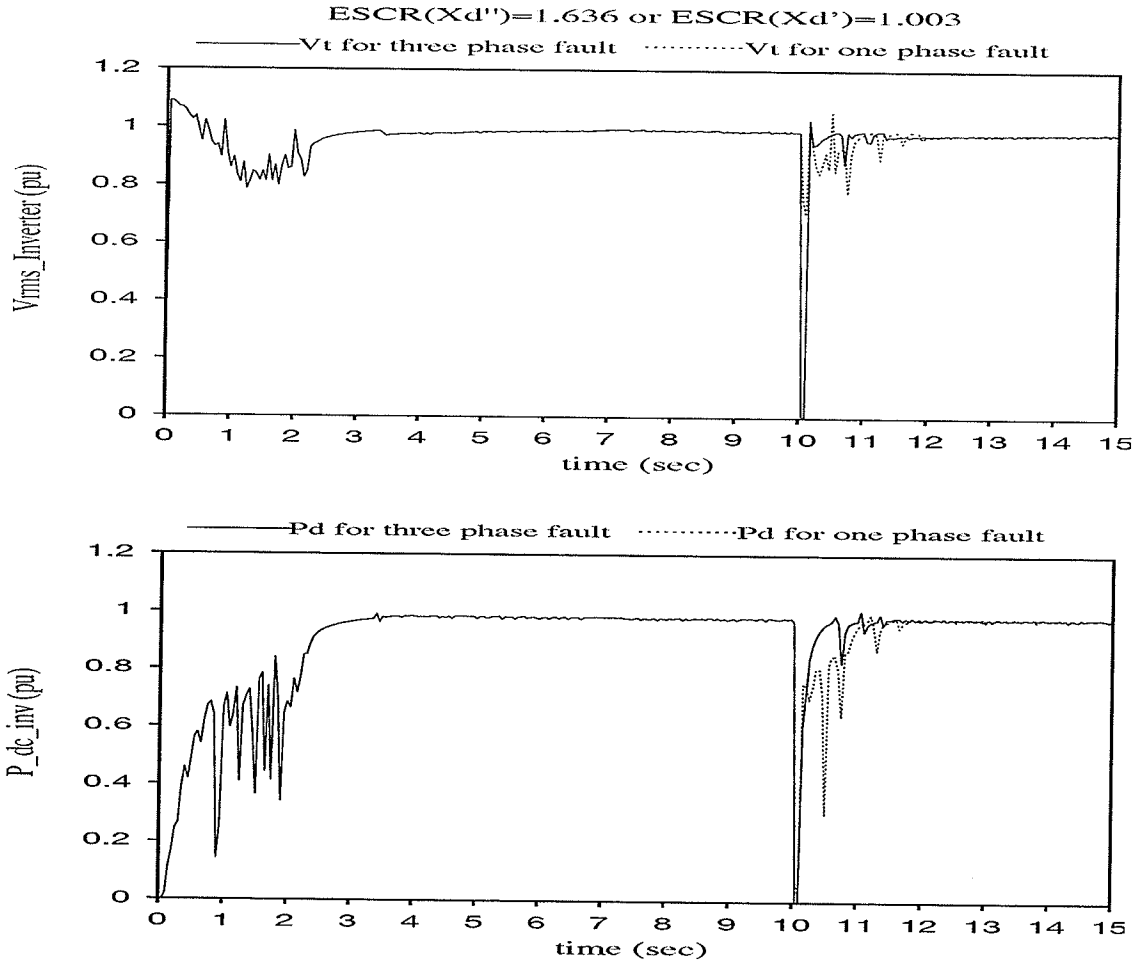

Figure 4.2.3: One phase fault and three phase fault recovery for model 1 with Xd".

The overall time domain results for model 1 are in excellent agreement with results from CSI and MPC analysis. This means the CSI and the MPC calculations agree with transient simulations of similar system representations. However, the real machine has more detail,

and results may be different. The more detailed machine representation is considered in the next section.

4. 3 Model 2 Time Domain Simulation Results

We now add one more level of accuracy in our system representation by including a full machine model, but still ignore the excitation system (section 2.4.2). For the theoretical calculation of CSI and MPC for this case we consider the model where the machine's real power is zero. The model 2 steady state is described by the steady state equations 3.2.

Simulations are conducted as in the previous case. The strength of the ac system i.e. ESCR at the inverter end is reduced by increasing Zs. Using the steady state equations 3.2 of the system and assuming that the synchronous machine supplies 260 MVar into the system, Esys is calculated for every ESCR. After that, the Efield is manually adjusted so that the terminal voltage remains at 1pu in the steady state.

The simulation results show that the system can not operate stably below ESCR equal to 1.622 while the system can not recover from the three phase faults and the one phase faults for the ESCR's less than ESCR equal to 1.881 and ESCR equal to 2.003, respectively. It is found that a one phase fault is more severe than a three phase fault. The only concern during simulation and determination of these critical ESCR's is the steady state stability, whereas the quality of the system response during transients is not considered.

However, during faults recovery the terminal voltage decreasing oscillations with frequency approximately around 1Hz are observed. These oscillations can be attributed to the mechanical dynamics of the detailed synchronous machine model. The oscillations become more significant as the ESCR decreases. In practice, due to these oscillations, system response in a very weak ac system, after fault recovery, wouldn't be acceptable even if the system is stable in the steady state. This implies that the lowest ESCR of the ac system should be higher than that found above in order for the system to operate satisfactorily.

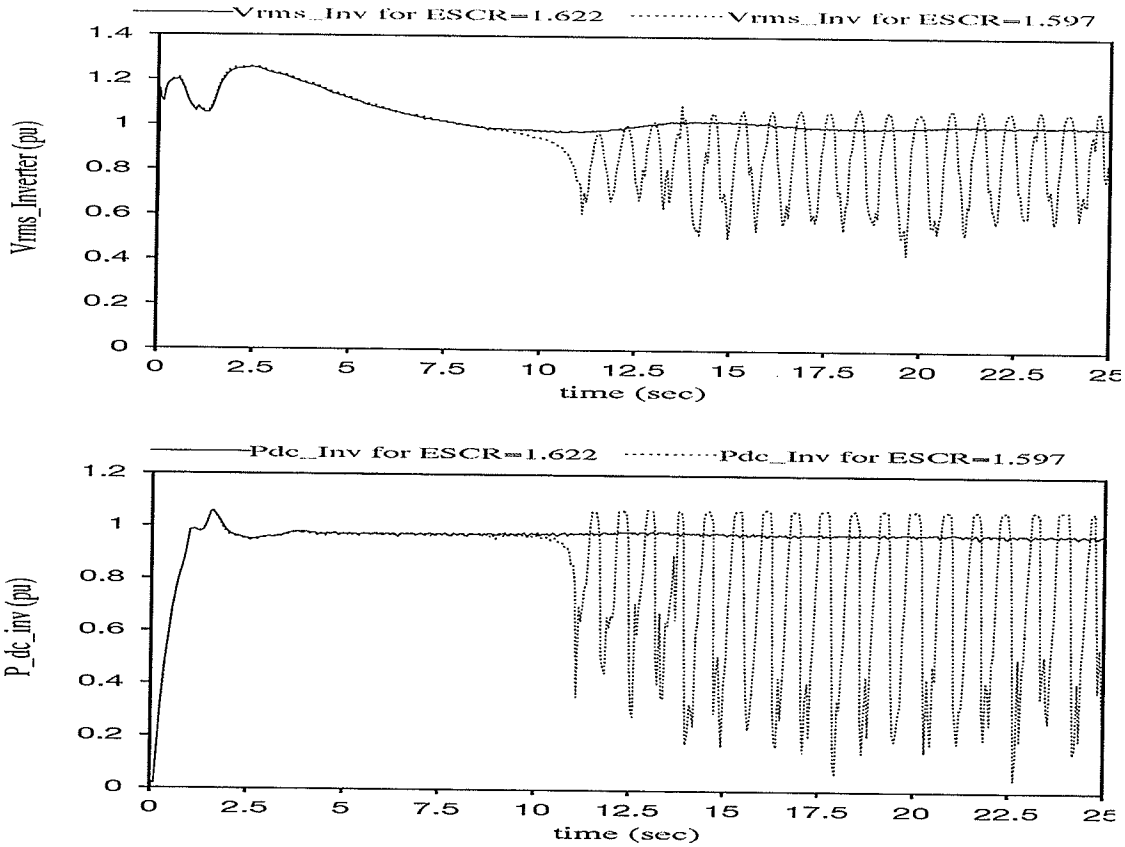

Figure 4.3.1: Steady state stability and instability for model 2.

If in equations 3.2 the machine is represented by transient reactance Xd', the CSI analysis

gives that the critical ESCR is equal to 1.597. The simulation yielded a steady state critical ESCR of 1.622; slightly higher than the theoretically found critical ESCR. On the other hand, if the machine in equations 3.2 is represented by the sub-transient reactance Xd" the CSI analysis gives that the critical ESCR is equal to 1.355 which is significantly lower than the simulation critical ESCR. It is then obvious that it is more accurate to represent the machine by the transient reactance Xd' than by the sub-transient reactance Xd" when the CSI and the MPC analysis are conducted.

Figures 4.3.1, 4.3.2, and 4.3.3 show stable and unstable steady state system response, stable and unstable three phase and one phase fault system recovery, respectively.

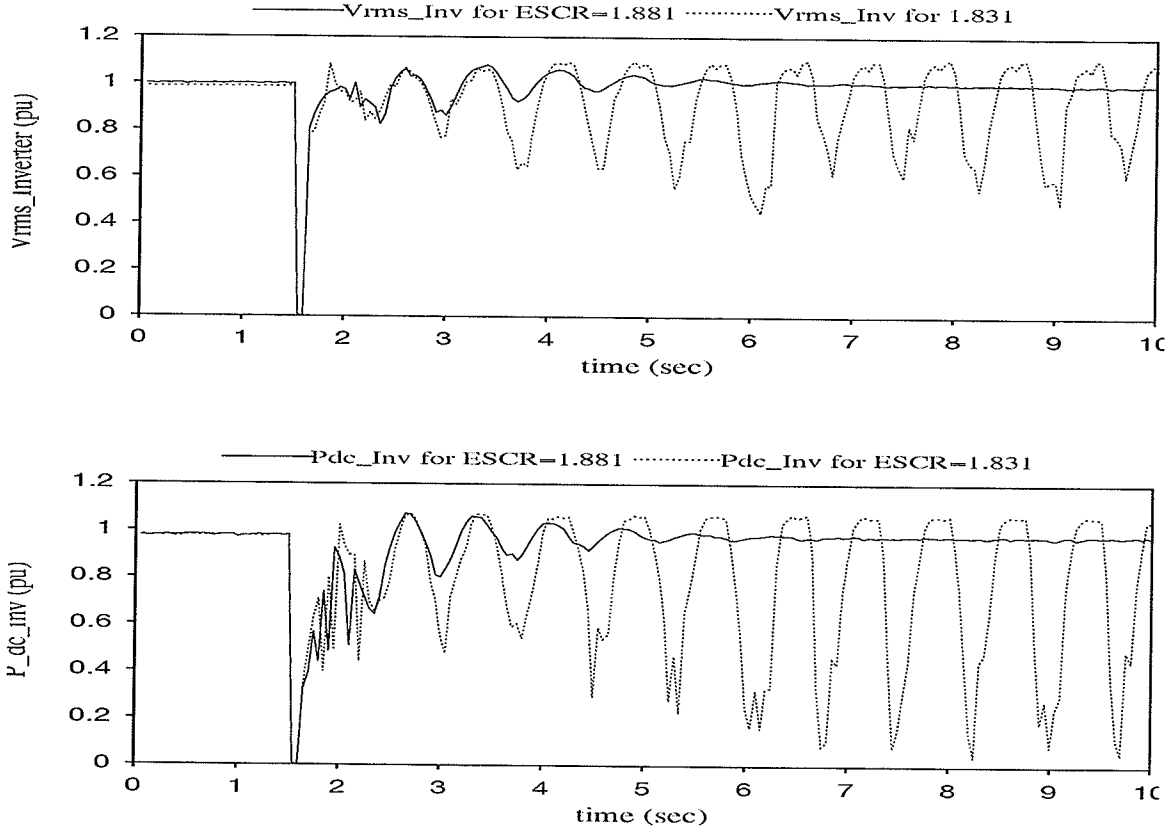

Figure 4.3.2: Three phase fault stability and instability for model 2.

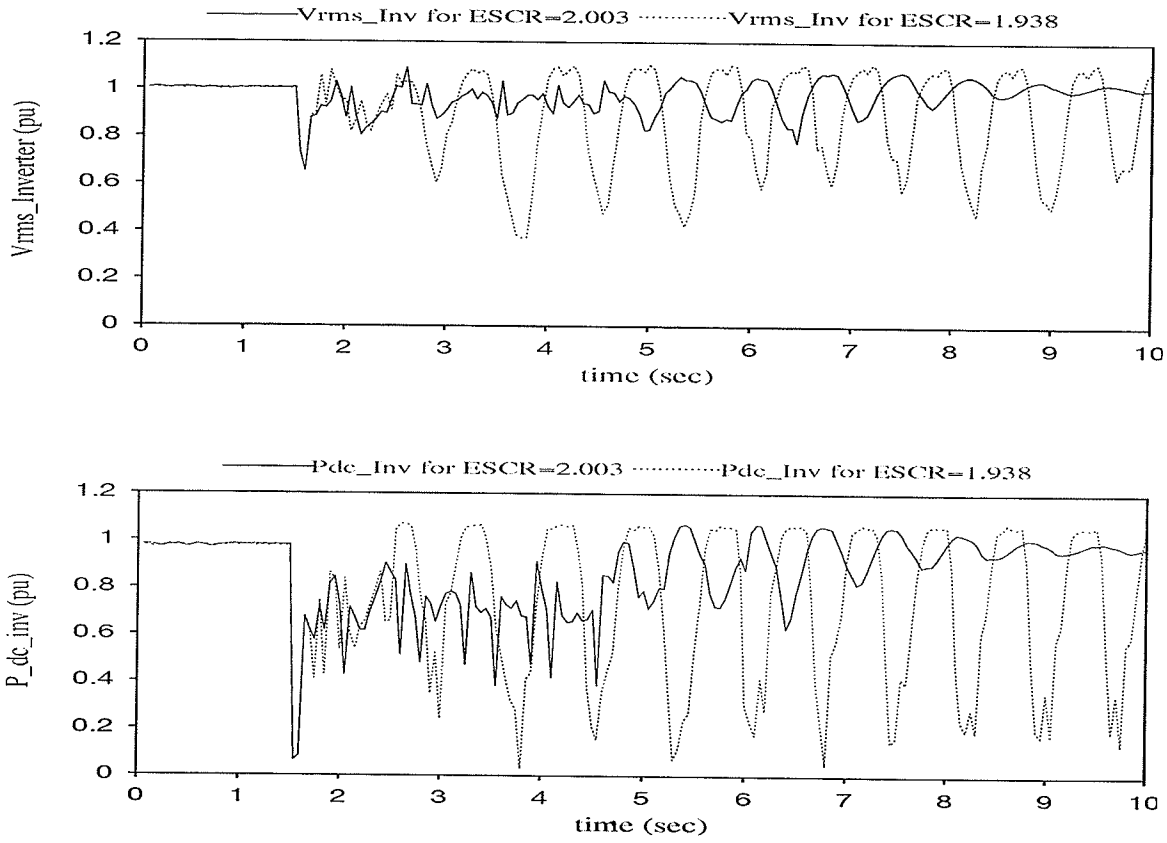

Figure 4.3.3: One phase fault stability and instability for model 2.

4.4 Model 3 Time Domain Simulation Results

The performance of the real system is affected by the inherent dynamics and delays of the machine and exciter. Therefore, in order to get a more accurate picture about the system performance which corresponds to the real system behaviour, the system in model 3 is simulated. In this model the machine is fully modelled, and the exciter is employed to dynamically adjust the machine's field voltage to keep bus voltage at 1pu (section 2.4.3).

Simulations were conducted as in the two previous models. From the steady state equations Esys is calculated for every simulated ac system strength ESCR such that the synchronous machine supplies 260 Mvar into the system. The machine field voltage is dynamically adjusted by the exciter/voltage regulator to keep terminal voltage at the inverter ac bus at 1pu. Therefore, the system dynamics and stability are affected by the exciter parameters. For this reason, the effect of the exciter gain Ka on the critical ESCR in the three cases steady state stability, three phase and one phase recovery is investigated. Two different types of exciter (section 2.4.3) were considered. The results for exciter model 1 are given in the table 2 while results for exciter model 2 are given in the table 3.

Table 2: The Critical ESCR's for the Exciter Model 1

Ka	Steady State	Three Phase Fault	One Phase Fault
223.	1.746	2.393	2.735
200.	1.831	2.393	2.735
150.	1.881	2.269	2.393
100.	2.165	2.545	2.393

From Table 2 it can be seen that as gain increases the critical ESCR for steady state decreases. However, in the case of one phase fault recovery the critical ESCR decreases as gain decreases. The gain Ka=150 gives the lowest critical ESCR for three phase fault recovery while for higher Ka gains the critical ESCR's are slightly higher. Generally, the one phase fault is most severe for the system stability. However, for Ka equal to 100 the critical ESCR for the one phase fault is lower than for the three phase fault.

Table 3: The Critical ESCR's for the Exciter Model 2

Ka	Steady State	Three Phase Fault	One Phase Fault
200	2.003	2.165	2.393
150	1.938	2.078	2.393
120	2.003	2.393	2.393
100	2.078	2.393	2.393

From Table 3 for exciter model 2, the steady state and three phase recovery critical ESCR's are lowest for Ka equal to 150 while for lower and higher gains critical ESCR's are higher. The critical ESCR's for one phase fault recovery are same for every investigated gain value. The overall performance of the system is better if exciter model 1 is used as the automatic voltage regulator.

Here, it should be emphasized again that only steady state stability is considered without regarding the quality of the system response during transients. Likewise in model 2., the terminal voltage during transients is oscillatory, and the oscillations are more pronounced as the ECSR is decreased.

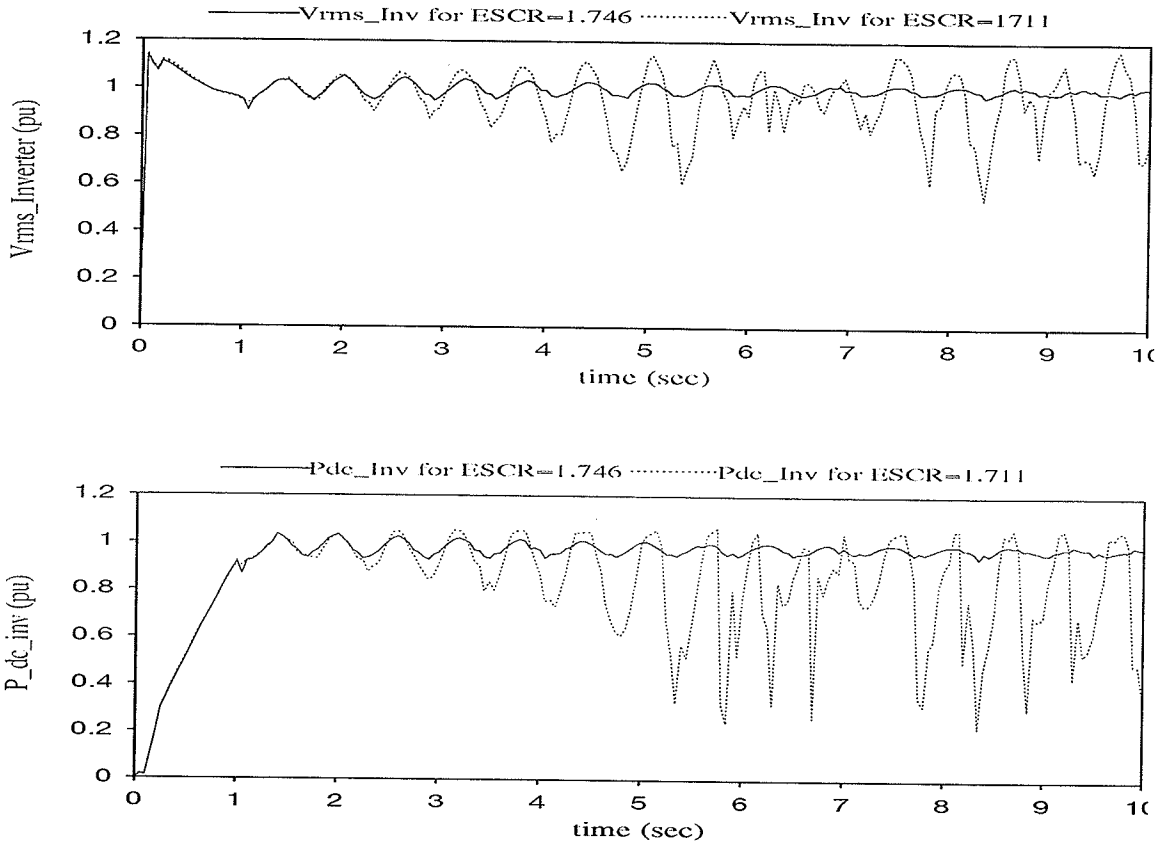

Fig. 4.4.1: Steady state stability and instability for model 3 with exciter model and gain Ka=223.

Figures 4.4.1-4.4.3 show steady state, three phase fault, and one phase recovery rms inverter voltage and dc power for ESCR equal to or lower than critical ESCR. In the case of steady state and three phase fault instability, the figures 4.4.1 and 4.4.2, increasing voltage oscillations due to exciter dynamics cause instability. On the other hand in the case of one phase fault instability figure 4.4.3, due to dynamics after fault clearing the exciter hits its upper limit and thus no longer achieves voltage control. This causes the inverter ac voltage to collapse.

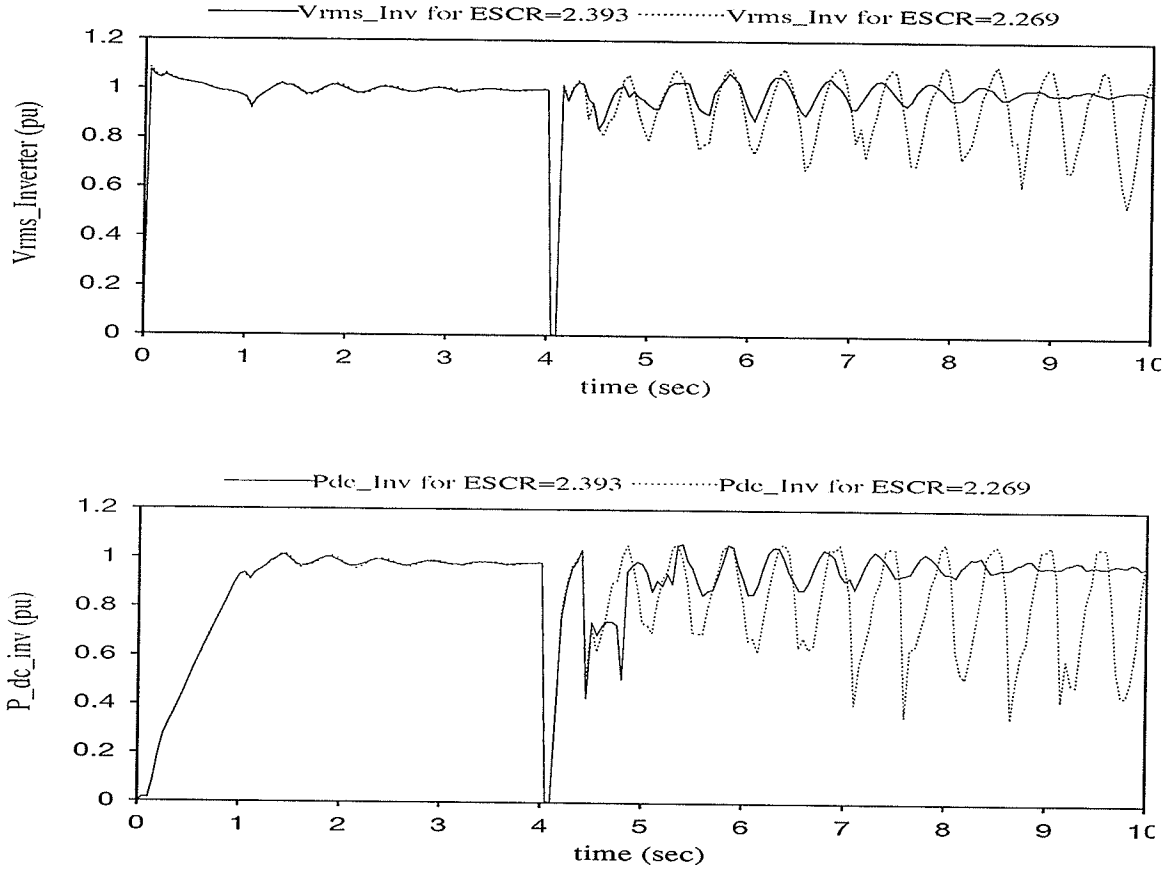

Fig. 4.4.2: Three phase fault stability and instability for model 3 with exciter model 1 and gain Ka=223.

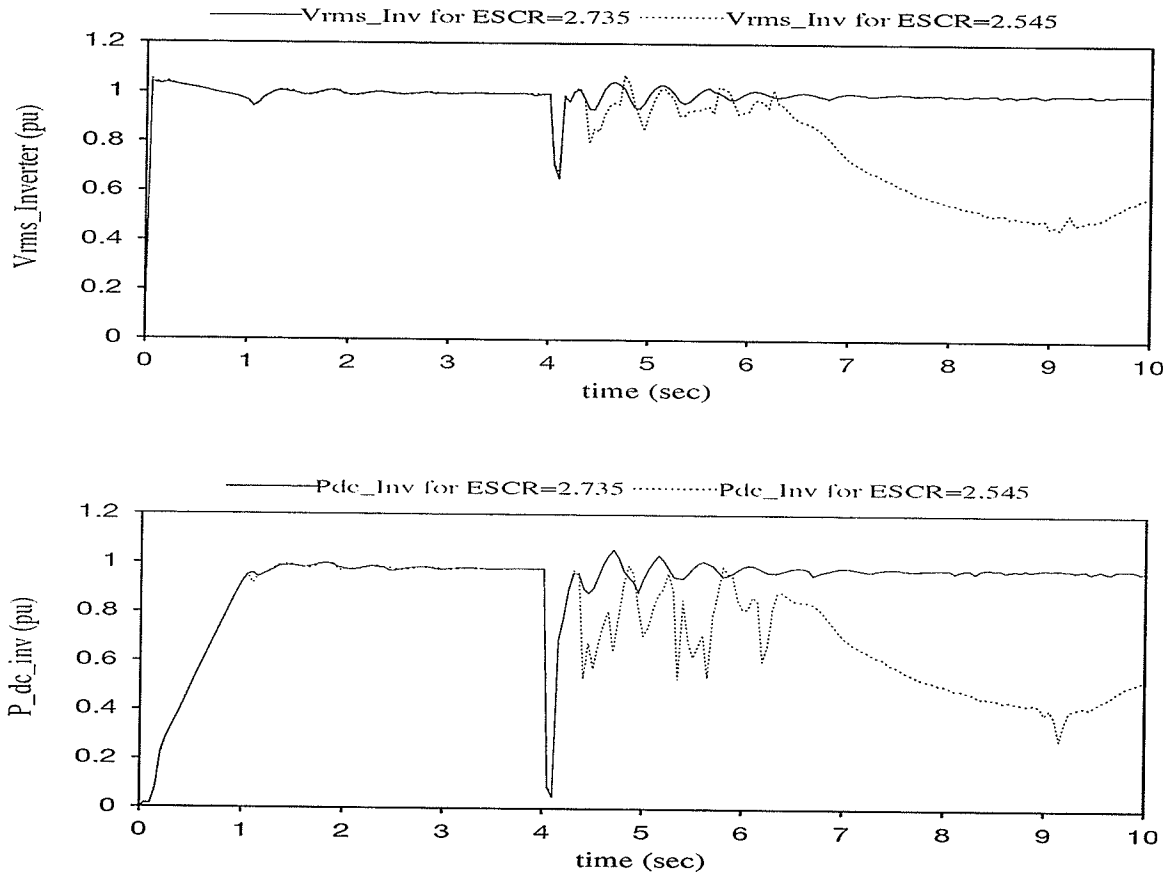

Fig. 4.4.3: One phase fault stability and instability for model 3 with exciter model 1 and gain Ka=223.

4.4.1 Model 3 With Two and Three Synchronous Machines

The synchronous machine is connected with the ac system impedance in parallel increasing the ESCR viewed from the converters. In this way the synchronous machine makes the ac system stronger. Adding more synchronous machines in to the system is expected to make the system stronger. The objective of this section is to investigate how the number of the synchronous machines affects the critical ESCR.

We now consider the case of having additional synchronous machines at the converter bus. In addition to the original case with one (300MVar/-165Mvar rating) synchronous machine we add first one and then two identical machines on the bus. Naturally, to maintain the steady state operating conditions each machine is required now to provide only a portion of the total 260MVar requirement. For this study the exciter model 1 is used with different gain Ka values to investigate how the number of synchronous machines and how the exciter gains affects the critical ESCR.

In order to have unique reference to compare the results for the system with different number of synchronous machines two entries are given in Tables 4, 5, and 6. It is of our interest to see how high the system impedance (how low the ESCR) can be such that system is stable. Also, whether the critical system impedance can be increased (critical ESCR reduced) by adding more machines into the system. Therefore, the first entry labelled as ESCRr is the critical short ratio calculated such that the system impedance Zs, the local load impedance Zll, and filter impedance Zf contribution to the system strength are considered (equation 4.1) while the machines contribution to the system strength is neglected. This entry is the only relevant number for the system performance comparison when a different number of the synchronous machines are employed.

$$ESCRr = Zbase\left(\frac{1}{kZsys} + \frac{1}{Zll} + \frac{1}{Zf}\right) \qquad (4.1)$$

The ESCR's labelled as ESCR1, ESCR2, and ESCR3 are actual ESCR values for system

with one, two, and three synchronous machines. In the calculation of the ESCR1, ESCR2 and ESCR3 the contribution of the one, two, and three machine to the ac system strength are taken into ESCR calculation, respectively. The equations 4.2 shows how ESCR1, ESCR2, and ESCR3 are calculated.

$$
\begin{aligned}
ESCR1 &= Zbase\left(\frac{1}{kZsys}+\frac{1}{Xd'}+\frac{1}{Zll}+\frac{1}{Zf}\right)\\
ESCR2 &= Zbase\left(\frac{1}{kZsys}+\frac{2}{Xd'}+\frac{1}{Zll}+\frac{1}{Zf}\right) \qquad (4.2)\\
ESCR3 &= Zbase\left(\frac{1}{kZsys}+\frac{3}{Xd'}+\frac{1}{Zll}+\frac{1}{Zf}\right)
\end{aligned}
$$

Table 4: The critical ESCR's for Ka=223

Ka=223	Steady State ESCRr	ESCR1	Three Phase Fault ESCRr	ESCR2	One Phase Fault ESCRr	ESCR3
One Synchronous Machine	0.616	1.746	1.225	2.393	1.56	2.735
Two Synchronous Machine	0.556	2.864	0.789	3.125	1.104	3.458
Three Synchronous Machine	0.472	3.954	0.651	4.167	0.85	4.385

The results given in Tables 4, 5, and 6 are critical ESCR's for different values of the exciter gains. The results from the tables (looking at ESCRr values) leads to conclusion that adding more synchronous machines improves system operation from the Zs point of view. In other words, the more the number of synchronous machines are in operation, the

system can operate with the higher system impedance magnitude |Zs|. This conclusion is based looking at the ESCRr values from the tables. However, looking at the actual effective system strength, ESCR1 for one machine, ESCR2 for two machines, and ESCR3 for three machines, it is obvious that critical ESCR as a value increases by adding more machines in to the system.

The proper tuning of the exciter gains plays an important role in making the system operate satisfactorily. From the tables it seems that by reducing exciter gain the critical steady state ESCR's increases. However, this conclusion is based only on the experimental simulation results. To get better insight about effect of the exciter parameters on the critical ESCR more detailed stability analysis has to be developed, and is left for the future researcher.

Table 5: The Critical ESCR's for Ka=200

Ka=200	Steady State ESCRr ESCR1	Three Phase Fault ESCRr ESCR2	One Phase Fault ESCRr ESCR3
One Synchronous Machine	0.691 1.831	1.225 2.393	1.56 2.735
Two Synchronous Machine	0.556 2.864	0.85 3.19	1.225 3.582
Three Synchronous Machine	0.532 4.028	0.691 4.212	0.789 4.319

Table 6: The Critical ESCR for Ka=150

Ka=150	Steady State ESCRr ESCR1	Three Phase Fault ESCRr ESCR2	One Phase Fault ESCRr ESCR3
One Synchronous Machine	0.737 1.881	1.104 2.269	1.225 2.393
Two Synchronous Machine	0.584 2.897	0.737 3.068	1.104 3.458
Three Synchro-nous Machine	0.616 4.127	0.691 4.212	0.789 4.315

4.5 Model 4 Time Domain Simulation Results

Model 4 is a hypothetical model which assumes an idealized exciter that is able to rapidly control the bus voltage. In the simulation, we represent this via a fast acting control system controlling the voltage source behind the machine's transient reactance Xd' (section 2.4.4).

This model is the closest to the ideal bus voltage control. The simulation results show that system is stable for every ESCR, and system does not show recovery problems after one and three phase fault clearing. In other words, the model 4 in time domain analysis does not show signs of the power/voltage instability at all. This is in agreement with theory which tells that the ideal bus voltage control increases the ac system strength such that the system is not in the jeopardy of power/voltage instability.

Figure 3.5.1 shows system bus voltage for the steady state, one phase fault recovery, and

three phase fault recovery for ESCR equal to 1.033. This ESCR is the lowest ESCR for the ac system. This ESCR is calculated such that system impedance (Zs) contribution to the ESCR is equal to zero (i.e. Zs tends to infinity or disconnected ac system). During simulation the ac system thevenin equivalent is disconnected, and voltage source Esys behind transient reactance Xd' is dynamically adjusted by the PI controller (section 2.4.4) to keep bus voltage at 1pu.

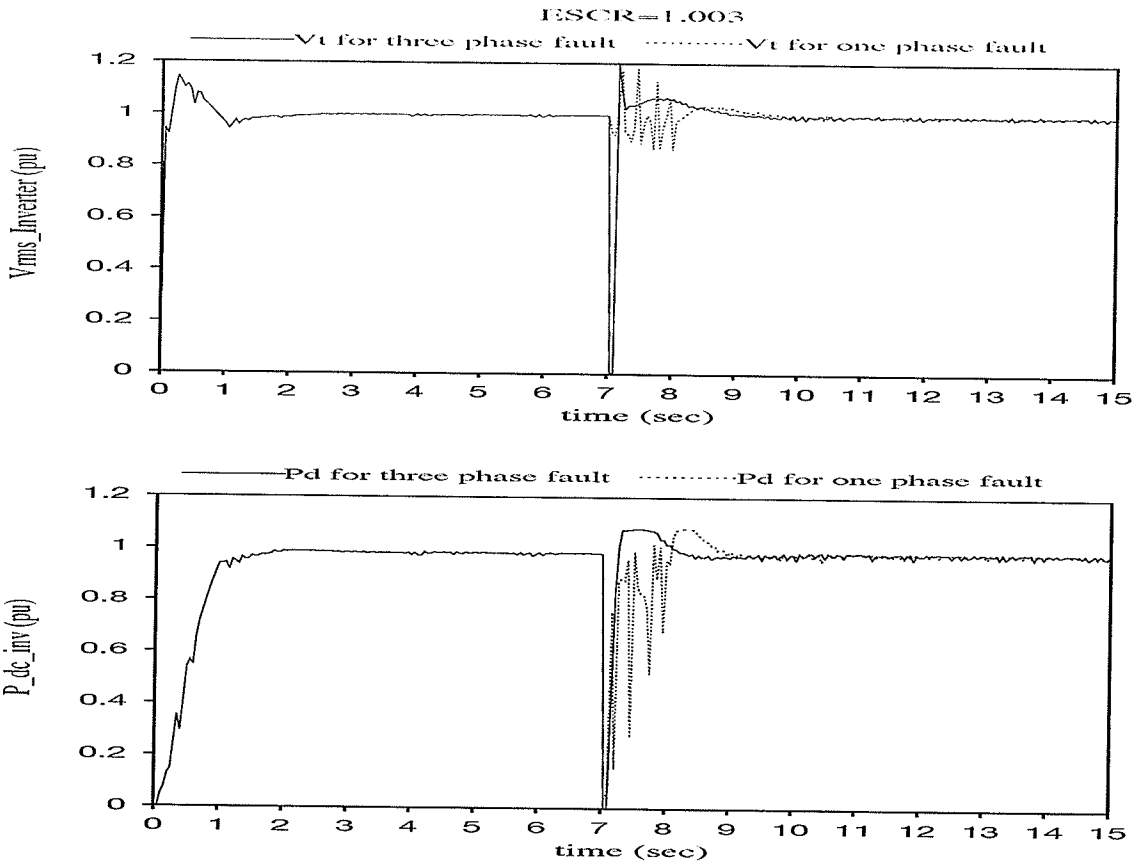

Figure 4.5.1: The steady state, one phase fault, and three phase fault stability for model 4.

4.6 Summary

To allow easier comparison of the four system models, the results for critical ESCR's are given in the Table 7. The simplest machine model 1 has the same critical ESCR for steady state, one phase fault recovery, and three phase fault recovery. However, if the detailed machine model (either with or without exciter) described by the Park's equations is used as in model 2 or model 3, instabilities occur for ESCR's larger than the theoretically calculated values using a simple equivalent (or as simulated in model 1). It is clear then that the model 1, where the synchronous machine is replaced by the fixed voltage source behind the transient reactance Xd' is too simplified for power/voltage stability analysis; especially if recovery from faults is considered. Furthermore, model 2 and model 3 show significant oscillatory system response during transients, particularly for the low ESCR values. In the estimation of the lowest ESCR for which the system can operate reliably, analysis of these transient oscillations plays an important role. Although in a strict sense the system is stable if it eventually recovers, in a practical sense an excessively oscillatory response is undesirable. However, we have not considered this aspect in this thesis because of the subjectivity of deciding how much oscillation is unacceptable. These oscillations can not be observed in model 1, so these oscillation can be attributed to the machine and exciter dynamics.

Model 1 has the lowest simulation steady state critical ESCR. It also agrees with the theoretical critical ESCR found by the CSI and the MPC analysis using equations 3.1. Similarly, agreement between the theoretically calculated (for modified steady state equations

as in equations 3.2 where machine real power is zero) and simulated steady state ESCR for model 2 is quite good. The critical ESCR's are highest for model 3. This leads to the conclusion that the internal synchronous machine dynamics and the exciter dynamics significantly affect the critical ESCR. The critical ESCR's are also dependant on the exciter parameters. The time domain simulation results for model 4 confirm theory which tells that if it is possible to ideally control voltage on the infinite ac bus the system will be stable for every ESCR.

Table 7: The Critical ESCR's for Different Machine Representations

MODEL	Critical ESCR's (CESCR)	Theoretical CESCR	Steady State CESCR (Simulation)	Three Phase Fault Recovery CESCR (Simulation)	One Phase Fault Recovery CESCR (Simulation)
Model 1	Fixed voltage source behind synchronous impedance	1.554	1.554	1.554	1.554
Model 2.	Detailed machine model with fixed field voltage	1.597	1.622	1.881	2.003
Model 3.	Detailed machine model with exciter model 1 Ka=223.	stable for all ESCR	1.746	2.393	2.735
Model 4.	Adjustable voltage source behind synchronous impedance	stable for all ESCR's	stable for all ESCR's	stable for all ESCR's	stable for all ESCR's

The simplified system model 1 (machine represented as Thevenin equivalent) always recovers from fault if its ESCR is above theoretically calculated steady state critical ESCR. However, if a detailed machine model is used as in model 2 the system can not recover after fault clearing for ESCR higher than steady state critical ESCR. Furthermore,

the system performance is more degraded by adding detailed machine and exciter model as in model 3. This can be attributed to the machine and exciter transient dynamics.

Comparing model 3 (full machine model with exciter) and model 4 (ideal bus voltage control), it appears that it is incorrect to simplify the model of a machine which is controlling voltage at a bus as an ideal voltage controller. It can be seen that the ideal voltage controller does not in fact lead to any instability which is clearly not demonstrated in the detailed simulation. The internal machine dynamics and the exciter inherited dynamics and limits puts additional constraints on the system operations.

CHAPTER 5

CONCLUSION

5.1. Conclusions

Based on the results presented in the previous chapters, the following conclusions can be drawn:

◆ *The critical ESCR calculation is dependant of the steady state equations by which the system is described.* Modelling a synchronous machine such that machine in the steady state does not deliver real power gives a more accurate critical ESCR than if the machine is modelled as mere fixed voltage behind reactance.

◆ *The transient reactance Xd' should be taken into account during ESCR analysis.* It is found that replacing the machine with its sub-transient reactance Xd", the system strength is significantly increased. The system modelled in such a manner may incorrectly result in a stable solution although the detailed simulation produces results to the contrary.

◆ *From the terminal voltage stability point of view, modelling the synchronous condenser as a fixed voltage behind a synchronous reactance is over simplified, and analysis based*

only on ESCR's is not sufficient. The reason for this lies in fact that synchronous machine in the steady state does not absorb real power. On the other hand, if the machine is modelled as a voltage source the effect of this constraint on the system stability is neglected because unlike the real synchronous condenser the voltage source can absorb real power. Furthermore, the detailed model of the synchronous machine with exciter has highest critical ESCR's which means that the fast exciter doesn't improve system performance from the steady state point of view. Therefore, detailed model of the synchronous machine with exciter should be applied in order to get a better insight into the system performance, especially during transients and fault recovery when electro-mechanical oscillations involving the machine become significant.

◆ *The fault recovery critical ESCR's (one phase fault and three phase fault) are significantly higher then steady state critical ESCR.* This conclusion is based on observing the system's ability to recover after fault clearing. It is found that in each case the one phase fault is the most severe i.e. critical ESCR's have the highest values. This fact should be taken into account in determining the lowest ESCR up to which the system can run.

◆ *The critical ESCR and dynamics of the system are significantly affected by the exciter gain.* The steady state critical ESCR can be reduced by increasing the exciter gain. On the other hand, that will cause that critical ESCR for a one phase fault to increase. Therefore, it is very important to properly tune the exciter in order to get better system performance.

The above results and conclusions are made regarding only 1pu steady state stability with-

out regarding whether the system response is acceptable during transients and fault recovery. However, in real applications these should be taken into consideration.

5. 2. Future Work

◈ The method "Control Sensitivity Index (CSI)" analysis based on the steady state equations have been demonstrated. However, during CSI calculation the system and control dynamics are neglected. Including the system and control dynamics in the CSI calculation would be the next step in developing the CSI method for the control stability analysis.

◆ It is shown that on hvdc system can not recover after fault clearing for the ESCR much higher than the steady state critical ESCR. This conclusion is based on the system inherent ability to recover from faults. However, applying some of the strategies for the fault clearing may reduce fault clearing critical ESCR. Finding such appropriate fault clearing strategy would improve system performance. A further study can be carried out in this respect.

◆ It is found that the critical ESCR is significantly affected by the exciter parameters. In this thesis the conclusion how critical ESCR is affected by exciter gain is based on the experimental simulation results. An approach as described in [7] where steady-state equations are combined with controller dynamic equations is recommended. With this approach frequency-domain control system design tools (such as root locus) can be applied to the problem solution.

REFERENCES:

[1] A. Gavrilovic, "AC/DC System Strength as Indicated by Short Circuit Ratios", IEE Fifth International Conference on AC and DC Power Transmission, London, September 1991, pp 27-32.

[2] J.D. Ainsworth, A. Gavrilovic, H.L.Thanawala, "Static and Synchronous Compensators for Hvdc Transmission Converters Connected to Weak Ac System", GIGRE Conference, Paris, 1980, Paper No. 31-01.

[3] O. B. Nayak, "Dynamic Performance of Static and Synchronous Compensators at an Inverter Bus in a Very Weak Ac System", Ph.D Thesis, University of Manitoba, Canada, September 1993.

[4] O.B. Nayak, A.M. Gole, D.G.Chapman & J.B. Davies, "Control Sensitivity Indices for Stability Analysis of Hvdc Converters", Canadian Electrical and Computer Engineering Conference (CECEC), Vancouver, 14-17 September 1993.

[5] CIGRE WG 14.07, "Guide for planning - Dc Links terminating at Ac Systems Locations Having Low Short Circuit Capacities, Part 1: AC/DC System Interaction Phenomena", December 1991.

[6] C.V. Thio & J.B. Davies, "New Synchronous Compensators for the Nelson River Hvdc System-Planing Requirements and Specifications", IEEE Trans. on Power Delivery, Vol. 6, No. 2, April 1991, pp 922-928.

[7] A.M.Gole, G.B.Mazur, O.B.Nayak," Application of Control Sensitivity Indices to Hvdc Controller Tuning", Stockholm Power Tech Power Electronics, Stockholm, Sweden, June 1995, pp 7-11.

[8] M.Szechtman, et al., "First Benchmark Model for Hvdc Control Studies", Electra, Vol. 135, April 1991, pp 55-73.

[9] A.E.HAmmad, et al., "A New Approach for the Analysis and Solution of Ac Voltage Stability Problems at Hvdc Terminals", International Conference on Dc Power Transmission, Montreal, June 1984, pp 164-170.

[10] B.Franken & G.Andersson, "Analysis of Hvdc Converters Connected to Weak Ac Systems", IEEE Transactions on Power Systems, Vol. 5, No. 1, February 1990, pp 235-242.

[11] T.Smed, G. Andersson, G.B. Sheble, L.L.Grigsby, " A New Approach to ac/dc power Flow", IEEE Transactions on Power Systems, Vol. 6, No.31, August 1991, pp 1238-1244.

[12] G.Gaba, et al., "Comparative Analysis and Study of the Dynamic Stability of Ac/dc Systems", IEEE Transactions on Power Systems, Vol. 3, No. 3, August 1988, pp 978-985.

[13] A. Gavrilovic. " Interaction Between Ac and Dc Systems", Paper submitted at request of the chairman of SC 14.

[14] C. Concordia, "Steady-State Stability of Synchronous Machine as Affected by Voltage-Regulator Characteristics", AIEE Transactions, May 1944, Vol. 63, pp 215-220.

[15] A.E.Hammad, C.T.Taylor, "Sensitivity of Transient Voltage Stability to Dynamic Load Characteristics, and HVDC and SVC Dynamic Control Characteristics", CIGRE SC 38, Florianopolis Brazil, 22-23 September 1993.

[16] M.L.Crow, B.C.Lesieutre, "Voltage Collapse", IEEE Potentials, 1994, pp 18-21.

[17] E.W. Kimbark, "*Direct Current Transmission - Volume 1*", John Wiley & Sons, Inc. 1971.

[18] *Mathcad, Version 6.0,* MathSoft, Inc., 201 Broadway, Cambridge, Massachusetts, 02139.

[19] W.H. Press, S.A. Teukolsky, W. T.Vetterling, B.P. Flannery, "*Numerical Recipes in C*", Second Edition, Cambridge University Press.

[20] "*EMTDC Users's Manual*", Manitoba HVDC Research Centre, Winnipeg, Canada, 1994.

[21] J. Arrillaga."*High Voltage Direct Current Transmission*", IEE Power Engineering Series 6, Peter Peregrinus 1988.

APPENDIX I: The ac system impedance Zs frequency response

The system impedance magnitude frequency response(pu).

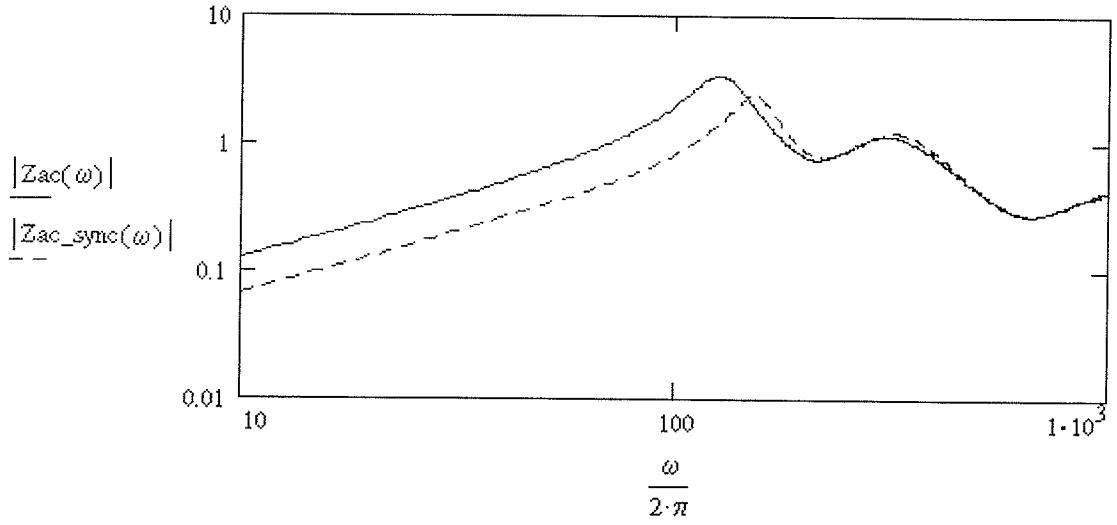

The system impedance phase angle frequency response(deg).

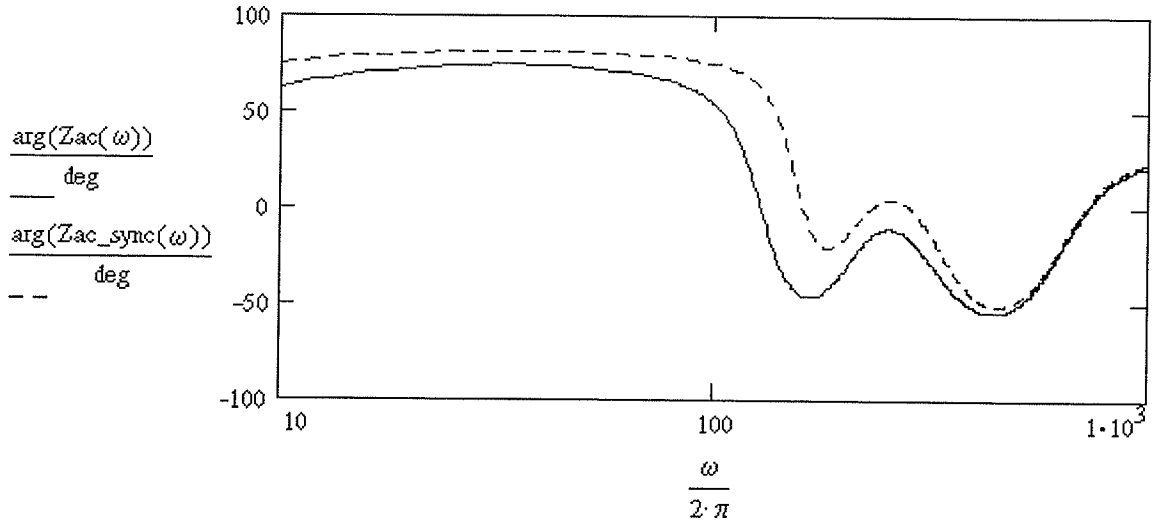

APPENDIX II: The SCR and Corresponding ESCR Table

The tables below gives SCRtr and corresponding ESCRtr calculated by using machine transient reactance Xd' and corresponding ESCRsub_tr and SCRsub_tr calculated by using machine sub-transient reactance Xd". During the simulations the ac system with different strengths given in the table below is investigated.

k	|SCRtr (k)|	|ESCRtr (k)|	|SCRsub_tr (k)|	|ESCRsub_tr (k)|	arg (ESCRtr (k)) deg
0.7	3.277	2.979	3.891	3.592	- 81.629
0.8	3.033	2.735	3.646	3.347	- 81.269
0.9	2.842	2.545	3.455	3.157	- 80.941
1	2.69	2.393	3.303	3.005	- 80.641
1.1	2.566	2.269	3.178	2.88	- 80.366
1.2	2.462	2.165	3.075	2.776	- 80.112
1.3	2.374	2.078	2.987	2.689	- 79.878
1.4	2.299	2.003	2.911	2.613	- 79.661
1.5	2.234	1.938	2.846	2.548	- 79.459
1.6	2.177	1.881	2.789	2.491	- 79.271
1.7	2.127	1.831	2.739	2.441	- 79.096
1.8	2.082	1.786	2.694	2.396	- 78.932
1.9	2.042	1.746	2.654	2.356	- 78.778
2	2.006	1.711	2.618	2.32	- 78.633
2.1	1.974	1.678	2.585	2.287	- 78.496
2.2	1.944	1.649	2.555	2.258	- 78.368
2.3	1.917	1.622	2.528	2.231	- 78.246
2.4	1.892	1.597	2.503	2.206	- 78.131
2.5	1.87	1.574	2.481	2.183	- 78.022
2.6	1.849	1.554	2.46	2.162	- 77.919
2.7	1.829	1.534	2.44	2.142	- 77.821
2.8	1.811	1.516	2.422	2.124	- 77.727
2.9	1.794	1.499	2.405	2.107	- 77.638
3	1.779	1.484	2.389	2.092	- 77.553

Appendix III: Synchronous Compensator Data

Table 8: Synchronous Compensator Data

Parameters	Values	Units
Rated RMS Phase Voltage	7.96743	kV
Rated RMS Phase Current	12.55	kA
Vt terminal Voltage Magnitude	1.021	pu
Mechanical Damping	1	pu
Base Angular Frequency	376.99	rad/s
Inertia Specified Through a VAR	2.15	MWs/MVA
Portier Reactance Xp	0.15	pu
Direct-Axis Reactance Xd	1.35	pu
Direct-Axis Transient Reactance Xd'	0.25	pu
Direct-Axis Sub-Transient Reactance Xd"	0.165	pu
Damper-Field Mutual Reactance Xkf	0.0	pu
Quad-Axis Reactance Xq	0.815	pu
Quad-Axis Sub-Transient Reactance Xq"	0.19	pu
Armature Resistance Ra	0.00174	pu
Armature Time Constant Ta	0.27	sec
Direct-Axis Transient Time Constant Tdo'	8.2	sec
Direct-Axis Sub-Transient Time Constant Tdo"	0.1	sec
Quad_Axis Sub_transient Time Constant Tqo"	0.275	sec
Air Gap Factor AGFC	0.8	

Machine rating is -165-+300Mvar.

Appendix IV: Program listings for the CSI calculation.

Program listing for calculation of the CSI for power control mode for equations (3.1):

```
#include<stdio.h>
#include<malloc.h>
#include<math.h>

#define SQ(x) ((x)*(x))

double **mat_alloc();
double *vector();

/*** The steady state and CSI for power control mode calculation   ***
 *** for the hvdc/ac system with synchronous machine for different  ***
 *** system impendance Zs.                                          ***/

main()
{
 FILE *fp,*fpst;
 double **Jac, **Jred, **Jinv;
 double sq2, pi, cons1, deg, KV, Mvar;
 double Vt, Vd, Es, Id, Pd;
 double alpha, gama, phi, theta;
 double Rs, Xs, Zs, Rf, Xf, Zf, Zbase, t;
 double Rsys, Xsys, Zsys, Xc, Xd, Zll, Rll, Xll;
 double *x,*dx,*f,*res,*svi,*scal;
 double SCR, ESCR, scrang, K, dK;
  int i, j , k, l, d;
 int loop;
 int Jrow=6, Jcol=9;

 sq2=1.41423562;
 pi=3.141592652;
 deg=pi/180.0;
 cons1=3.0*sq2/pi;
 KV=1000;
 Mvar=1000000;
 dK=0.05;

/*---------memory allocation-------*/

Jac=mat_alloc(1,Jrow,1,Jcol);
Jred=mat_alloc(1,Jrow,1,Jcol);
Jinv=mat_alloc(1,Jrow,1,Jcol);
x=vector(1,Jrow);
scal=vector(1,Jrow);
res=vector(1,Jrow);
```

```
dx=vector(1,Jrow);
f=vector(1,Jrow);
svi=vector(1,Jrow);

/*------- data -------*/

Zbase=230.*230./1000.;
Rf=0.095811;
Xf=175.928145;
Xc=13.315204*2.;
Xll=55.0404703;
Rll=167.55;
Rsys=2.921761;
Xsys=38.435098;
Xd=44.087226;
/*Xd=29.0975208;*/
Zf=SQ(Rf)+SQ(Xf);
Zll=SQ(Rll)+SQ(Xll);
Zsys=SQ(Rsys)+SQ(Xsys);
t=0.90969*2.;

/*------- constraints conditions and initial conditions-----*/

Id=2.0;
gama=15.0*deg;
Vt=230.0;
Vd=245*2;
Es=230.0;
alpha=150.0*deg;
theta=0.0*deg;
phi=-150.*deg;
Pd=990.;

/*--------------ESCR iteration---------------*/

fpst=fopen("STDY6eq.out","w");
fp=fopen("CSI6eq.out","w");
for(K=1.;K<=3;K+=dK)
{

Rs=(-K*Rsys*K*Xsys*Xd+K*Rsys*Xd*(K*Xsys+Xd))/
(K*Rsys*K*Rsys+(Xd+Xsys*K)*(Xd+Xsys*K));
Xs=(K*Rsys*K*Rsys*Xd+K*Xsys*Xd*(K*Xsys+Xd))/(K*Rsys*K*Rsys+(Xd+Xsys*K)*(Xd+Xsys*K));
Zs=SQ(Rs)+SQ(Xs);

SCR=Zbase*sqrt((K*Rsys+Rll)*(K*Rsys+Rll)+(K*Xsys+Xll)*(K*Xsys+Xll))/(sqrt((K*Zsys)*(Zll)));
ESCRhelp=Zbase*sqrt((Rs+Rll)*(Rs+Rll)+(Xs+Xll)*(Xs+Xll))/(sqrt((Zs)*(Zll)));

ESCR=Zbase*sqrt(SQ(Rll*Rf+Rs*Rf+Rs*Rll+Xf*Xll+Xs*Xf-Xs*Xll)+SQ(Rf*Xll-Rll*Xf+Rf*Xs-
Rs*Xf+Rs*Xll+Rll*Xs))/sqrt(Zs*Zll*Zf);
/*---------x vector definition-------------*/

x[1]=alpha;
x[2]=phi;
```

```
x[3]=Vd;
x[4]=Es;
x[5]=theta;
x[6]=Pd;

/*---------f vector definition----------*/

f[1]=Vt-sq2*Xc*Id/(t*(cos(gama)+cos(alpha)));
f[2]=cos(phi)-(cos(alpha)-cos(gama))*0.5;
f[3]=Vd-(cons1*t*Vt*cos(gama)-Xc*Id*3.0/pi);
f[4]=Pd-Vd*Id;
f[5]=(Rs*(Vt-Es*cos(theta))-Xs*Es*sin(theta))/Zs-Pd/Vt+Vt*Rf/Zf+Vt*Rll/Zll;
f[6]=(-Rs*Es*sin(theta)-Xs*(Vt-Es*cos(theta)))/Zs-Pd*tan(phi)/Vt+Vt*Xf/Zf-Vt*Xll/Zll;

/*----------Newton-Raphson method for nonlinear equation root----------*/
for(loop=1;loop<=20;loop++)
{

/*---------definition of the Jacobian matrix----------*/

for(i=1;i<=Jrow;i++){
   for(j=1;j<=Jcol;j++) Jac[i][j]=0;
 }

Jac[1][1]=1.0;
Jac[1][2]=-sq2*Xc/(t*(cos(alpha)+cos(gama)));
Jac[1][3]=-sq2*Xc*Id*sin(alpha)/(t*SQ(cos(alpha)+cos(gama)));
Jac[1][4]=-sq2*Xc*Id*sin(gama)/(t*SQ(cos(alpha)+cos(gama)));

Jac[2][3]=sin(alpha)/2.0;
Jac[2][4]=-sin(gama)/2.0;
Jac[2][5]=-sin(phi);

Jac[3][1]=-cons1*t*cos(gama);
Jac[3][2]=3.*Xc/pi;
Jac[3][4]=cons1*Vt*t*sin(gama);
Jac[3][6]=1.;

Jac[4][2]=-Vd;
Jac[4][6]=-Id;
Jac[4][9]=1.;

Jac[5][1]=Rs/Zs+Pd/SQ(Vt)+Rf/Zf+Rll/Zll;
Jac[5][7]=(-Rs*cos(theta)-Xs*sin(theta))/Zs;
Jac[5][8]=Es*(Rs*sin(theta)-Xs*cos(theta))/Zs;
Jac[5][9]=-1./Vt;

Jac[6][1]=-Xs/Zs+Pd*tan(phi)/SQ(Vt)+Xf/Zf-Xll/Zll;
Jac[6][5]=-Pd/(Vt*SQ(cos(phi)));
Jac[6][7]=(-Rs*sin(theta)+Xs*cos(theta))/Zs;
Jac[6][8]=Es*(-Rs*cos(theta)-Xs*sin(theta))/Zs;
Jac[6][9]=-tan(phi)/Vt;

/*----------reduced Jacobian----------*/
```

```
for(k=1;k<=Jrow;k++){
Jred[k][1]=Jac[k][3]; /* alpha */
Jred[k][2]=Jac[k][5]; /* phi */
Jred[k][3]=Jac[k][6]; /* Vd */
Jred[k][4]=Jac[k][7]; /* Esys*/
Jred[k][5]=Jac[k][8]; /* theta */
Jred[k][6]=Jac[k][9]; /* Idc */
}
mat_inverse(Jred,Jinv,Jrow);
mtx_vect_multiplication(Jinv,f,dx,Jrow,-1.0);
vect_adding(x,dx,x,Jrow);

alpha=x[1];
phi=x[2];
Vd=x[3];
Es=x[4];
theta=x[5];
Pd=x[6];

f[1]=Vt-sq2*Xc*Id/(t*(cos(gama)+cos(alpha)));
f[2]=cos(phi)-(cos(alpha)-cos(gama))*0.5;
f[3]=Vd-(cons1*t*Vt*cos(gama)-Xc*Id*3.0/pi);
f[4]=Pd-Vd*Id;
f[5]=(Rs*(Vt-Es*cos(theta))-Xs*Es*sin(theta))/Zs-Pd/Vt+Vt*Rf/Zf+Vt*Rll/Zll;
f[6]=(-Rs*Es*sin(theta)-Xs*(Vt-Es*cos(theta)))/Zs-Pd*tan(phi)/Vt+Vt*Xf/Zf-Vt*Xll/Zll;
}
/*------- Printing Steady State Solution ----------------------------------*/
fprintf(fpst,"K=%4.4f\t Rsys=%4.4f\t Xsys=%4.4f\t SCR=%4.4f\n", K, K*Rsys, K*Xsys, SCR);
fprintf(fpst,"a=%4.4f\t g=%4.4f\t phi=%4.4f\t theta=%4.4f\t \n", alpha/deg, gama/deg, phi/deg, theta/deg);
fprintf(fpst,"Vd=%4.4f\t Vt=%4.4f\t Es=%4.4f\t\n", Vd, Vt, Es);
fprintf(fpst,"Pd=%4.4f\t Id=%4.4f\t \n", Pd, Id);
fprintf(fpst,"Qf=%4.4f\t Qd=%4.4f\t Qsys=%4.4f\n",SQ(Vt)*Xf/Zf,
-Pd*tan(phi), Vt*(Rs*Es*sin(theta)+Xs*(Vt-Es*cos(theta)))/Zs);
fprintf(fpst,"Pf=%4.4f\t Pd=%4.4f\t Psys=%4.4f\n", SQ(Vt)*Rf/Zf, Pd, Vt*(Rs*(Vt-Es*cos(theta))-
Xs*Es*sin(theta))/Zs);
fprintf(fpst,"\n /****************************** / \n");

/*-------------CSI calculation---------------*/
for(k=1;k<=Jrow;k++){
Jred[k][1]=Jac[k][1]; /*dVt csi[1] */
Jred[k][2]=Jac[k][3]; /*dALPHA csi[2] */
Jred[k][3]=Jac[k][5]; /*dPHI csi[3] */
Jred[k][4]=Jac[k][6]; /*dVd csi[4] */
Jred[k][5]=Jac[k][8]; /*dTHETA csi[5] */
Jred[k][6]=Jac[k][9]; /*dPdc csi[6] for power control mode*/
res[k]=Jac[k][2]; /*dId */
}
mat_inverse(Jred,Jinv,Jrow);
mtx_vect_multiplication(Jinv,res,svi,Jrow,-1.0);

fprintf(fp,"%4.6f\t %4.6f\t %4.6f\t %4.6f\t\n", K, SCR, svi[6], ESCR);
}
mat_free(Jac,1,Jrow,1,Jcol);
mat_free(Jred,1,Jrow,1,Jrow);
```

```
mat_free(Jinv,1,Jrow,1,Jrow);
free_vector(x,1,Jrow);
free_vector(scal,1,Jrow);
free_vector(dx,1,Jrow);
free_vector(f,1,Jrow);
free_vector(x,1,Jrow);
free_vector(res,1,Jrow);
free_vector(svi,1,Jrow);
fclose(fp);
fclose(fpst);
}
```

Program listing for calculation of the CSI for power control mode for equations (3.2):

```
#include<stdio.h>
#include<malloc.h>
#include<math.h>

#define SQ(x) ((x)*(x))

double **mat_alloc();
double *vector();

/*** The steady state and CSI for power control mode calculation     ***
 *** for the hvdc/ac system with synchronous machine for different  ***
 *** system impendance Zs.                                          ***/

main()
{
 FILE *fp,*fpst;
 double **Jac, **Jred, **Jinv;
 double sq2,pi, cons1, deg, sq3;
 double Vt, Vd, Es, Id, Ei;
 double alpha, gama, phi, theta, delta;
 double Pd, Qm;
double Rs, Xs,Zs, Rf, Xf, Zf, Zbase, t;
double Xc, Xd, Xll, Rll, Zll, Rsys, Xsys,Zsys, Req, Xeq, Zeq;
 double *x, *dx, *f, *res, *svi, *scal;
 double SCR, ESCR, K, dK;
 int i, j, l, k, d;
 int loop, iscr;
 int Jrow=7, Jcol=12;

sq3=1.732050808;
sq2=1.41423562;
pi=3.141592652;
deg=pi/180.0;
cons1=3.0*sq2/pi;
```

```
 dK=0.05;

 /*---------memory allocation-------*/
 Jac=mat_alloc(1,Jrow,1,Jcol);
 Jred=mat_alloc(1,Jrow,1,Jcol);
 Jinv=mat_alloc(1,Jrow,1,Jcol);
 x=vector(1,Jrow);
 scal=vector(1,Jrow);
 res=vector(1,Jrow);
 dx=vector(1,Jrow);
 f=vector(1,Jrow);
 svi=vector(1,Jrow);

 /*------- data -------*/

 Zbase=230.*230./1000.;
 Rf=0.095811;
 Xf=175.928145;
 Xc=13.315204*2;
 Xd=44.087152;
 /*Xd=29.0975208;*/
 Xll=55.0404703;
 Rll=167.55;
 Zll=SQ(Rll)+SQ(Xll);
 Zf=SQ(Rf)+SQ(Xf);
 t=0.90969*2;

 /*------- constraints conditions------*/
 Id=2.0;
 gama=15.0*deg;
 Vt=230.0;
 Qm=260.;
 delta=0.0*deg;

 /*-------initial conditions-------------*/
 Rsys=2.921761;
 Xsys=38.435098;
 Vd=500;
 Es=230.0;
 alpha=150.0*deg;
 theta=-26.9*deg;
 phi=-151.58*deg;
 Ei=350;
 Pd=1000;

 /*--------------scr iteration---------------*/
 fpst=fopen("reacSTEADY.out","w");
 fp=fopen("reacCSI.out","w");
 for(K=0.7;K<=10.;K+=dK)
 {
 Rs=K*Rsys;
 Xs=K*Xsys;
 Zs=SQ(Rs)+SQ(Xs);
 Req=(-K*Rsys*K*Xsys*Xd+K*Rsys*Xd*(K*Xsys+Xd))/
```

```
(K*Rsys*K*Rsys+(Xd+Xsys*K)*(Xd+Xsys*K));
Xeq=(K*Rsys*K*Rsys*Xd+K*Xsys*Xd*(K*Xsys+Xd))/
(K*Rsys*K*Rsys+(Xd+Xsys*K)*(Xd+Xsys*K));
Zeq=SQ(Req)+SQ(Xeq);
Zsys=SQ(Rsys)+SQ(Xsys);

SCR=Zbase*sqrt((K*Rsys+Rll)*(K*Rsys+Rll)+(K*Xsys+Xll)*(K*Xsys+Xll))/(sqrt((K*Zsys)*(Zll)));
ESCR=Zbase*sqrt(SQ(Rll*Rf+Req*Rf+Req*Rll+Xf*Xll+Xeq*Xf-Xeq*Xll)+SQ(Rf*Xll-Rll*Xf+Rf*Xeq-
Req*Xf+Req*Xll+Rll*Xeq))/sqrt(Zeq*Zll*Zf);

/*---------x vector definition----------*/

x[1]=alpha;
x[2]=phi;
x[3]=Vd;
x[4]=Es;
x[5]=theta;
x[6]=Pd;
x[7]=Ei;

/*---------f vector definition----------*/

f[1]=Vt-sq2*Xc*Id/(t*(cos(gama)+cos(alpha)));
f[2]=cos(phi)-(cos(alpha)-cos(gama))*0.5;
f[3]=Vd-(cons1*t*Vt*cos(gama)-Xc*Id*3.0/pi);
f[4]=Pd-Vd*Id;
f[5]=(Rs*(Vt-Es*cos(theta))-Xs*Es*sin(theta))/Zs-Pd/Vt+Vt*Rf/Zf+Vt*Rll/Zll;
f[6]=(-Rs*Es*sin(theta)-Xs*(Vt-Es*cos(theta)))/Zs-Pd*tan(phi)/Vt+Vt*Xf/Zf-Vt*Xll/Zll+Qm/Vt;
f[7]=Qm-sq3*Vt*(Ei*cos(delta)-Vt)/Xd;

/*-----Newton_Raphson Method for nonlinear equation root---*/
for(loop=1;loop<=500 ;loop++)
{
/*---------definition of the Jacobian matrix----------*/
for(i=1;i<=Jrow;i++){
   for(j=1;j<=Jcol;j++) Jac[i][j]=0;
 }
Jac[1][1]=1.0;
Jac[1][2]=-sq2*Xc/(t*(cos(alpha)+cos(gama)));
Jac[1][3]=-sq2*Xc*Id*sin(alpha)/(t*SQ(cos(alpha)+cos(gama)));
Jac[1][4]=-sq2*Xc*Id*sin(gama)/(t*SQ(cos(alpha)+cos(gama)));

Jac[2][3]=sin(alpha)/2.0;
Jac[2][4]=-sin(gama)/2.0;
Jac[2][5]=-sin(phi);

Jac[3][1]=-cons1*t*cos(gama);
Jac[3][2]=3.*Xc/pi;
Jac[3][4]=cons1*Vt*t*sin(gama);
Jac[3][6]=1.;

Jac[4][2]=-Vd;
Jac[4][6]=-Id;
Jac[4][9]=1.;
```

```
Jac[5][1]=Rs/Zs+Pd/SQ(Vt)+Rf/Zf+Rll/Zll;
Jac[5][7]=(-Rs*cos(theta)-Xs*sin(theta))/Zs;
Jac[5][8]=Es*(Rs*sin(theta)-Xs*cos(theta))/Zs;
Jac[5][9]=-1./Vt;

Jac[6][1]=-Xs/Zs+Pd*tan(phi)/SQ(Vt)+Xf/Zf-Xll/Zll-Qm/SQ(Vt);
Jac[6][5]=-Pd/(Vt*SQ(cos(phi)));
Jac[6][7]=(-Rs*sin(theta)+Xs*cos(theta))/Zs;
Jac[6][8]=Es*(-Rs*cos(theta)-Xs*sin(theta))/Zs;
Jac[6][9]=-tan(phi)/Vt;
Jac[6][12]=1/Vt;

Jac[7][1]=-sq3*(Ei*cos(delta)-2.*Vt)/Xd;
Jac[7][10]=-sq3*Vt*(cos(delta))/Xd;
Jac[7][11]=sq3*Vt*Ei*sin(delta)/Xd;
Jac[7][12]=1.;

/*----------------reduced Jacobian--------------*/

for(k=1;k<=Jrow;k++){
Jred[k][1]=Jac[k][3];
Jred[k][2]=Jac[k][5];
Jred[k][3]=Jac[k][6];
Jred[k][4]=Jac[k][7];
Jred[k][5]=Jac[k][8];
Jred[k][6]=Jac[k][9];
Jred[k][7]=Jac[k][10];
}

mat_inverse(Jred,Jinv,Jrow);
mtx_vect_multiplication(Jinv,f,dx,Jrow,-1.0);
vect_adding(x,dx,x,Jrow);

alpha=x[1];
phi=x[2];
Vd=x[3];
Es=x[4];
theta=x[5];
Pd=x[6];
Ei=x[7];

f[1]=Vt-sq2*Xc*Id/(t*(cos(gama)+cos(alpha)));
f[2]=cos(phi)-(cos(alpha)-cos(gama))*0.5;
f[3]=Vd-(cons1*t*Vt*cos(gama)-Xc*Id*3.0/pi);
f[4]=Pd-Vd*Id;
f[5]=(Rs*(Vt-Es*cos(theta))-Xs*Es*sin(theta))/Zs-Pd/Vt+Vt*Rf/Zf+Vt*Rll/Zll;
f[6]=(-Rs*Es*sin(theta)-Xs*(Vt-Es*cos(theta)))/Zs-Pd*tan(phi)/Vt+Vt*Xf/Zf-Vt*Xll/Zll+Qm/Vt;
f[7]=Qm-sq3*Vt*(Ei*cos(delta)-Vt)/Xd;
}

/*------- Printing Steady State Solution ------------------------------------*/
fprintf(fpst,"K=%4.4f\t Rsys=%4.4f\t Xsys=%4.4f\t \n",K,Rs,Xs);
fprintf(fpst,"a=%4.4f\t g=%4.4f\t phi=%4.4f\t  theta=%4.4f\t delta=%4.4f\n", alpha/deg, gama/deg, phi/deg,
```

```
theta/deg, delta/deg);
fprintf(fpst,"Vd=%4.4f\t Vt=%4.4f\t Es=%4.4f\t Ei=%4.4f\n",Vd,Vt, Es, Ei);
fprintf(fpst,"Pd=%4.4f\t Id=%4.4f\t \n", Pd, Id);
fprintf(fpst,"Qm=%4.4f\t    Qf=%4.4f\t    Qd=%4.4f\t    Qsys=%4.4f\n",        Vt*sq3*(Ei*cos(delta)-Vt)/
Xd,SQ(Vt)*Xf/Zf,-Pd*tan(phi),
Vt*(Rs*Es*sin(theta)-Xs*(Es*cos(theta)-Vt))/Zs);
fprintf(fpst,"Pm=%4.4f\t Pf=%4.4f\t Pd=%4.4f\t Psys=%4.4f\n", Vt*Ei*sin(delta)/Xd, SQ(Vt)*Rf/Zf, Pd,
Vt*(Rs*(Es*cos(theta)-Vt)+Xs*Es*sin(theta))/Zs);
fprintf(fpst,"\n /********************************* /\n");

 /*-------------CSI calculation---------------*/
for(k=1;k<=Jrow;k++){
Jred[k][1]=Jac[k][1];   /*Vt*/
Jred[k][2]=Jac[k][3];   /*alpha*/
Jred[k][3]=Jac[k][5];   /*phi*/
Jred[k][4]=Jac[k][6];   /*Vd*/
Jred[k][5]=Jac[k][8];   /*theta*/
Jred[k][6]=Jac[k][9];   /*Pdc*/
Jred[k][7]=Jac[k][12];  /*Qsync*/
res[k]=Jac[k][2];       /*Id*/
}

mat_inverse(Jred,Jinv,Jrow);
mtx_vect_multiplication(Jinv,res,svi,Jrow,-1.0);
fprintf(fp,"%4.6f\t %4.6f\t %4.6f\t %4.6f\t\n", K, SCR, svi[6],ESCR);
}

mat_free(Jac,1,Jrow,1,Jcol);
mat_free(Jred,1,Jrow,1,Jrow);
mat_free(Jinv,1,Jrow,1,Jrow);
free_vector(x,1,Jrow);
free_vector(scal,1,Jrow);
free_vector(dx,1,Jrow);
free_vector(f,1,Jrow);
free_vector(x,1,Jrow);
free_vector(res,1,Jrow);
free_vector(svi,1,Jrow);
fclose(fp);
fclose(fpst);
}
```

Appendix V: Program listings for the MAP calculation.

Program listing for the MPC calculation for equations (3.1):

```
#include<stdio.h>
#include<malloc.h>
#include<math.h>

#define SQ(x) ((x)*(x))

double **mat_alloc();
double *vector();

/*** This program calculate the MAP curve for the hvdc/ac model   ***
 *** with the synchronous  machine where the Vt-bus voltage is   ***
 *** not kept constant.                                          ***/

main()
{
 FILE *fp, *fpst;
 double **Jac,**Jred, **Jinv;
 double sq2, pi,cons1, deg;
 double Vt,Vd, Es,Id;
 double alpha, gama, phi, theta;
 double Pd;
 double Rs, Xs, Zs, Rf, Xf,Zf, Zbase, t;
 double Rsys, Xsys, Zsys, Xc, Xd, Zll, Rll, Xll;
 double Vdbase, Idbase, Vtbase, Pdbase;
 double *x,  *dx, *f, *res, *svi, *scal;
 double SCR, ESCR, scrang, K, dId;
 int i, j, k, l, d;
 int loop;
 int Jrow=6, Jcol=9;

 sq2=1.41423562;
 pi=3.141592652;
 deg=pi/180.0;
 cons1=3.0*sq2/pi;
 dId=0.01;

 Vdbase=500;
 Idbase=2.;
 Vtbase=230.;
 Pdbase=1000.;

/*---------memory allocation-------*/
Jac=mat_alloc(1,Jrow,1,Jcol);
Jred=mat_alloc(1,Jrow,1,Jcol);
Jinv=mat_alloc(1,Jrow,1,Jcol);
x=vector(1,Jrow);
scal=vector(1,Jrow);
```

```
res=vector(1,Jrow);
dx=vector(1,Jrow);
f=vector(1,Jrow);
svi=vector(1,Jrow);

/*------- data -------*/
Rf=0.095811;
Xf=175.928145;
Xc=13.315204*2;
Xll=55.0404703;
Rll=167.55;
Rsys=2.921761;
Xsys=38.435098;
Xd=44.087226;
/*Xd=29.0975208;*/
Zf=SQ(Rf)+SQ(Xf);
Zll=SQ(Rll)+SQ(Xll);
t=0.90969*2;
K=1.;
Rs=(-K*Rsys*K*Xsys*Xd+K*Rsys*Xd*(K*Xsys+Xd))/
(K*Rsys*K*Rsys+(Xd+Xsys*K)*(Xd+Xsys*K));
Xs=(K*Rsys*K*Rsys*Xd+K*Xsys*Xd*(K*Xsys+Xd))/(K*Rsys*K*Rsys+(Xd+Xsys*K)*(Xd+Xsys*K));
Zs=SQ(Rs)+SQ(Xs);

/*------- constraints conditions and initial conditions------*/
Es=265.571958;
theta=-11*deg;
Id=2.0;
gama=15.0*deg;
Vt=230;
Vd=496;
alpha=141.8026*deg;
phi=-151.1546*deg;
Pd=900;

/*--------------Current order changes loop ---------------*/
fp=fopen("MAP6eq.out","w");
for(Id=Idbase*0.5;Id<=Idbase*1.2;Id+=dId)
{

/*---------x vector definition-------------*/
x[1]=Vt;
x[2]=alpha;
x[3]=phi;
x[4]=Vd;
x[5]=theta;
x[6]=Pd;

/*---------f vector definition-------------*/
f[1]=Vt-sq2*Xc*Id/(t*(cos(gama)+cos(alpha)));
f[2]=cos(phi)-(cos(alpha)-cos(gama))*0.5;
f[3]=Vd-(cons1*t*Vt*cos(gama)-Xc*Id*3.0/pi);
f[4]=Pd-Vd*Id;
f[5]=(Rs*(Vt-Es*cos(theta))-Xs*Es*sin(theta))/Zs-Pd/Vt+Vt*Rf/Zf+Vt*Rll/Zll;
```

```
f[6]=(-Rs*Es*sin(theta)-Xs*(Vt-Es*cos(theta)))/Zs-Pd*tan(phi)/Vt+Vt*Xf/Zf-Vt*Xll/Zll;

/*----------------Newton Raphson Method for nonlinear equation root----------------*/
for(loop=1;loop<=50;loop++)
{
/*---------definition of the Jacobian matrix----------*/
for(i=1;i<=Jrow;i++){
   for(j=1;j<=Jcol;j++) Jac[i][j]=0;
 }
Jac[1][1]=1.0;
Jac[1][2]=-sq2*Xc/(t*(cos(alpha)+cos(gama)));
Jac[1][3]=-sq2*Xc*Id*sin(alpha)/(t*SQ(cos(alpha)+cos(gama)));
Jac[1][4]=-sq2*Xc*Id*sin(gama)/(t*SQ(cos(alpha)+cos(gama)));

Jac[2][3]=sin(alpha)/2.0;
Jac[2][4]=-sin(gama)/2.0;
Jac[2][5]=-sin(phi);

Jac[3][1]=-cons1*t*cos(gama);
Jac[3][2]=3.*Xc/pi;
Jac[3][4]=cons1*Vt*t*sin(gama);
Jac[3][6]=1.;

Jac[4][2]=-Vd;
Jac[4][6]=-Id;
Jac[4][9]=1.;

Jac[5][1]=Rs/Zs+Pd/SQ(Vt)+Rf/Zf+Rll/Zll;
Jac[5][7]=(-Rs*cos(theta)-Xs*sin(theta))/Zs;
Jac[5][8]=Es*(Rs*sin(theta)-Xs*cos(theta))/Zs;
Jac[5][9]=-1./Vt;
Jac[6][1]=-Xs/Zs+Pd*tan(phi)/SQ(Vt)+Xf/Zf-Xll/Zll;
Jac[6][5]=-Pd/(Vt*SQ(cos(phi)));
Jac[6][7]=(-Rs*sin(theta)+Xs*cos(theta))/Zs;
Jac[6][8]=Es*(-Rs*cos(theta)-Xs*sin(theta))/Zs;
Jac[6][9]=-tan(phi)/Vt;

/*----------------reduced Jacobian---------------*/
for(k=1;k<=Jrow;k++){
Jred[k][1]=Jac[k][1];   /* Vt   */
Jred[k][2]=Jac[k][3];   /* alpha */
Jred[k][3]=Jac[k][5];   /* phi */
Jred[k][4]=Jac[k][6];   /* Vd */
Jred[k][5]=Jac[k][8];   /* theta */
Jred[k][6]=Jac[k][9];   /* Pd */
}

mat_inverse(Jred,Jinv,Jrow);
mtx_vect_multiplication(Jinv,f,dx,Jrow,-1.0);
vect_adding(x,dx,x,Jrow);

Vt=x[1];
alpha=x[2];
phi=x[3];
```

```
 Vd=x[4];
 theta=x[5];
 Pd=x[6];

 f[1]=Vt-sq2*Xc*Id/(t*(cos(gama)+cos(alpha)));
 f[2]=cos(phi)-(cos(alpha)-cos(gama))*0.5;
 f[3]=Vd-(cons1*t*Vt*cos(gama)-Xc*Id*3.0/pi);
 f[4]=Pd-Vd*Id;
 f[5]=(Rs*(Vt-Es*cos(theta))-Xs*Es*sin(theta))/Zs-Pd/Vt+Vt*Rf/Zf+Vt*Rll/Zll;
 f[6]=(-Rs*Es*sin(theta)-Xs*(Vt-Es*cos(theta)))/Zs-Pd*tan(phi)/Vt+Vt*Xf/Zf-Vt*Xll/Zll;

 }
 fprintf(fp,"%4.6f\t %4.6f\t %4.6f\t %4.6f\t \n", Id/Idbase,Pd/Pdbase,Vt/Vtbase,Vd/Vdbase);
 }
 mat_free(Jac,1,Jrow,1,Jcol);
 mat_free(Jred,1,Jrow,1,Jrow);
 mat_free(Jinv,1,Jrow,1,Jrow);
 free_vector(x,1,Jrow);
 free_vector(scal,1,Jrow);
 free_vector(dx,1,Jrow);
 free_vector(f,1,Jrow);
 free_vector(x,1,Jrow);
 free_vector(res,1,Jrow);
 free_vector(svi,1,Jrow);
 fclose(fp);
 }
```

Program listing for the MPC calculation for equations (3.2):

```
#include<stdio.h>
#include<malloc.h>
#include<math.h>

#define SQ(x) ((x)*(x))

double **mat_alloc();
double *vector();

/*** This program calculate the MAP curve for the hvdc/ac model    ***
 *** with the synchronous  machine where the Vt-bus voltage is      ***
 *** not kept constant.                                            ***/

main()
{
 FILE *fp,*fpst;
 double **Jac,**Jred,**Jinv;
 double sq2, pi, cons1, deg, sq3;
 double Vt, Vd, Es, Id, Ei, dId;
 double alpha, gama, phi, theta, delta;
 double Pd, Qm;
```

```
double Rs, Xs, Zs, Rf, Xf, Zf, Zbase, t, Xc, Xd, Xll, Rll, Zll;
double *x, *dx, *f, *res,*svi,*scal;
double SCR, ESCR, K;
double Idbase=2, Vdbase=500, Vtbase=230, Pdbase=1000;
int i, j, l, k, d;
int loop;
int Jrow=7, Jcol=12;

sq3=1.732050808;
sq2=1.41423562;
pi=3.141592652;
deg=pi/180.0;
cons1=3.0*sq2/pi;
dId=0.01;

/*---------memory allocation-------*/
Jac=mat_alloc(1,Jrow,1,Jcol);
Jred=mat_alloc(1,Jrow,1,Jcol);
Jinv=mat_alloc(1,Jrow,1,Jcol);
x=vector(1,Jrow);
scal=vector(1,Jrow);
res=vector(1,Jrow);
dx=vector(1,Jrow);
f=vector(1,Jrow);
svi=vector(1,Jrow);

/*------- data -------*/
Zbase=230*230/1000;
Rf=0.095811;
Xf=175.928145;
Xc=13.315204*2;
Xd=44.087152;
/*Xd=29.0975208;*/
Xll=55.0404703;
Rll=167.55;
Zll=SQ(Rll)+SQ(Xll);
Zf=SQ(Rf)+SQ(Xf);
t=0.90969*2;

/*------- constraints conditions and initial conditions------*/
Id=2.;
gama=15.0*deg;
Vt=230;
Qm=260.;
delta=0.0*deg;
Es=372.57;
Vd=550;
alpha=150.0*deg;
theta=-26.9*deg;
phi=-151.58*deg;
Ei=258.773583;
/*Ei=248.990555;*/
Pd=900;
K=2.4;
```

```
Rs=K*2.921761;
Xs=K*38.435098;
Zs=SQ(Rs)+SQ(Xs);
ESCR=Zbase*sqrt(SQ(Rf/Zf+Rs/Zs)+SQ(Xf/Zf-Xs/Zs));

/*fpst=fopen("mapsdsync.out","w");*/
fp=fopen("mapsync.out","w");

for(Id=0.5*Idbase;Id<=1.2*Idbase;Id+=dId)
{
/*---------x vector definition-------------*/
x[1]=alpha;
x[2]=phi;
x[3]=Vd;
x[4]=theta;
x[5]=Pd;
x[6]=Qm;
x[7]=Ei;


/*---------f vector definition-------------*/
f[1]=Vt-sq2*Xc*Id/(t*(cos(gama)+cos(alpha)));
f[2]=cos(phi)-(cos(alpha)-cos(gama))*0.5;
f[3]=Vd-(cons1*t*Vt*cos(gama)-Xc*Id*3.0/pi);
f[4]=Pd-Vd*Id;
f[5]=(Rs*(Vt-Es*cos(theta))-Xs*Es*sin(theta))/Zs-Pd/Vt+Vt*Rf/Zf+Vt*Rll/Zll;
f[6]=(-Rs*Es*sin(theta)-Xs*(Vt-Es*cos(theta)))/Zs-Pd*tan(phi)/Vt+Vt*Xf/Zf-Vt*Xll/Zll+Qm/Vt;
f[7]=Qm-sq3*Vt*(Ei*cos(delta)-Vt)/Xd;

/*----------------Newton-Raphson nonlinear equation root----------------*/
for(loop=1;loop<=50 ;loop++)
{

/*---------definition of the Jacobian matrix------------------*/
for(i=1;i<=Jrow;i++){
   for(j=1;j<=Jcol;j++) Jac[i][j]=0;
 }

Jac[1][1]=1.0;
Jac[1][2]=-sq2*Xc/(t*(cos(alpha)+cos(gama)));
Jac[1][3]=-sq2*Xc*Id*sin(alpha)/(t*SQ(cos(alpha)+cos(gama)));
Jac[1][4]=-sq2*Xc*Id*sin(gama)/(t*SQ(cos(alpha)+cos(gama)));

Jac[2][3]=sin(alpha)/2.0;
Jac[2][4]=-sin(gama)/2.0;
Jac[2][5]=-sin(phi);

Jac[3][1]=-cons1*t*cos(gama);
Jac[3][2]=3.*Xc/pi;
Jac[3][4]=cons1*Vt*t*sin(gama);
Jac[3][6]=1.;

Jac[4][2]=-Vd;
Jac[4][6]=-Id;
```

```
Jac[4][9]=1.;

Jac[5][1]=Rs/Zs+Pd/SQ(Vt)+Rf/Zf+Rll/Zll;
Jac[5][7]=(-Rs*cos(theta)-Xs*sin(theta))/Zs;
Jac[5][8]=Es*(Rs*sin(theta)-Xs*cos(theta))/Zs;
Jac[5][9]=-1./Vt;

Jac[6][1]=-Xs/Zs+Pd*tan(phi)/SQ(Vt)+Xf/Zf-Xll/Zll-Qm/SQ(Vt);
Jac[6][5]=-Pd/(Vt*SQ(cos(phi)));
Jac[6][7]=(-Rs*sin(theta)+Xs*cos(theta))/Zs;
Jac[6][8]=Es*(-Rs*cos(theta)-Xs*sin(theta))/Zs;
Jac[6][9]=-tan(phi)/Vt;
Jac[6][12]=1/Vt;

Jac[7][1]=-sq3*(Ei*cos(delta)-2.*Vt)/Xd;
Jac[7][10]=-sq3*Vt*(cos(delta))/Xd;
Jac[7][11]=sq3*Vt*Ei*sin(delta)/Xd;
Jac[7][12]=1.;

/*----------------reduced Jacobian--------------*/
for(k=1;k<=Jrow;k++){
Jred[k][1]=Jac[k][3];
Jred[k][2]=Jac[k][5];
Jred[k][3]=Jac[k][6];
Jred[k][4]=Jac[k][8];
Jred[k][5]=Jac[k][9];
Jred[k][6]=Jac[k][12];
Jred[k][7]=Jac[k][10];
}
mat_inverse(Jred,Jinv,Jrow);
mtx_vect_multiplication(Jinv,f,dx,Jrow,-1.0);
vect_adding(x,dx,x,Jrow);

alpha=x[1];
phi=x[2];
Vd=x[3];
theta=x[4];
Pd=x[5];
Qm=x[6];
Ei=x[7];

f[1]=Vt-sq2*Xc*Id/(t*(cos(gama)+cos(alpha)));
f[2]=cos(phi)-(cos(alpha)-cos(gama))*0.5;
f[3]=Vd-(cons1*t*Vt*cos(gama)-Xc*Id*3.0/pi);
f[4]=Pd-Vd*Id;
f[5]=(Rs*(Vt-Es*cos(theta))-Xs*Es*sin(theta))/Zs-Pd/Vt+Vt*Rf/Zf+Vt*Rll/Zll;
f[6]=(-Rs*Es*sin(theta)-Xs*(Vt-Es*cos(theta)))/Zs-Pd*tan(phi)/Vt+Vt*Xf/Zf-Vt*Xll/Zll+Qm/Vt;
f[7]=Qm-sq3*Vt*(Ei*cos(delta)-Vt)/Xd;
}

fprintf(fp,"%4.6f\t %4.6f\t %4.6f\t %4.6f\t \n", Id/Idbase,Pd/Pdbase,Vt/Vtbase,Vd/Vdbase);
}
mat_free(Jac,1,Jrow,1,Jcol);
mat_free(Jred,1,Jrow,1,Jrow);
```

```
mat_free(Jinv,1,Jrow,1,Jrow);
free_vector(x,1,Jrow);
free_vector(scal,1,Jrow);
free_vector(dx,1,Jrow);
free_vector(f,1,Jrow);
free_vector(x,1,Jrow);
free_vector(res,1,Jrow);
free_vector(svi,1,Jrow);
fclose(fp);
}
```